

**Polyelectrolyte Multilayers:  
Nanofabricated Architectures for Bio-interface Materials**

by

**Jonas Daniel Mendelsohn**

**B.S. Biomedical Engineering  
The Johns Hopkins University, 1997**

**Submitted to the Department of Materials Science and Engineering  
in Partial Fulfillment of the Requirements for the Degree of**

**Doctor of Philosophy  
in Polymer Science**

at the

**Massachusetts Institute of Technology**

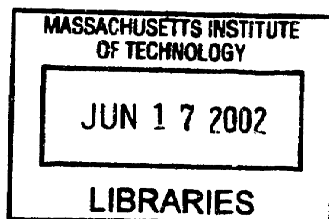
**June 2002**

**© 2002 Massachusetts Institute of Technology. All rights reserved.**

Signature of Author: \_\_\_\_\_  
Department of Materials Science and Engineering  
May 7, 2002

Certified by: \_\_\_\_\_  
Michael F. Rubner  
TDK Professor of Materials Science and Engineering  
Thesis Supervisor

Accepted by: \_\_\_\_\_  
Harry L. Tuller  
Professor of Ceramics and Electronic Materials  
Chair, Departmental Committee on Graduate Students



**ARCHIVES**



# **Polyelectrolyte Multilayers: Nanofabricated Architectures for Bio-interface Materials**

By  
Jonas D. Mendelsohn

Submitted to the Department of Materials Science and Engineering  
and the Program in Polymer Science and Technology on May 7, 2002  
in Partial Fulfillment of the Requirements for the  
Degree of Doctor of Philosophy in Polymer Science

## **ABSTRACT**

The layer-by-layer process, whereby aqueous solutions of oppositely charged polymers are alternately and repeatedly deposited onto a substrate, has emerged in recent years as a promising approach for creating thin films with nanoscale control of structure, composition, and surface properties. Applications ranging from surface modification to optical and electronic devices have arisen from the versatility of this nanocomposite fabrication technique. The additional ability to assemble into films a wide variety of biological entities, such as enzymes and DNA, has expanded the use of polyelectrolyte multilayers for biosensor and other biomaterials applications.

This thesis further explores the rationale of using multilayers as biomaterials, with particularly emphasis on the importance of the underlying molecular architecture. Many of the results presented here concern films assembled from weak polyions, i.e., ones with pH-dependent charge densities, including poly(acrylic acid) (PAA) and poly(allylamine hydrochloride) (PAH). Using weak polyions enables the creation of thin films with chemical and structural properties controlled with nanoscale precision by simply adjusting the pH of the polymer solutions.

Under certain assembly conditions, initially nonporous PAA/PAH films become nano- and/or microporous through a simple pH-induced phase separation in acidic water (pH ~ 2.4), even with an exposure time of just a few seconds. By adjusting several processing parameters (e.g., the time, temperature, ionic strength, and a secondary rinse with neutral water), it is possible to generate either interconnected or discrete porous morphologies. The interaction of a highly adhesive mammalian NR6WT fibroblast cell line with various PAA/PAH films and other multilayer systems of differing compositions, structures, and charge densities has also been explored. This thesis demonstrates that by manipulating the multilayer pH assembly conditions, which in turn dictates the molecular architecture of the thin films, one may powerfully direct a single multilayer combination to be either cell adhesive or cell resistant. Highly ionically stitched multilayers attract cells, whereas weakly ionically crosslinked multilayers, which swell substantially in physiological conditions and thereby present richly hydrated surfaces, resist cell attachment. This unprecedented ability to fine-tune a multilayer to be either cell adhesive or bioinert, along with the unique feature of controllable porosity, allows polyelectrolyte multilayers to be envisioned for membranes, controlled release, and biocompatible implant coating applications.

Thesis Supervisor: Michael F. Rubner

Title: TDK Professor of Materials Science and Engineering





## Table of Contents

<b>Title Page .....</b>	<b>1</b>
<b>Abstract .....</b>	<b>3</b>
<b>Table of Contents .....</b>	<b>5</b>
<b>List of Figures and Tables.....</b>	<b>9</b>
<b>Acknowledgments.....</b>	<b>11</b>
<b>1. Introduction and Background .....</b>	<b>13</b>
<b>1.1 The Field of Biomaterials .....</b>	<b>13</b>
1.1.1 Biocompatibility .....	14
1.1.2 Bioinert Materials .....	16
<b>1.2 Polyelectrolyte Complexes as Biomaterials.....</b>	<b>17</b>
<b>1.3 The Layer-by-Layer Processing of Polyelectrolytes .....</b>	<b>19</b>
1.3.1 Introductory Remarks.....	19
1.3.2 The Mechanism of Multilayer Assembly.....	21
1.3.3 Controlling Multilayer Properties .....	22
<b>1.4 Previous Biomedical Applications of Polyelectrolyte Multilayers .....</b>	<b>24</b>
1.4.1 Introductory Remarks.....	24
1.4.2 Previous Cell Interaction Studies with Polyelectrolyte Multilayers.....	25
<b>1.5 Thesis Outline and Aims.....</b>	<b>26</b>
<b>1.6 References .....</b>	<b>28</b>
<b>2. Fundamental Assembly Characteristics of Polyelectrolyte Multilayers.....</b>	<b>35</b>
<b>2.1 Introductory Remarks.....</b>	<b>35</b>
<b>2.2. Materials and Methods.....</b>	<b>36</b>
2.2.1 General Multilayer Deposition and Assembly .....	36
2.2.2 Thickness Determination.....	37
2.2.3 Wettability Measurements.....	38
2.2.4 Methylene Blue and Rose Bengal Dye Staining.....	38
2.2.5 Chemical Analysis: UV-visible and FT-IR Spectroscopy .....	38
2.2.6 Surface Morphology and Roughness: Atomic Force Microscopy (AFM).....	38
<b>2.3 Representative PAA/PAH Polyelectrolyte Multilayer Systems.....</b>	<b>39</b>
2.3.1 The 6.5/6.5 PAA/PAH System .....	39
2.3.2 The 3.5/7.5 PAA/PAH System .....	40
2.3.3 The 2.0/2.0 PAA/PAH System .....	41
<b>2.4 Other Polyelectrolyte Multilayer Systems .....</b>	<b>43</b>
2.4.1 Introductory Remarks.....	43

2.4.2 Polyacrylamide Systems.....	43
2.4.3 PMA/PAH Systems.....	44
2.4.4 SPS/PAH Systems .....	44
2.4.5 SPS/PDAC Systems.....	45
<b>2.5 Conclusion.....</b>	<b>45</b>
<b>2.6 References .....</b>	<b>47</b>
<b>3. The Development of Porosity in Polyelectrolyte Multilayers .....</b>	<b>49</b>
<b>3.1 Introductory Remarks.....</b>	<b>49</b>
<b>3.2 Materials and Methods.....</b>	<b>50</b>
3.2.1 General Multilayer Deposition and Assembly .....	50
3.2.2 The Porosity Process .....	51
3.2.3 Characterization of the Porous Multilayers.....	51
3.2.4 Thermal Crosslinking.....	52
<b>3.3 Results and Discussion.....</b>	<b>52</b>
3.3.1 General Findings.....	52
3.3.2 The pH Parameter .....	54
3.3.3 Multilayer System.....	55
3.3.4 Layer Number and the Identity of the Outermost Layer.....	57
3.3.5 Time, Temperature, and Rinsing Parameters .....	57
3.3.6 Extended Immersions in Neutral Water.....	68
3.3.7 Ionic Strength.....	70
3.3.8 Mechanism of Porosity Formation in Polyelectrolyte Multilayers.....	72
<b>3.4 Applications of Porous Polyelectrolyte Multilayers .....</b>	<b>79</b>
<b>3.5 Conclusion and Future Work.....</b>	<b>80</b>
<b>3.6 References .....</b>	<b>83</b>
<b>4. Protein Interactions with Polyelectrolyte Multilayers .....</b>	<b>87</b>
<b>4.1 Introductory Remarks.....</b>	<b>87</b>
<b>4.2 Materials and Methods.....</b>	<b>90</b>
4.2.1 Materials.....	90
4.2.2 Surface Plasmon Resonance.....	90
<b>4.3 Results and Discussion.....</b>	<b>91</b>
4.3.1 Assembly of Polyelectrolyte Multilayers.....	91
4.3.2 Protein Adsorption to Polyelectrolyte Multilayers .....	93
<b>4.4 Conclusion and Future Work.....</b>	<b>97</b>
<b>4.5 References .....</b>	<b>98</b>
<b>5. Cell Interactions with Polyelectrolyte Multilayers.....</b>	<b>101</b>
<b>5.1 Introductory Remarks.....</b>	<b>101</b>
<b>5.2 Materials and Methods.....</b>	<b>102</b>
5.2.1 General Multilayer Deposition and Assembly .....	102
5.2.2 Cell Culture.....	102
5.2.3 Characterization Methods.....	103
5.2.4 In Situ Swelling Experiments .....	104

<b>5.3 Results .....</b>	<b>104</b>
5.3.1 General Findings: PAA/PAH Multilayers.....	104
5.3.2 General Findings: PMA/PAH, SPS/PAH, and SPS/PDAC Multilayers.....	109
5.3.3 General Findings: PAA/PAAm and PMA/PAAm Multilayers .....	111
<b>5.4 Discussion .....</b>	<b>113</b>
5.4.1 General Remarks.....	113
5.4.2 Wettability Studies.....	115
5.4.3 Roughness and Topography .....	117
5.4.4 Protein Adhesiveness .....	120
5.4.5 Swelling Studies .....	121
<b>5.5 Conclusion and Future Work.....</b>	<b>122</b>
<b>5.6 References .....</b>	<b>126</b>
<b>6. Conclusions and Outlook .....</b>	<b>129</b>
6.1 Thesis Summary and Outlook.....	129
6.2 References .....	134



## List of Figures and Tables

Figure 1.1. Schematic of the biocompatibility concept of creating a bioactive system for medical implant surfaces.....	16
Figure 1.2. Schematic of the layer-by-layer process .....	21
Figure 1.3. Schematic of train and loop-rich conformations in multilayers .....	23
Figure 2.1. Chemical structures of some of the common polymers for multilayer thin film assembly.....	36
Figure 2.2. Schematics of proposed molecular architectures for the 6.5/6.5, 3.5/7.5, and 2.0/2.0 PAA/PAH multilayer thin films .....	42
Figure 2.3. Graph of the mean total film thickness vs. the number of layers deposited for the 3.5/7.5, 6.5/6.5, and 2.0/2.0 PAA/PAH multilayers .....	43
Figure 3.1. Flowchart depicting the various processing routes and variables used to fabricate porous polyelectrolyte multilayer thin films.....	51
Figure 3.2. Representative AFM images of nonporous and porous 3.5/7.5 PAA/PAH films .....	53
Figure 3.3. % pore volume vs. pH curve for the 3.5/7.5 PAA/PAH system.....	55
Figure 3.4. Array of AFM images of porous multilayers conditioned in pH ~ 2.4 water for various exposure times and acid bath temperatures, without rinsing .....	59
Figure 3.5. Array of AFM images of porous multilayers conditioned in pH ~ 2.4 water for various exposure times and acid bath temperatures, with rinsing .....	60
Figure 3.6. AFM images of the percolating, microporous morphoplogy and the rounded, discrete throughpore structure.....	61
Figure 3.7. Processing paths to create interconnected microporous or discrete, rounded throughpore morphologies.....	62
Figure 3.8. Graphs of the mean pore size of the porous multilayers vs. time.....	63
Figure 3.9. Graphs of the expansion factor or thickness increase for porous films vs. time .....	65
Figure 3.10. Graphs of the porous refractive index, $n_{\text{pore}}$ , vs. time.....	67
Figure 3.11. Graphs of the AFM-derived RMS roughness values for porous films vs. time .....	68
Figure 3.12. AFM image of a typical porous multilayer conditioned for several hours in neutral water after the initial acid treatment.....	69
Figure 3.13. Graph of the % pore volume vs. pH curve for the 3.5/7.5 PAA/PAH system treated in acidic water of various ionic strengths.....	71
Figure 3.14. AFM image of a nanoporous multilayer .....	71
Figure 3.15. FT-IR spectra of the 3.5/7.5 PAA/PAH multilayer before and after the porosity treatment .....	73
Figure 3.16. Graph of the FT-IR-derived COOH/COO <sup>-</sup> absorbance ratio for various PAA/PAH combinations .....	73
Figure 3.17. Schematics of the “ladder conformation” and the “scrambled salt” arrangement to describe polyelectrolyte complexes.....	75
Figure 4.1. Schematic of the experimental flow cell used in SPR detection .....	89
Figure 4.2. Representative response units vs. time graph obtained from SPR data.....	92

Figure 4.3. SPR-derived adsorption data for lysozyme and fibrinogen on an uncoated gold surface and gold coated with 3.5/7.5 or 2.0/2.0 PAA/PAH multilayers .....	94
Figure 5.1. Graph of the number of fibroblasts attached on various PAA/PAH multilayers and on a TCPS control .....	105
Figure 5.2. Phase contrast photographs of NR6WT fibroblasts seeded onto various PAA/PAH multilayers and a TCPS control .....	107
Figure 5.3. Phase contrast photograph of NR6WT fibroblasts transplanted from a bioinert 2.0/2.0 PAA/PAH multilayer surface to a TCPS surface.....	108
Figure 5.4. Phase contrast photographs of NR6WT fibroblasts seeded onto various PMA/PAH multilayers.....	109
Figure 5.5. Phase contrast photographs of NR6WT fibroblasts seeded onto various SPS/PAH multilayers.....	111
Figure 5.6. Phase contrast photographs of NR6WT fibroblasts seeded onto various SPS/PDAC multilayers .....	112
Figure 5.7. Phase contrast photographs of NR6WT fibroblasts seeded onto various PAA/PAAm and PMA/PAAm multilayers .....	112
Figure 5.8. Advancing and receding contact angles with water on the 3.5/7.5 and 2.0/2.0 PAA/PAH multilayers, after being treated in various solutions used in cell culture .....	116
Figure 5.9. Phase contrast photographs of NR6WT fibroblasts seeded onto nonporous and porous 3.5/7.5 PAA/PAH multilayers .....	119
Figure 5.10. Phase contrast photographs of NR6WT fibroblasts seeded onto a patterned TCPS dish with an uncoated side and a PAA/PAAm multilayer-coated side .....	125
Table 2.1. Comparison of important physical and chemical properties of various PAA/PAH multilayers. ....	42
Table 2.2. Comparison of the average layer thickness and RMS roughness values for various multilayer combinations.....	46

## Acknowledgments

First and foremost, I must acknowledge my thesis advisor, Professor Michael F. Rubner, who allowed me to embark on such an exciting thesis in a truly fascinating research field. I admire his willingness to let me explore a very different area than what was previously typical in the lab; starting anything biologically-related is a daunting task, but with his guidance, I think we managed quite well. I appreciate the help from my thesis committee as well—Professors Linn Hobbs, Anne Mayes, and ChoKyun Rha—who provided me with useful advice and insight into this project.

I would also like to acknowledge the support and companionship of all my past and present fellow group members: Erika Abbas, Mike Berg, Bo Chen, Jeeyoung Choi, Anita Chung, Michael Durstock, Erik Handy, Jeri' Ann Hiller, Ilsoon Lee, Adam Nolte, Amlan Pal, Hartmut Rudmann, Satoru Shimada, Nobuaki Takane (and his wife Kaori), Sung Yun Yang, Peter Wan, Tom Wang, Aleks White, Haipeng Zheng, and Stephanie Hansen. I appreciate the help of several UROPs—Allon Hochbaum, Colleen Colson, Aaron Raphel, Venetia Chan, Alicia Jackson, Lisa Scoppettuolo, and Nicole Zacharia. Thanks to all of these group members for putting up with my humor and satire and accompanying me to free food venues, of which there were so many!

Thanks also to several members from Professor Mayes's group: Chris Barrett, who helped with much of the initial work on this project, as well as Stella Park, Jonathan Hester, Ariya Akthakul, and Metin Acar for helpful discussions. For teaching me cell culture techniques and for the NR6WT cell line, I am indebted to Lily Koo and Professor Linda Griffith. I must thank Lily as well as Ley Richardson from the Griffith lab for answering my numerous questions during my cell culture studies. I am grateful to Shuguang Zhang for allowing me to use the Center for Bioengineering cell culture facilities and to Carlos Semino for help along the way. I must acknowledge Joonil Seog in Prof. Christine Ortiz's lab for help with the AFM swelling experiments. I am thankful to Libby Shaw and Tim McClure for help in using the CMSE Analytical Facilities as well as to the NSF grants which supported this work financially. My former college professors—Manny Horowitz, Ed Mueller, Mark Saltzman, Kam Leong, Norm Sheppard, John D. Hoffman, and James Wagner—deserve my thanks as well for inspiring me and introducing me to biomaterials and polymers.

Of course, I must acknowledge the love and support of my family—my parents, Bob and Lindy, and my brothers and sisters-in-law, Seth and Amy, Aaron and Kelly—for all that they've done for me, questioning (and not really understanding) what I've been working on at MIT, their encouragement, and their humor. To my longtime friends, Ruth, Marc, Jason, Go, Roger, Ed, cousin Rick and Amanda, and Ben—thanks for the friendship and getting me out of the lab every once and awhile.

I dedicate this thesis to those who are not around to see this great milestone, although I know they are still watching my progress closely and proudly—my friend Brian Patrick Smith and my grandparents, Louise and Samuel Bloom and Emanuel Mendelsohn. I am also grateful to G-d for all of life's many gifts, including the wonderful occasion of the fulfillment of this degree. L'chaim!



# **Chapter 1: Introduction and Background**

## **1.1 The Field of Biomaterials**

The merging of medicine, biology, and engineering in recent decades has provided many new opportunities to treat disease, particularly at the molecular level. Magnetic resonance imaging (MRI), minimally invasive surgery, organ transplantation, and even genetic engineering are just a few examples of cutting-edge technologies that are now becoming routine ways to diagnose and heal patients. Another remarkable advance that has had a significant impact and improvement on many people's lives is the field of biomaterials, whereby typically synthetic materials replace or repair injured or diseased body tissues.<sup>1-3</sup> Dissolvable sutures, contact lenses, dental implants, bone screws, and hip joint replacements are just some of the many diverse biomaterial devices used by the millions today. Two of the more nascent, state-of-the-art subdisciplines of biomaterials—controlled drug delivery<sup>4</sup> and tissue engineering<sup>5-9</sup>—will surely become important and commonplace technologies in the 21<sup>st</sup> century. All of these medical devices and biomaterial applications involve a complex interplay between the cells and tissues of the physiological environment and the implanted material(s); this interaction is captured by the concept of biocompatibility.

### 1.1.1 Biocompatibility

One of the most obvious requirements for any biomaterial, whether synthetic or natural, is to be non-toxic and safe to the host body. Though it has been defined in several different ways, the concept of biocompatibility summarizes these essential needs of any medical device. Biocompatibility may be thought of as the harmonious integration of the body with the biomaterial without evoking any significant inflammatory or immunological responses; the biomaterial should not irritate or harm the surrounding tissues or the body as a whole, and the body should similarly not damage the implant.<sup>1</sup> While the host physiology perceives nearly all medical implants as “foreign,” which then typically results in an inflammatory reaction to some degree, a major aim in biomaterials is to abate any negative response and instead induce desirable material-tissue interactions. Thus, making implant materials more biocompatible is a high priority.

Much of the body’s reaction to a foreign implant resembles the natural process of wound healing. Both a short-term acute response and a longer-term chronic response constitute general wound healing as well as the typical reaction to any biomaterial. Upon implantation, virtually any biomaterial rapidly adsorbs a *nonspecific* layer of proteins that then attract the body’s immune cells, including neutrophils, macrophages, and foreign body multinuclear giant cells (composed of many macrophages) to deposit onto the implant surface.<sup>1,10</sup> Ratner has appropriately termed this common albeit undesirable and nonspecific physiological response a “blah” reaction.<sup>11</sup> Furthermore, this acute reaction may induce migrating fibroblast cells to form an encapsulating layer of scar-like, collagenous tissue<sup>10,12</sup> in order to “wall-off” the biomaterial<sup>11</sup>; this “walling-off” effect is the body’s attempt to get rid of the foreign material, which, of course, undermines the very reason the biomaterial was implanted in the first place. Depending on how irritating or biocompatible the implant is, the body may either accept the material with a relatively mild reaction (i.e., with little or even no fibrous encapsulation) or, on the contrary, elicit a strong negative response marked by a thicker, persistent capsule with long-term inflammation typically. Chronic fibrous encapsulation may hinder device performance, necessitate implant removal, increase the risk of infection, or cause clinical complications and patient dissatisfaction, as was, for example, frequently reported and well-publicized by patients with silicone breast implants.<sup>13</sup> Additionally, in blood-contacting medical devices, it should be noted that the nonspecific

protein adsorption onto the implant surface might trigger platelet activation and a dangerous biochemical cascade that may potentially lead to thrombosis (blood clots).<sup>10</sup>

In the past, many researchers even perceived the common “walling-off” phenomenon as indicative of good biocompatibility. However, an emerging theme that challenges that view suggests instead that true biocompatibility involves the body integrating with the implant in a specific, presumably predictable and engineered way, and certainly not in reactions whereby the body tries to exclude or “wall-off” the device.<sup>11</sup> Central to Ratner’s theory and now many other emerging perspectives on biocompatibility is to first and foremost control (i.e., usually eliminate) the nonspecific adsorption of proteins to the biomaterial, since proteins mediate cell adhesion.<sup>11</sup> After having prevented uncontrolled protein adhesion, specific biomolecular cues, such as the protein adhesive sequences like the well-known RGD (arginine-glycine-aspartic acid) tripeptide, may be reintroduced to signal cell activities, encourage cell binding, and promote cell proliferation in a controlled manner.<sup>12,14-16</sup>

The promising biomaterials field of tissue engineering<sup>5-9</sup>—which aims to restore damaged tissue often with both a synthetic polymer scaffold and living cells, could benefit greatly from controlled cell behavior. Typically, the polymers, which may resorb or degrade over time, are seeded with cells and occasionally beneficial growth factors or other signaling biomolecules as well. The polymer acts as a supporting scaffold for directing the cells to grow, regenerate lost function, and organize into healthy tissue that can incorporate into the surrounding tissue. Thus, having specific adhesive molecules that bind only the desired cell type(s) necessary to regenerate new tissue—and not unwanted or inflammatory cells—is important. Figure 1.1 depicts this emerging demand in tissue engineering and biomedicine to create truly bioactive systems—the approach of being able to block uncontrolled cell and protein adhesion and then to re-establish cell-material interactions in a predictable fashion, often with precisely engineered geometries as well.<sup>12,14,15</sup>

With such an approach as that shown in Figure 1.1, it is also possible to have multiple cell types coexist, such as a primary cell type plus other supporting cells for tissue regrowth. Besides tissue engineering and biomaterials in general, other biotechnology and industrial processes, including nonfouling membranes and separation filters, bioreactors, biosensors, novel cell and protein arrays, and high-throughput combinatorial synthetic processes, among others, could also greatly benefit from controlled biological-materials interactions.

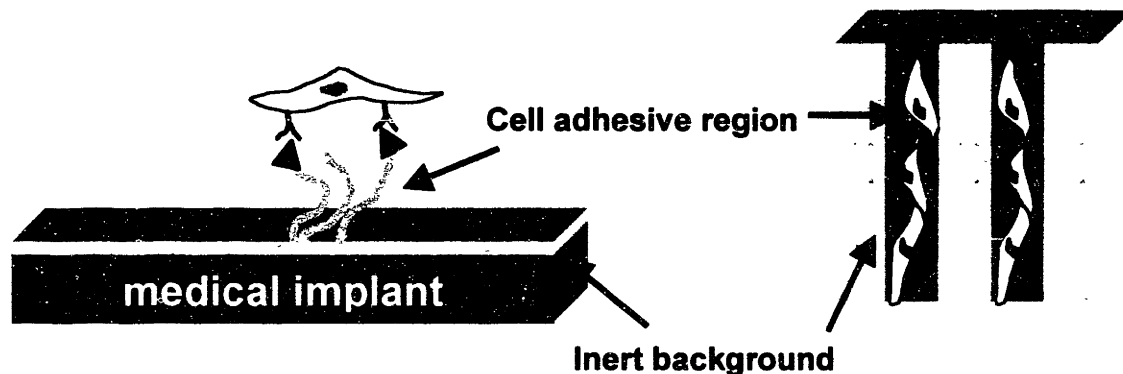


**Figure 1.1:** Schematic of the biocompatibility concept of creating a bioactive system for medical implant surfaces. The important elements are: 1) a bioinert background to resist nonspecific cell attachment, and 2) the inclusion of specific binding molecules (e.g., RGD or other peptide ligands, depicted by the ▲ symbol) to encourage desired cell attachment. The patterning of these two elements in precise geometries can also be accomplished, as illustrated above.

### 1.1.2 Bioinert Materials

To accomplish the goal of eliminating nonspecific protein adhesion and thus undesirable cell attachment, numerous protein-resistant or so-called “bioinert” materials have been developed. While some researchers may claim that no material can be truly inert in the physiological environment, there are indeed some substances that significantly reduce uncontrolled protein and cell attachment. Ideally, these bioinert materials provide a cell-resistant background, which then can be modified with appropriate biochemical signals to enable the growth of desirable and useful cells for the end-goal application. Polymeric or oligomeric ethylene glycol (PEO, PEG, or o-EG), a hydrophilic material with a proven ability to resist protein adhesion, often exemplifies the bioinert background material in such an approach. While there is some debate as to the exact mechanism of its protein resistance, researchers speculate that PEO’s attributes—its neutral charge, strong hydrogen bonding interactions with water, and chain flexibility (but only in its polymeric not oligomeric form)—render it a hydrated molecule that can sterically repel proteins.<sup>17,18</sup>

Unfortunately, PEO succumbs to auto-oxidation and hydrolytic degradation over time and thus has poor stability in long-term clinical applications. Consequently, other materials, including PEO-based hydrogels,<sup>19,20</sup> dextran,<sup>21,22</sup> mannitol,<sup>23</sup> poly(vinyl alcohol),<sup>24</sup> polyacrylamide,<sup>25</sup> and phosphatidylcholine,<sup>26</sup> have been explored as viable bioinert alternatives. Among the processing schemes to achieve the bioinert background is to utilize self-assembled monolayers (SAMs)<sup>23,26-31</sup> or one of a number of various grafting or polymerization approaches<sup>16,32,33</sup> to present one of these resistant materials onto the surface of

interest. However, potential problems with incomplete, non-uniform surface coverage, the need in many cases for multiple synthetic steps, and for the case of SAMs, its restriction to silicon or gold substrates, tend to limit somewhat these approaches for creating bioinert coatings. As will be discussed in this thesis, yet another method based on polyelectrolyte complexes may offer a unique way by which to manipulate virtually any material surface, such as rendering the surface cell-resistant and/or bioactive in order to achieve controllable and desirable biomaterial-tissue interactions. Moreover, this technique—known as the layer-by-layer processing of polyelectrolytes—forms nanostructured, conformal, highly tailorable as well as patternable coatings with the further potential for becoming porous, which would be useful for controlled release applications. Before detailing this process, it is worth explaining some background on polyelectrolyte complexes and their use in biomedical applications.

## **1.2 Polyelectrolyte Complexes as Biomaterials**

Compared to non-charged polymers, polyelectrolytes are macromolecules with a high percentage of ionizable functional groups. The presence of charges in the chain backbone or on pendant groups allows polyelectrolytes to bind to oppositely charged surfaces and produce complexes (also known as symplexes) with oppositely charged polymers. Consequently, oppositely charged polyelectrolytes in solution can form water-soluble or insoluble, precipitated complexes depending on their specific binding interactions as well as the pH, ionic strength, molecular weight, and the stoichiometric ratio between the polymers.<sup>34</sup> Usually, the complexation of two oppositely charged polyelectrolytes leads to a phase separation from the solution. In one type of phase separation process known as complex coacervation, two oppositely charged polyelectrolytes aggregate together as they undergo a so-called liquid-liquid phase separation or partial desolvation from solution. The resulting two liquid phases are: 1) a hydrated, polymer-rich, gel-like phase called the “coacervate phase,” and 2) a polymer-deficient, liquid phase termed the “coacervate medium.”<sup>35</sup> Typically, complex coacervation yields an interfacial ionic thin film between the two polyelectrolytes, which may become a porous membrane resulting from the interfacial diffusion of the chains during the phase transition.<sup>36</sup>

Both precipitated and coacervated polyelectrolyte complexes have potential use in biomedical applications in the form of thin films and porous membranes. Furthermore, due to their ionic nature, hydrogel structure, and permeability to bodily fluids, polyelectrolyte complexes possess many features similar to proteins and biological tissues.<sup>34,37</sup> This protein resemblance along with their low toxicity, hydrophilicity, good mechanical strength, inherent ability to bind with molecules of opposite charge, and unique phase separation behavior have made polyelectrolyte complexes attractive candidates for biomedical use.<sup>34,37</sup> In fact, polyelectrolytes have a long history as implant materials, with applications as contact lenses, drug delivery systems, dental adhesives, blood compatible and anti-clotting coatings, membranes, scaffold materials for tissue regeneration, and enteric coatings for drugs.<sup>34,37,38</sup>

One of the most studied biomedical applications of polyelectrolyte complexes is for encapsulating cells (or cell products, drugs, genes, or enzymes) for novel therapeutic purposes, such as cell-based internal artificial organs. In 1972, Chang first pioneered the possibility of encapsulating enzymes or cell components into synthetic nylon, polystyrene, or cellulose nitrate polymer membranes.<sup>39</sup> In 1980, there was the well-known report by Lim and Sun who demonstrated the complex coacervation of the polyanion alginate with the polycation poly-L-lysine as an effective method to encapsulate pancreatic islets (clusters of glucose-sensing and insulin-secreting cells) for the treatment of diabetes.<sup>40</sup> Since then, the encapsulation of healthy, foreign cells (i.e., cross-species xenografts or human allografts) in order to isolate them from the recipient patient's immune system has emerged as a potential high-tech treatment for many ailments, including neurological conditions and chronic pain.<sup>41</sup> In such an approach, a semipermeable membrane entraps the foreign cells from the host's immune system by sterically controlling the passage of molecules via the size of its pores. Small molecules, such as oxygen, nutrients, wastes, and secreted proteins or other cell products, may freely diffuse through the permselective membrane, while much larger antibody molecules and immune cells are excluded. Therefore, the cells can survive and remain functional by receiving necessary nutrients and oxygen without being recognized and attacked by the host's immune system. It is also important for the membrane materials to be biocompatible and not succumb to significant fibrous encapsulation, which would severely hinder the transport of solutes through the membrane, thus possibly detrimentally depriving

the trapped cells of much needed oxygen and nutrients. Consequently, a bioinert membrane coating would be quite advantageous for immunoisolation applications.

Many researchers have tried to improve upon the classic alginate-polylysine coacervate chemistry in hopes of simultaneously optimizing the biocompatibility, permeability, and mechanical integrity of polyelectrolyte complex capsules. Due to biocompatibility concerns that polylysine may be toxic to cells, an additional layer of alginate is often adsorbed to the microcapsule to produce a tri-layered alginate/polylysine/alginate complex coating.<sup>42</sup> Thus, several groups have realized this process could be extended to include not two but three or even more layers for additional improvement of the capsule properties. For example, Pommersheim et al. have successfully applied to alginate capsules containing enzymes or islets many alternate layers of the polyanion poly(acrylic acid) (PAA) and the polycation poly(ethyleneimine) (PEI).<sup>43,44</sup> In addition, the same group has assembled alternating multilayers of PAA and poly(*N*-vinylamine) (PNVA) to enzyme-containing alginate beads.<sup>45</sup> Using these multiple layers of polyelectrolytes, they report better control of the permeability and mechanical strength compared to single-step membrane-forming complexation. Prokop et al. similarly observed that polyelectrolyte complex membranes formed in several steps excelled over the ordinary binary complex coacervation that yields an interfacial membrane in one step.<sup>46</sup> Therefore, it appears that the most optimal method for creating semipermeable polyelectrolyte complexes is to use a multilayering scheme.

## **1.3 The Layer-by-Layer Processing of Polyelectrolytes**

### **1.3.1 Introductory Remarks**

As discussed in Section 1.2, polyelectrolyte complexes have been proposed to be useful biomaterials due to their resemblance to physiological tissues and proteins. Furthermore, many drug and cell encapsulation strategies rely on polyelectrolyte complexation, particularly on a single two-layer polycation-polyanion system. As mentioned above, the repetitive layering of polyions to form capsule walls is also a possibility, as demonstrated by Pommersheim et al.<sup>43-45</sup> Their alternate deposition of polycations and polyanions onto capsule cores is an example of a recently developed thin film fabrication method known as the layer-by-layer processing of polyelectrolytes.

The layer-by-layer process effectively assembles polyelectrolyte complexes one molecular layer at a time to form what are known as polyelectrolyte multilayers. Introduced by Decher et al.<sup>47-49</sup> in the early 1990's, polyelectrolyte multilayer deposition is a simple yet highly versatile technique whereby ultrathin films are assembled electrostatically from the repetitive, sequential adsorption of oppositely charged polyelectrolytes from dilute aqueous solution onto a substrate. However, in certain polymeric systems, hydrogen bonding, rather than electrostatic attraction, is the assembly mechanism.<sup>50-53</sup> This layer-by-layer technique enables the development of complex heterostructures and the control of thickness and surface properties at the nanoscale level, resulting in uniform, highly interpenetrated ultrathin films. Moreover, because the layer-by-layer method assembles polyelectrolyte complexes onto a substrate, the problem of forming complexes that precipitate in solution is avoided. Since it builds films one molecular layer at a time, the technique additionally affords better control over the molecular architecture than other more conventional thin film fabrication techniques, such as the Langmuir-Blodgett (LB) method. It should be noted that dip coating with alternate polyion solutions is a common way to prepare multilayer films, yet spin coating<sup>54,55</sup> and spray-coating<sup>56</sup> are alternative useful processing schemes to deposit multilayers.

Essentially any synthetic or natural polyion can be used to fabricate the multilayer thin films in this customizable, environmentally sound, aqueous-based process, which is additionally easily automated and able to be upscaled for mass production. A wide variety of materials, such as synthetic polyelectrolytes,<sup>57,58</sup> conductive and light emitting polymers,<sup>59-62</sup> dyes,<sup>63,64</sup> inorganic/clay molecules,<sup>65,66</sup> and biopolymers, such as chitosan,<sup>67</sup> DNA,<sup>68-71</sup> proteins/enzymes,<sup>69,72-76</sup> and even viruses,<sup>77</sup> have effectively been constructed into multilayer assemblies. The resulting polyelectrolyte multilayers can coat reproducibly substrates of any type, size, shape, or texture with well defined properties of film thickness, composition, conformation, degree of interchain ionic bonding, roughness, and wettability. With its unprecedented potential in creating ultrathin films with tailorable nanoscale features, the layer-by-layer approach has been investigated for a diverse range of applications including, but not limited to, light emitting devices,<sup>62,78</sup> surface coatings with tailored wettabilities,<sup>57,58</sup> chemical sensors,<sup>79</sup> biosensors,<sup>69,74,75,80,81</sup> and potential biomaterials applications.<sup>67,82-85</sup> As a whole, the field of polyelectrolyte multilayers has been reviewed recently,<sup>86-88</sup> with respect to both its fundamentals and applications.



### 1.3.2 The Mechanism of Multilayer Assembly

The layer-by-layer process, as depicted in Figure 1.2, generally involves sequentially immersing clean substrates into dilute solutions of a polycation and a polyanion. Virtually any substrate, including silicon, glass, polystyrene and other plastics, quartz, and inorganic crystals such as zinc selenide, may easily be used in the technique. Even colloids and nanoparticles have been frequently employed as substrates.<sup>76,89-97</sup> In a typical layer construction, the charges of an adsorbing polyelectrolyte molecule bind to the oppositely charged previous layer. Charge overcompensation on the adsorbing polymer layer reverses the net surface charge to facilitate the binding of the next layer. Rinsing with neutral, ultrapure water between the polyelectrolyte baths removes any loosely bound molecules. The substrate is then dipped into an oppositely charged polyelectrolyte that readily adsorbs to the oppositely charged film surface; this single alternating polycation/polyanion combination, which makes one bilayer, may be repeated as many times as needed to achieve a desired film thickness. Thus, the electrostatic interactions occurring between the oppositely charged ions on the polymers usually enable the construction of multilayer thin films.

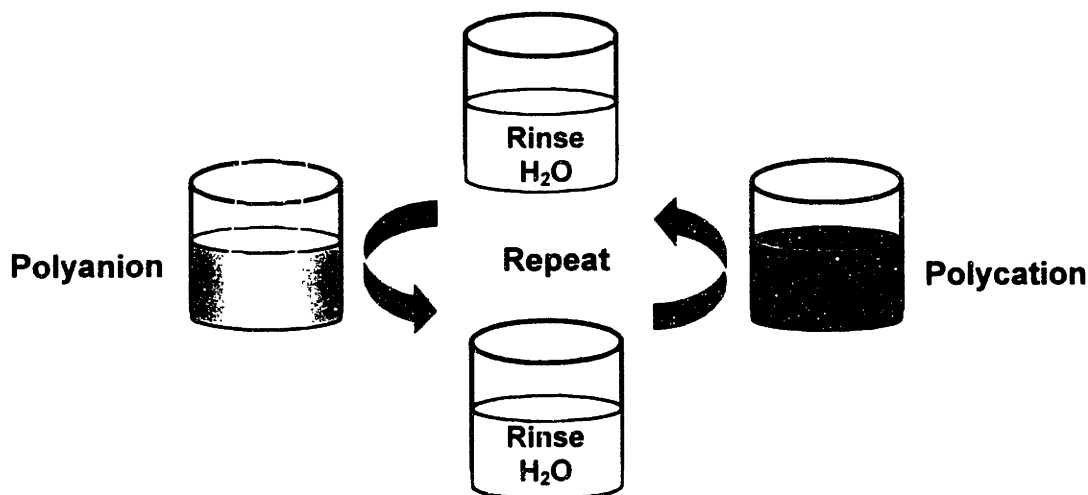


**Figure 1.2:** Schematic of the layer-by-layer process showing the sequential absorption of alternating polyions onto an immersed substrate. The cycle may be repeated as indicated to form films with a desired thickness. Automation of this simple process has also become routine.

Commonly, the layer-by-layer approach uses two polyelectrolytes, but additional polymers or other non-polymeric charged species may be included to form even more

complex structures, as long as there exists an alternation in charge. As mentioned previously, hydrogen bonding can alternatively serve as the assembly mechanism for certain polymeric systems.<sup>50-53</sup> Additionally, more sophisticated, specific molecular interactions involving enzyme-substrate binding, such as avidin-biotin chemistry, may be used to engineer protein-containing multilayer films.<sup>98,99</sup> Therefore, the layer-by-layer approach advantageously enables the researcher to be quite flexible in fabricating useful, ultrathin films with complete control in determining the final multilayer architecture and composition.

### 1.3.3 Controlling Multilayer Properties

Perhaps the primary advantage of the polyelectrolyte multilayer process is being able to control the thin film architecture with nanoscale precision. The layer-by-layer technique's efficacy in creating these high quality thin films with controllable structure and surface properties derives from its facile manipulation of the processing variables. The molecular weight of the polyelectrolytes, the concentration and pH of the dipping solutions, the number of layers assembled, the identity of the outermost layer, and the solution ionic strength (i.e., the presence and concentration of salt), are important parameters that enable the formation of functional thin film polymer materials. Various properties, such as the film's wettability, surface roughness, degree of layer interpenetration, number of free ions, and layer thickness, may easily be modified by appropriately adjusting these processing conditions.

The pH of the polyelectrolyte dipping solutions is of particular importance in manipulating the multilayer's molecular architecture. Strong polyelectrolytes possess a degree of ionization ( $\alpha$ ) relatively independent of their solution pH. However, weak polyelectrolytes are strongly influenced by pH and can change their linear charge density in solution, with respect to their  $pK_a$  values, according to a modified Henderson-Hasselbach equation<sup>100</sup>:

$$pH = pK_a - \log\left(\frac{1-\alpha}{\alpha}\right) + 0.434 \frac{\Delta G_{el}}{RT} \quad (1)$$

where  $\Delta G_{el}$  is the free energy change involved in dissociating functional groups on the molecule, R is the universal gas constant, and T is the temperature. In fact, weak polyelectrolytes can readily alter their  $pK_a$  over several pH units depending on their environment.<sup>58</sup> For example, poly(acrylic acid) (PAA), a common weak polyanion having a

$pK_a$  in aqueous solution of about 4.5–5.5, may substantially change its  $pK_a$  to well below 3 during the assembly of some multilayers.

Simply adjusting the pH of the polyion dipping solutions easily enables one to control the bilayer thickness, composition, and the degree of layer interpenetration. For instance, either depositing strong polyelectrolytes (in the absence of salt) or adsorbing weak polyions at pH conditions where the polyelectrolytes are fully charged, will create a strong force of Coulombic attraction between the absorbing layer and the previous layer; this results in high degrees of opposite ion pairing (“train” conformations) and consequently thin layers (i.e., less than a few angstroms thick) that are molecularly smooth. However, for weak polyelectrolytes adsorbed at pH values when the charge density of one (or both) molecule(s) is low, the electrostatic forces are reduced, so the opposite ions cannot pair up as readily. Therefore, non-fully charged molecules deposit with a high number of loops and tails, forming thicker, so-called loopy, and rougher layers. With the additional of salt, strong polyelectrolytes may also be formed into thicker, loopier layers,<sup>101</sup> since the added salt screens charges on the polyion backbones. Using weak polyions allows pH-induced charge screening effects without adding salt. To summarize the concept of fully- and non-fully- ionized layers, Figure 1.3 portrays schematically the train and loopy conformations that may be exhibited by weak polyelectrolyte multilayers simply via pH adjustments.

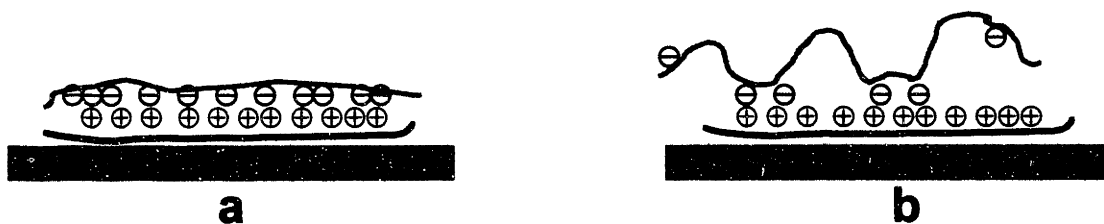


**Figure 1.3:** Schematic of: a) thinner, higher charge density, train conformations due to coordinated ionic pairing; b) thicker, lower charge density, loop-rich conformations due to uncoordinated ionic stitching in layers.

The Rubner group has extensively studied multilayers assembled from weak polyions, particularly the weak polyanion PAA and the weak polycation poly(allylamine hydrochloride) (PAH) and has compiled a 3-D matrix of how the PAA/PAH bilayer thickness varies as a function of the deposition pH of PAA and PAH.<sup>58</sup> Again, the  $pK_a$  of PAA, a polyacid, in aqueous solution is about 4.5–5.5, so it is ~ 50% charged in solution at pH ~ 5, much less

charged at a pH  $\ll$  5, and fully charged a few units above its  $pK_a$ . For PAH, a polybase with a  $pK_a \sim 8.0$ – $10.0$ , it is essentially fully charged only several units below its  $pK_a$  and partially charged near and above its  $pK_a$ . Consequently, variations in pH, even by just one or two pH units, can dramatically alter the PAA/PAH bilayer thickness.<sup>57,58</sup> As stated earlier, pH combinations where the polymers are both fully charged yields ultrathin, smooth layers with a bilayer thickness of just a few angstroms, such as that exhibited by PAA/PAH films deposited each at pH 6.5. However, much of the matrix exhibits substantially thicker bilayers due to the PAA or PAH not being fully charged, which results in loopier and thus more expanded conformations. Several specific PAA/PAH multilayer combinations will be presented in detail in Chapter 2.

## **1.4 Previous Biomedical Applications of Polyelectrolyte Multilayers**

### **1.4.1 Introductory Remarks**

As nanofabricated polyelectrolyte complexes, polyelectrolyte multilayers should offer much promise for biomaterial applications. During 2002, certain types of extended-wear contact lenses that have been coated with hydrophilic multilayers for better patient compliance will be manufactured and soon available to the public. Developed from research from the Rubner group, these lenses will be some of the first commercial products based on polyelectrolyte multilayer technology.

Other biomedical applications are surely to arise out of multilayer processing. Numerous groups have already elicited layer-by-layer schemes to assemble hybrid protein-polymer thin films. Some of the specific biomolecules used to create these nanocomposite protein-synthetic polyion multilayers include hemoglobin, myoglobin, lysozyme, and glucose oxidase, among many others<sup>73,93,102</sup>; if the proteins (e.g., glucose oxidase) are enzymatic in nature, it is believed that the multilayer films may provide a range of enzyme-based biosensor applications. In fact, researchers report that enzymes or antibodies contained within multilayers often exhibit more sensing activity than those immobilized via other methods.<sup>81</sup> Furthermore, the enzymatic or antibody activity increases with an increasing number of the protein layers.<sup>81</sup> Multilayer processing also easily enables the production of several-step enzymatic thin film biosensors in which multiple types of enzymes—which share dependent,

cascading reactions—are located in different parts of the film with nanoscale-controlled spacing.<sup>74,75</sup>

Drug delivery capabilities using polyelectrolyte multilayers also seem viable. Chung and Rubner have used the small molecular weight, cationic dye methylene blue and the anesthetic drug procaine to represent how drugs could be loaded into the layers of PAA/PAH films and subsequently be released.<sup>103</sup> Additionally, since polyelectrolyte multilayers may be assembled onto virtually any type, topology, size, or shape of substrate imaginable, several groups have deposited multilayers directly onto sub-micron or micron-sized colloids. Notably, Caruso's and Möhwald's groups have published extensively on the fabrication of multilayers directly onto colloids or polystyrene latex nanoparticles, typically several hundred nanometers in size.<sup>76,89-97</sup> Furthermore, an appropriate chemistry, such as a specific solvent or pH, may be used to dissolve the colloidal core, leaving behind a hollow capsule with a polyelectrolyte multilayer shell, which would be quite useful for entrapping useful therapeutic agents.<sup>76,89-97</sup> In a logical extension of that work, those groups have coated enzyme crystals,<sup>104</sup> drug crystals,<sup>105</sup> and glutaraldehyde-fixed human blood cells.<sup>90,92,95,106</sup> Moreover, the controlled release of fluorescent molecules<sup>107-109</sup> and ibuprofen drug molecules<sup>105</sup> from polyelectrolyte multilayer core-shell capsules has recently been demonstrated. Overall, these core-shell multilayer systems appear to be quite useful approaches for enzyme bioreactors and biosensors, controlled release and drug delivery systems, and cell encapsulation purposes.

#### **1.4.2 Previous Cell Interaction Studies with Polyelectrolyte Multilayers**

While many groups have investigated incorporating active proteins into multilayer assemblies, there has been little work examining the interactions of living cells with polyelectrolyte multilayers. As discussed in section 1.4.1, some groups have fabricated multilayer films onto chemically fixed cells,<sup>90,92,95,106</sup> and Pommersheim et al. successfully encapsulated living islets with multiple polyionic layers as well.<sup>43-45</sup> Nevertheless, those researchers report only that they were effectively able to encapsulate the cells and have not rigorously addressed the biocompatibility interactions of those cells with the multilayers.

A few other cell-multilayer studies have been reported, although they also do not explore in depth the *in vitro* behavior in terms of cell attachment, spreading, and proliferation. Chluba et al. demonstrated the ability of melanoma cells to respond in a specific biological

manner to signaling hormone molecules immobilized within multilayers.<sup>82</sup> Kotov's group has reported how both muscle and neuronal precursor cells readily attached to multilayers assembled from collagen, a natural biopolymer, and the synthetic polyelectrolyte sulfonated polystyrene (SPS).<sup>84</sup> Serizawa et al. fabricated biopolymer-based multilayers of chitosan and dextran sulfate and demonstrated how the outermost layer could definitively affect the biological activity of the entire film.<sup>67</sup> Depending on whether the chitosan or the dextran sulfate was the surface layer, the films *alternately* showed either pro- or anticoagulant properties, respectively, with human blood.<sup>67</sup> Overall, all of these papers suggest just how powerful the layer-by-layer method is for constructing uniform, nanoscaled-controlled bio-interfacing thin films.

Another study, that of Hubbell's group,<sup>83</sup> has investigated more thoroughly how (fibroblast) cells behave onto various polyelectrolyte multilayers. The researchers examined multilayer films of polylysine and alginate, the classic biopolymer-based system often used in many cell coacervate capsule formulations. Their study reveals that alginate/polylysine films, when deposited onto otherwise cell-adhesive substrates, such as extracellular matrix (ECM), collagen, and ordinary tissue culture polystyrene (TCPS), could actually render those surfaces to be quite cell resistant; an increasing degree of cell adhesion resistance correlated with an increasing number of adsorbed alginate/polylysine layers.<sup>83</sup> In contrast to the report of Serizawa et al.,<sup>67</sup> the alginate/polylysine films did not show any alternating bioactivity; films with either polymer as the outermost layer were cell resistant. It should also be emphasized that the individual alginate and polylysine layers were much thicker and gel-like rather than molecular monolayers as what is typical of most polyelectrolyte multilayers in the literature. Thus, to date, while there have been some basic studies regarding the general interaction of multilayers with living cells, there has been no rigorous, systematic study of how the molecular-level processing and characteristics of multilayer thin films affects the resulting cell behavior.

## **1.5 Thesis Outline and Aims**

This thesis in general addresses several different aspects of polyelectrolyte multilayers—1) their fundamental assembly and structure, 2) their ability to undergo pH-induced morphological changes that may lead to nano- and microporous thin films, and 3)

their basic interactions with proteins and living cells—all of which should provide a solid foundation for determining the rationale and utility of polyelectrolyte multilayers for potential biomaterial applications. Specifically, Chapter 2 describes the experimental protocol and analytical methods used to assemble and characterize the polyelectrolyte multilayers discussed throughout this thesis. In particular, the chapter presents the defining characteristics and properties of several different representative PAA/PAH systems along with some other weak and strong polyion multilayer combinations. Chapter 3 details a unique nano- and microporosity-inducing morphological transformation that may have implications in creating porous biomedically-relevant thin films, along with other useful optical- and/or microelectronic coatings. The interrelated Chapters 4 and 5 concern the protein and cell interactions with polyelectrolyte multilayers, respectively, which are essential components in evaluating and manipulating their biocompatibility. Those chapters importantly demonstrate how multilayer assembly schemes enable the researcher to have complete control over the cell adhesiveness of nanofabricated polymer surfaces; remarkably, one can direct the same multilayer system to be either highly cell-adhesive or completely cell-resistant simply by adjusting the pH conditions of the constituent polyelectrolyte dipping solutions. Therefore, this thesis attempts, for the first time, to relate in vitro cell responses with the molecular-level assembly features of multilayer thin films. Finally, Chapter 6 summarizes the thesis as a whole and provides ideas for future work.

Overall, this thesis attempts to show that processing synthetic polyions and/or other molecules of biological interest via the layer-by-layer approach enables the unprecedented superior nanoscale control over the chemical, physical, and even the biological properties of polymeric thin films. As Chapter 5 will show, the underlying molecular architecture of multilayers can remarkably dictate substantially different cell responses. Thus, since one can easily direct the interaction of multilayer thin films with living cells, it is possible to engineer materials and surfaces with predictable biocompatibility responses. To reiterate, the multilayer processing of polyelectrolytes will soon be utilized in the manufacture of certain contact lens coatings. As will be discussed in this thesis, multilayers may be tailored in many useful ways, such as being micropatterned, made nanoporous or microporous, and/or made cell adhesive or cell resistant. These unique features should allow polyelectrolyte multilayers to be suitable tailorable nanoengineered architectures for many biomaterial applications,

including useful bioinert implant coatings, porous biomedical thin films or membranes, controlled release systems, and substrates for biosensors and patterned cell arrays, among many others.

## 1.6 References

- (1) Park, J. B.; Lakes, R. S. *Biomaterials: An Introduction*, 2nd ed.; Plenum Press: New York, 1992.
- (2) Ratner, B. D.; Hoffman, A. S.; Schoen, F. J.; Lemons, J. E., eds. *Biomaterials Science: An Introduction to Materials in Medicine*; Academic Press: New York, 1996.
- (3) Langer, R. Biomaterials: Status, Challenges, and Perspectives. *AIChE J.* **2000**, *46*, 1286.
- (4) Langer, R. New Methods of Drug Delivery. *Science* **1990**, *249*, 1527.
- (5) Langer, R.; Vacanti, J. P. Tissue Engineering. *Science* **1993**, *260*, 920.
- (6) Griffith, L. G.; Naughton, G. Tissue Engineering—Current Challenges and Expanding Opportunities. *Science* **2002**, *295*, 1009.
- (7) Lanza, R. P.; Langer, R.; Chick, W. L., eds. *Principles of Tissue Engineering*; Academic Press: Georgetown, TX, 1997.
- (8) Hubbell, J. A. Biomaterials in Tissue Engineering. *Bio-technology* **1995**, *13*, 565.
- (9) Hubbell, J. A.; Langer, R. Tissue Engineering. *Chem. Eng. News* **1995**, 42.
- (10) Anderson, J. M. Biological Responses to Materials. *Annu. Rev. Mater. Res.* **2001**, *31*, 81.
- (11) Ratner, B. D. New Ideas in Biomaterials—A Path to Engineered Biomaterials. *J. Biomed. Mater. Res.* **1993**, *27*, 837.
- (12) Griffith, L. G. Polymeric Biomaterials. *Acta. Mater.* **2000**, *48*, 263.
- (13) Herdman, R. C.; Bondurant, S.; Ernster, V. L. Safety of Silicone Breast Implants: The 1999 Institute of Medicine Report. *Trans. Sixth World Biomaterials Congress: Kamuela, HI, 2000*; p 328.
- (14) Hubbell, J. A. Bioactive Biomaterials. *Curr. Opin. Biotech.* **1999**, *10*, 123.
- (15) Hench, L. L.; Polak, J. M. Third-Generation Biomedical Materials. *Science* **2002**, *295*, 1014.
- (16) Irvine, D. J.; Mayes, A. M.; Griffith, L. G. Nanoscale Clustering of RGD Peptides at Surfaces Using Comb Polymers. 1. Synthesis and Characterization of Comb Thin Films. *Biomacromolecules* **2001**, *2*, 85.
- (17) Malmsten, M.; Emoto, K.; Van Alstine, J. M. Effect of Chain Density on Inhibition of Protein Adsorption by Poly(ethylene glycol) Based Coatings. *J. Colloid Interface Sci.* **1998**, *202*, 507.
- (18) Wang, R. L. C.; Kreuzer, H. J.; Grunze, M. Molecular Conformation and Solvation of Oligo(ethylene glycol)-Terminated Self-Assembled Monolayers and Their Resistance to Protein Adsorption. *J. Phys. Chem. B* **1997**, *101*, 9767.
- (19) Quirk, R. A.; Davies, M. C.; Tendler, S. J. B.; Chan, W. C.; Shakesheff, K. M. Controlling Biological Interactions with Poly(lactic acid) by Surface Entrapment Modification. *Langmuir* **2001**, *17*, 2817.



- (20) Tziampazis, E.; Kohn, J.; Moghe, P. V. PEG-Variant Biomaterials as Selectively Adhesive Protein Templates: Model Surfaces for Controlled Cell Adhesion and Migration. *Biomaterials* **2000**, *21*, 511.
- (21) Frazier, R. A.; Matthijs, G.; Davies, M. C.; Roberts, C. J.; Schacht, E.; Tendler, S. J. B. Characterization of Protein-Resistant Dextran Monolayers. *Biomaterials* **2000**, *21*, 957.
- (22) Massia, S. P.; Stark, J.; Letbetter, D. S. Surface-Immobilized Dextran Limits Cell Adhesion and Spreading. *Biomaterials* **2000**, *21*, 2253.
- (23) Luk, Y.-Y.; Kato, M.; Mrksich, M. Self-Assembled Monolayers of Alkanethiols Presenting Mannitol Groups Are Inert to Protein Adsorption and Cell Attachment. *Langmuir* **2000**, *16*, 9604.
- (24) Dai, W. S.; Barbari, T. A. Gel-Impregnated Pore Membranes with Mesh-size Asymmetry for Biohybrid Artificial Organs. *Biomaterials* **2000**, *21*, 1363.
- (25) Oka, J. A.; Weigel, P. H. Binding and Spreading of Hepatocytes on Synthetic Galatose [sic] Culture Surfaces Occur as Distinct and Separable Threshold Responses. *J. Cell Biol.* **1986**, *103*, 1055.
- (26) Tegoulia, V. A.; Rao, W.; Kalambur, A. T.; Rabolt, J. F.; Cooper, S. L. Surface Properties, Fibrinogen Adsorption, and Cellular Interactions of a Novel Phosphorylcholine-Containing Self-Assembled Monolayer on Gold. *Langmuir* **2001**, *17*, 4396.
- (27) López, G. P.; Albers, M. W.; Schreiber, S. L.; Carroll, R.; Peralta, E.; Whitesides, G. M. Convenient Methods for Patterning the Adhesion of Mammalian Cells to Surfaces Using Self-Assembled Monolayers of Alkanethiolates on Gold. *J. Am. Chem. Soc.* **1993**, *115*, 5877.
- (28) Ghosh, P.; Amirpour, M. L.; Lackowski, W. M.; Pishko, M. V.; Crooks, R. M. A Simple Lithographic Approach for Preparing Patterned, Micron-Scale Corrals for Controlling Cell Growth. *Angew. Chem. Int. Ed.* **1999**, *38*, 1592.
- (29) Ostuni, E.; Chapman, R. G.; Holmlin, R. E.; Takayama, S.; Whitesides, G. M. A Survey of Structure-Property Relationships of Surfaces that Resist the Adsorption of Protein. *Langmuir* **2001**, *17*, 5605.
- (30) Ostuni, E.; Chapman, R. G.; Liang, M. N.; Meluleni, G.; Pier, G.; Ingber, D. E.; Whitesides, G. M. Self-Assembled Monolayers That Resist the Adsorption of Proteins and the Adhesion of Bacterial and Mammalian Cells. *Langmuir* **2001**, *17*, 6336.
- (31) Chapman, R. G.; Ostuni, E.; Takayama, S.; Holmlin, R. E.; Yan, L.; Whitesides, G. M. Surveying for Surfaces that Resist the Adsorption of Proteins. *J. Am. Chem. Soc.* **2000**, *122*, 8303.
- (32) Lee, S.-D.; Hsiue, G.-H.; Chang, P. C.-T.; Kao, C.-Y. Plasma-Induced Grafted Polymerization of Acrylic Acid and Subsequent Grafting of Collagen onto Polymer Film as Biomaterials. *Biomaterials* **1996**, *17*, 1599.
- (33) Chapman, R. G.; Ostuni, E.; Liang, M. N.; Meluleni, G.; Kim, E.; Yan, L.; Pier, G.; Warren, H. S.; Whitesides, G. M. Polymeric Thin Films That Resist the Adsorption of Proteins and the Adhesion of Bacteria. *Langmuir* **2001**, *17*, 1225.
- (34) Michaels, A. S. Polyelectrolyte Complexes. *Ind. Eng. Chem.* **1965**, *57*, 32.
- (35) Arshady, R. Microspheres and Microcapsules, a Survey of Manufacturing Techniques. Part II: Coacervation. *Polym. Eng. Sci.* **1990**, *30*, 905.
- (36) Hunkeler, D. Polymers for Bioartificial Organs. *Trends Polym. Sci.* **1997**, *5*, 286.

- (37) Kötzt, J. Polyelectrolyte Complexes (Overview), in *Polymeric Materials Encyclopedia*; CRC Press, Inc.: Boca Raton, FL, 1996; p 5762.
- (38) Scranton, A. B.; Rangarajan, B.; Klier, J. Biomedical Applications of Polyelectrolytes. *Adv. Polym. Sci.* **1995**, *122*, 1.
- (39) Chang, T. M. S. *Artificial Cells*; C. C. Thomas: Springfield, IL, 1972.
- (40) Lim, F.; Sun, A. M. Microencapsulated Islets as Bioartificial Endocrine Pancreas. *Science* **1980**, *210*, 908.
- (41) Li, R. H. Materials for Immunoisolated Cell Transplantation. *Adv. Drug Del. Rev.* **1998**, *33*, 87.
- (42) Thu, B.; Bruheim, P.; Espevik, T.; Smidsrød, O.; Soon-Shiong, P.; Skjåk-Bræk, G. Alginate Polycation Microcapsules. I. Interaction between Alginate and Polycation. *Biomaterials* **1996**, *17*, 1031.
- (43) Pommersheim, R.; Schrezenmeir, J.; Vogt, W. Immobilization of Enzymes by Multilayer Microcapsules. *Macromol. Chem. Phys.* **1994**, *195*, 1557.
- (44) Schneider, S.; Feilen, P. J.; Slotty, V.; Kampfner, D.; Preuss, S.; Berger, S.; Beyer, J.; Pommersheim, R. Multilayer Capsules: A Promising Microencapsulation System for Transplantation of Pancreatic Islets. *Biomaterials* **2001**, *22*, 1961.
- (45) Rilling, P.; Walter, T.; Pommersheim, R.; Vogt, W. Encapsulation of Cytochrome C by Multilayer Microcapsules. A Model for Improved Enzyme Immobilization. *J. Membrane Sci.* **1997**, *129*, 283.
- (46) Prokop, A.; Hunkeler, D.; Powers, A. C.; Whitesell, R. R.; Wang, T. G. Water Soluble Polymers for Immunoisolation II: Evaluation of Multicomponent Microencapsulation Systems. *Adv. Polym. Sci.* **1998**, *136*, 53.
- (47) Decher, G.; Hong, J. D.; Schmitt, J. Buildup of Ultrathin Multilayer Films by a Self-Assembly Process: III. Consecutively Alternating Adsorption of Anionic and Cationic Polyelectrolytes on Charged Surfaces. *Thin Solid Films* **1992**, *210/211*, 831.
- (48) Hong, J. D.; Lowack, K.; Schmitt, J.; Decher, G. Layer-by-Layer Deposited Multilayer Assemblies of Polyelectrolytes and Proteins: From Ultrathin Films to Protein Arrays. *Progr. Colloid Polym. Sci.* **1993**, *93*, 98.
- (49) Lvov, Y.; Decher, G.; Möhwald, H. Assembly, Structural Characterization, and Thermal Behavior of Layer-by-Layer Deposited Ultrathin Films of Poly(vinylsulfate) and Poly(allylamine). *Langmuir* **1993**, *9*, 481.
- (50) Stockton, W. B.; Rubner, M. F. Molecular-Level Processing of Conjugated Polymers. 4. Layer-by-Layer Manipulation of Polyaniline via Hydrogen-Bonding Interactions. *Macromolecules* **1997**, *30*, 2717.
- (51) Wang, L.; Fu, Y.; Wang, Z.; Fan, Y.; Zhang, X. Investigation into an Alternating Multilayer Film of Poly(4-Vinylpyridine) and Poly(acrylic acid) Based on Hydrogen Bonding. *Langmuir* **1999**, *15*, 1360.
- (52) Yang, S. Y.; Rubner, M. F. Micropatterning of Polymer Thin Films with pH-Sensitive and Cross-linkable Hydrogen-Bonded Polyelectrolyte Multilayers. *J. Am. Chem. Soc.* **2002**, *124*, 2100.
- (53) Sukhishvili, S. A.; Granick, S. Layered, Erasable, Ultrathin Polymer Films. *J. Am. Chem. Soc.* **2000**, *122*, 9550.
- (54) Lee, S.-S.; Hong, J.-D.; Kim, C. H.; Kim, K.; Koo, J. P.; Lee, K.-B. Layer-by-Layer Deposited Multilayer Assemblies of Ionene-Type Polyelectrolytes Based on the Spin-Coating Method. *Macromolecules* **2001**, *34*, 5358.

- (55) Chiarelli, P. A.; Johal, M. S.; Holmes, D. J.; Casson, J. L.; Robinson, J. M.; Wang, H.-L. Polyelectrolyte Spin-Assembly. *Langmuir* **2002**, *18*, 168.
- (56) Schlenoff, J. B.; Dubas, S. T.; Farhat, T. Sprayed Polyelectrolyte Multilayers. *Langmuir* **2000**, *16*, 9968.
- (57) Yoo, D.; Shiratori, S. S.; Rubner, M. F. Controlling Bilayer Composition and Surface Wettability of Sequentially Adsorbed Multilayers of Weak Polyelectrolytes. *Macromolecules* **1998**, *31*, 4309.
- (58) Shiratori, S. S.; Rubner, M. F. pH-Dependent Thickness Behavior of Sequentially Adsorbed Layers of Weak Polyelectrolytes. *Macromolecules* **2000**, *33*, 4213.
- (59) Cheung, J. H.; Stockton, W. B.; Rubner, M. F. Molecular-Level Processing of Conjugated Polymers. 3. Layer-by-Layer Manipulation of Polyaniline via Electrostatic Interactions. *Macromolecules* **1997**, *30*, 2712.
- (60) Kellogg, G. J.; Mayes, A. M.; Stockton, W. B.; Ferreira, M.; Rubner, M. F.; Satija, S. K. Neutron Reflectivity Investigations of Self-Assembled Conjugated Polyion Multilayers. *Langmuir* **1996**, *12*, 5109.
- (61) Tarabia, M.; Hong, H.; Davidov, D.; Kirstein, S.; Steitz, R.; Neumann, R.; Avny, Y. Neutron and X-ray Reflectivity Studies of Self-Assembled Heterostructures Based on Conjugated Polymers. *J. Appl. Phys.* **1998**, *83*, 725.
- (62) Clark, S. L.; Handy, E. S.; Rubner, M. F.; Hammond, P. T. Creating Microstructures of Luminescent Organic Thin Films Using Layer-by-Layer Assembly. *Adv. Mater.* **1999**, *11*, 1031.
- (63) Cooper, T. M.; Campbell, A. L.; Crane, R. L. Formation of Polypeptide-Dye Multilayers by an Electrostatic Self-Assembly Technique. *Langmuir* **1995**, *11*, 2713.
- (64) Ariga, K.; Lvov, Y.; Kunitake, T. Assembling Alternate Dye-Polyion Molecular Films by Electrostatic Layer-by-Layer Adsorption. *J. Am. Chem. Soc.* **1997**, *119*, 2224.
- (65) Lvov, Y.; Ariga, K.; Ichinose, I.; Kunitake, T. Formation of Ultrathin Multilayer and Hydrated Gel from Montmorillonite and Linear Polycations. *Langmuir* **1996**, *12*, 3038.
- (66) Kotov, N. A.; Haraszti, T.; Turi, L.; Zavala, G.; Geer, R. E.; Dékány, I.; Fendler, J. H. Mechanism of and Defect Formation in the Self-Assembly of Polymeric Polycation-Montmorillonite Ultrathin Films. *J. Am. Chem. Soc.* **1997**, *119*, 6821.
- (67) Serizawa, T.; Yamaguchi, M.; Matsuyama, T.; Akashi, M. Alternating Bioactivity of Polymeric Layer-by-Layer Assemblies: Anti- vs Procoagulation of Human Blood on Chitosan and Dextran Sulfate Layers. *Biomacromolecules* **2000**, *1*, 306.
- (68) Lvov, Y.; Decher, G.; Sukhorukov, G. Assembly of Thin Films by Means of Successive Deposition of Alternate Layers of DNA and Poly(allylamine). *Macromolecules* **1993**, *26*, 5396.
- (69) Decher, G.; Lehr, B.; Lowack, K.; Lvov, Y.; Schmitt, J. New Nanocomposite Films for Biosensors: Layer-by-Layer Adsorbed Films of Polyelectrolytes, Proteins or DNA. *Biosens. Bioelect.* **1994**, *9*, 677.
- (70) Sukhorukov, G. B.; Möhwald, H.; Decher, G.; Lvov, Y. M. Assembly of Polyelectrolyte Multilayer Films by Consecutively Alternating Adsorption of Polynucleotides and Polycations. *Thin Solid Films* **1996**, *284/285*, 220.
- (71) Pei, R.; Cui, X.; Yang, X.; Wang, E. Assembly of Alternating Polycation and DNA Multilayer Films by Electrostatic Layer-by-Layer Adsorption. *Biomacromolecules* **2001**, *2*, 463.

- (72) Lvov, Y.; Ariga, K.; Kunitake, T. Layer-by-Layer Assembly of Alternate Protein/Polyion Ultrathin Films. *Chem. Lett.* **1994**, 2323.
- (73) Lvov, Y.; Ariga, K.; Ichinose, I.; Kunitake, T. Assembly of Multicomponent Protein Films by Means of Electrostatic Layer-by-Layer Adsorption. *J. Am. Chem. Soc.* **1995**, *117*, 6117.
- (74) Onda, M.; Lvov, Y.; Ariga, K.; Kunitake, T. Sequential Reaction and Product Separation on Molecular Films of Glucoamylose and Glucose Oxidase Assembled on an Ultrafilter. *J. Ferment. Bioeng.* **1996**, *82*, 502.
- (75) Onda, M.; Lvov, Y.; Ariga, K.; Kunitake, T. Sequential Actions of Glucose Oxidase and Peroxidase in Molecular Films Assembled by Layer-by-Layer Alternate Adsorption. *Biotech. Bioeng.* **1996**, *51*, 163.
- (76) Caruso, F.; Möhwald, H. Protein Multilayer Formation on Colloids Through a Stepwise Self-Assembly Technique. *J. Am. Chem. Soc.* **1999**, *121*, 6039.
- (77) Lvov, Y.; Haas, H.; Decher, G.; Möhwald, H.; Mikhailov, A.; Mtchedlishvily, B.; Morgunova, E.; Vainshtein, B. Successive Deposition of Alternate Layers of Polyelectrolytes and a Charged Virus. *Langmuir* **1994**, *10*, 4232.
- (78) Wu, A.; Yoo, D.; Lee, J.-K.; Rubner, M. F. Solid-State Light-Emitting Devices Based on the Tris-Chelated Ruthenium(II) Complex: 3. High Efficiency Devices via a Layer-by-Layer Molecular-Level Blending Approach. *J. Am. Chem. Soc.* **1999**, *121*, 4883.
- (79) Yamada, M.; Shiratori, S. S. Smoke Sensor Using Mass Controlled Layer-by-Layer Self-Assembly of Polyelectrolytes Films. *Sens. Actuators B* **2000**, *64*, 124.
- (80) Sun, Y.; Zhang, X.; Sun, C.; Wang B.; Shen, J. Fabrication of Ultrathin Film Containing Bienenzyme of Glucose Oxidase and Glucoamylase Based on Electrostatic Interaction and Its Potential Application as a Maltose Sensor. *Macromol. Chem. Phys.* **1996**, *197*, 147.
- (81) Caruso, F.; Niikura, K.; Furlong, D. N.; Okahata, Y. 2. Assembly of Alternating Polyelectrolyte and Protein Multilayer Films for Immunosensing. *Langmuir* **1997**, *13*, 3427.
- (82) Chluba, J.; Voegel, J.-C.; Decher, G.; Erbacher, P.; Schaaf, P.; Ogier, J. Peptide Hormone Covalently Bound to Polyelectrolytes and Embedded into Multilayer Architectures Conserving Full Biological Activity. *Biomacromolecules* **2001**, *2*, 800.
- (83) Elbert, D. L.; Herbert, C. B.; Hubbell, J. A. Thin Polymer Layers Formed by Polyelectrolyte Multilayer Techniques on Biological Surfaces. *Langmuir* **1999**, *15*, 5355.
- (84) Grant, G. G. S.; Koktysh, D. S.; Yun, B.; Matts, R. L.; Kotov, N. A. Layer-By-Layer Assembly of Collagen Thin Films: Controlled Thickness and Biocompatibility. *Biomed. Microdevices* **2001**, *3*, 301.
- (85) Mendelsohn, J. D.; Barrett, C. J.; Chan, V. V.; Pal, A. J.; Mayes, A. M.; Rubner, M. F. Fabrication of Microporous Thin Films from Polyelectrolyte Multilayers. *Langmuir* **2000**, *16*, 5017.
- (86) Decher, G. Fuzzy Nanoassemblies: Toward Layered Polymeric Multicomposites. *Science* **1997**, *277*, 1232.
- (87) Hammond, P. T. Recent Explorations in Electrostatic Multilayer Thin Film Assembly. *Curr. Opin. Coll. Interface Sci.* **2000**, *4*, 430.

- (88) Bertrand, P.; Jonas, A.; Laschewsky, A.; Legras, R. Ultrathin Polymer Coatings by Complexation of Polyelectrolytes at Interfaces: Suitable Materials, Structure and Properties. *Macromol. Rapid Commun.* **2000**, *21*, 319.
- (89) Sukhorukov, G. B.; Donath, E.; Lichtenfeld, H.; Knippel, E.; Knippel, M.; Budde, A.; Möhwald, H. Layer-by-Layer Self-Assembly of Polyelectrolytes on Colloidal Particles. *Colloids Surf. A* **1998**, *137*, 253.
- (90) Moya, S.; Sukhorukov, G. B.; Auch, M.; Donath, E.; Möhwald, H. Microencapsulation of Organic Solvents in Polyelectrolyte Multilayer Micrometer-Sized Shells. *J. Colloid Interface Sci.* **1999**, *216*, 297.
- (91) Sukhorukov, G. B.; Brumen, M.; Donath, E.; Möhwald, H. Hollow Polyelectrolyte Shells: Exclusion of Polymers and Donnan Equilibrium. *J. Phys. Chem. B* **1999**, *103*, 6434.
- (92) Voigt, A.; Lichtenfeld, H.; Sukhorukov, G. B.; Zastrow, H.; Donath, E.; Bäuml, H.; Möhwald, H. Membrane Filtration for Microencapsulation and Microcapsules Fabrication by Layer-by-Layer Polyelectrolyte Adsorption. *Ind. Eng. Chem. Res.* **1999**, *38*, 4037.
- (93) Caruso, F.; Schüler, C. Enzyme Multilayers on Colloid Particles: Assembly, Stability, and Enzymatic Activity. *Langmuir* **2000**, *16*, 9595.
- (94) Caruso, F.; Fiedler, H.; Haage, K. Assembly of  $\beta$ -glucosidase Multilayers on Spherical Colloidal Particles and Their Use as Active Catalysts. *Colloids Surf. A* **2000**, *169*, 287.
- (95) Leporatti, S.; Voigt, A.; Mitlöhner, R.; Sukhorukov, G.; Donath, E.; Möhwald, H. Scanning Force Microscopy Investigation of Polyelectrolyte Nano- and Microcapsule Wall Texture. *Langmuir* **2000**, *16*, 4059.
- (96) Möhwald, H. From Langmuir Monolayers to Nanocapsules. *Colloids Surf. A* **2000**, *171*, 25.
- (97) Sukhorukov, G. B.; Donath, E.; Moya, S.; Susha, A. S.; Voigt, A.; Hartmann, J.; Möhwald, H. Microencapsulation by Means of Step-wise Adsorption of Polyelectrolytes. *J. Microencapsulation* **2000**, *17*, 177.
- (98) Anzai, J.; Nishimura, M. Layer-by-Layer Deposition of Avidin and Polymers on a Solid Surface to Prepare Thin Films: Significant Effects of Molecular Geometry of the Polymers on the Deposition Behaviour. *J. Chem. Soc. Perkin Trans. 2* **1997**, 1887.
- (99) Anicet, N.; Bourdillon, C.; Moiroux, J.; Savéant, J.-M. Step-by-Step Avidin-Biotin Construction of Bienzyme Electrodes. Kinetic Analysis of the Coupling between the Catalytic Activities of Immobilized Monomolecular Layers of Glucose Oxidase and Hexokinase. *Langmuir* **1999**, *15*, 6527.
- (100) Dautzenberg, H.; Jaeger, W.; Kötz, J.; Philipp, B.; Seidel, C.; Stscherbina, D. *Polyelectrolytes: Formation, Characterization, and Application*; Hanser Publishers: New York, 1994.
- (101) Clark, S. L.; Montague, M. F.; Hammond, P. T. Ionic Effects of Sodium Chloride on the Templated Deposition of Polyelectrolytes Using Layer-by-Layer Ionic Assembly. *Macromolecules* **1997**, *30*, 7237.
- (102) Lvov, Y.; Munge, B.; Giraldo, O.; Ichinose, I.; Suib, S. L.; Rusling, J. F. Films of Manganese Oxide Nanoparticles with Polycations or Myoglobin from Alternate-Layer Adsorption. *Langmuir* **2000**, *16*, 8850.

- (103) Chung, A. J.; Rubner, M. F. Methods of Loading and Releasing Low Molecular Weight Cationic Molecules in Weak Polyelectrolyte Multilayer Films. *Langmuir* **2002**, *18*, 1176.
- (104) Caruso, F.; Trau, D.; Möhwald, H.; Renneberg, R. Enzyme Encapsulation in Layer-by-Layer Engineered Polymer Multilayer Capsules. *Langmuir* **2000**, *16*, 1485.
- (105) Qui, X.; Leporatti, S.; Donath, E.; Möhwald, H. Studies on the Drug Release Properties of Polysaccharide Multilayers Encapsulated Ibuprofen Microparticles. *Langmuir* **2001**, *17*, 5375.
- (106) Moya, S.; Dähne, L.; Voigt, A.; Leporatti, S.; Donath, E.; Möhwald, H. Polyelectrolyte Multilayer Capsules Templated on Biological Cells: Core Oxidation Influences Layer Chemistry. *Colloids Surf. A* **2001**, *183-185*, 27.
- (107) Shi, X.; Caruso, F. Release Behavior of Thin-Walled Microcapsules Composed of Polyelectrolyte Multilayers. *Langmuir* **2001**, *17*, 2036.
- (108) Antipov, A. A.; Sukhorukov, G. B.; Donath, E.; Möhwald, H. Sustained Release Properties of Polyelectrolyte Multilayer Capsules. *J. Phys. Chem. B* **2001**, *105*, 2281.
- (109) Sukhorukov, G. B.; Antipov, A. A.; Voigt, A.; Donath, E.; Möhwald, H. pH-Controlled Macromolecule Encapsulation in and Release from Polyelectrolyte Multilayer Nanocapsules. *Macromol. Rapid Comm.* **2001**, *22*, 44.

## **Chapter 2: Fundamental Assembly Characteristics of Polyelectrolyte Multilayers**

### **2.1 Introductory Remarks**

As introduced in section 1.3, the layer-by-layer approach is a versatile method by which to prepare thin film heterostructures with molecular-level control of film thickness, composition, conformation, roughness, and wettability. A rich library of various multilayer features has been reported simply by blending poly(acrylic acid) (PAA) and poly(allylamine hydrochloride) (PAH) at different deposition pH conditions,<sup>1</sup> as presented previously in section 1.3.3. Even one pH unit could result in dramatically different chain conformations, layer thicknesses (ranging from only a few angstroms to many tens of angstroms), and compositions (i.e., the relative ratio of PAH to PAA).

This chapter provides the experimental protocols used to fabricate and characterize the polyelectrolyte multilayer thin films discussed throughout in this thesis. The assembly process and analytical tools detailed herein may similarly be applied to any other multilayer combination that one may wish to study. Finally, several PAA/PAH multilayer systems representative of different thickness and conformation regimes are described, followed by the

introduction of some other weak and strong polyelectrolyte multilayer combinations also discussed in this thesis. The structures of the repeat units of the polymers mentioned in this thesis are depicted in Figure 2.1.

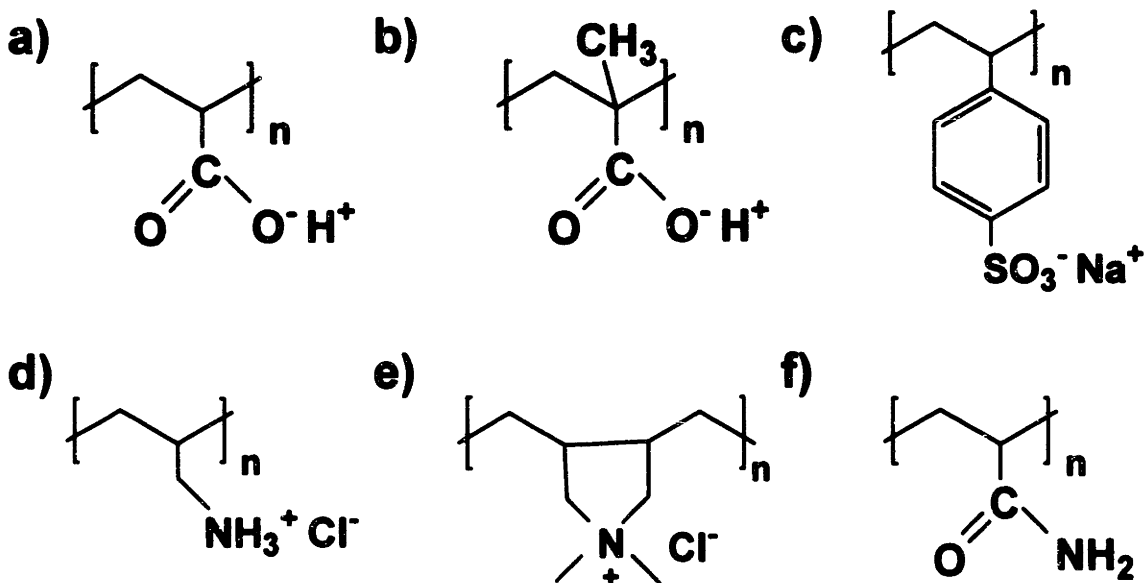


**Figure 2.1:** Chemical structures of some of the common polymers for multilayer thin film assembly. Some negatively-charged polyanions include: a) poly(acrylic acid) (PAA), b) poly(methacrylic acid) (PMA), and c) poly(styrene sulfonate) (SPS); some positively-charged polycations include: d) poly(allylamine hydrochloride) (PAH) and e) poly(diallyldimethylammonium chloride) (PDAC); a neutral polymer is f) polyacrylamide (PAAm).

## 2.2. Materials and Methods

### 2.2.1 General Multilayer Deposition and Assembly

**Reagents.** Poly(acrylic acid) (PAA) ( $M_w \sim 90\,000$ ), poly(methacrylic acid) (PMA) ( $M_w \sim 90\,000$ ), and polyacrylamide (PAAm) were obtained from Polysciences as 25% aqueous solutions. Poly(allylamine hydrochloride) (PAH) ( $M_w \sim 70\,000$ ), poly(styrene sulfonate), sodium salt, (SPS), ( $M_w \sim 70\,000$ ), poly(diallyldimethylammonium chloride) (PDAC) ( $M_w \sim 100\,000 - 200\,000$ ) as a 20 wt. % solution, the methylene blue dye, and the rose bengal dye were purchased from Aldrich Chemical. The polymers were used without any further purification, and their deposition baths were prepared as  $10^{-2}$  M solutions (based on the repeat unit molecular weight) using ultrapure  $18\text{ M}\Omega\text{-cm}$  Millipore water. The polymer solutions were pH-adjusted with either HCl or NaOH. Prior to multilayer assembly, all



polymer solutions were filtered through a 0.45  $\mu\text{m}$  cellulose acetate membrane. The methylene blue and rose bengal dyes were prepared as  $10^{-3}$  M solutions in Millipore water.

**Multilayer thin film deposition.** Polyelectrolyte multilayer thin films were deposited directly onto any number of substrates, including polished <100> silicon wafers (Wafernet), glass slides (VWR Scientific), ZnSe crystals (SpectraTech), standard or Permax tissue culture polystyrene (TCPS) slides (Nalgene), and TCPS petri dishes and multiwell plates (Falcon) via an automatic dipping procedure using an HMS programmable slide stainer from Zeiss, Inc. All multilayer fabrication was done at room temperature. The silicon wafers and glass slides were normally first rinsed well with ultrapure water and then plasma etched in a Harrick plasma cleaner for 2 minutes and blown dry with compressed, filtered air. The TCPS slides were simply rinsed and blown dry, while the TCPS petri dishes and multiwell plates were used as received.

All substrates for basic multilayer assemblies were first immersed in the polycationic solution (e.g., PAH or PDAC) for 15 minutes followed by rinsing in 3 successive baths of neutral water ( $\text{pH} \approx 5.5\text{--}6.5$ ) with light agitation, for 2, 1, and 1 minute(s), respectively. The substrates were then immersed into the oppositely charged polyanionic solution (e.g., PAA, PMA, or SPS) for 15 minutes and subjected to the same rinsing procedure. This process was repeated until the desired number of layers was assembled, after which the coated substrates were removed from the automatic dipping machines, blown dry with compressed, filtered air, and stored at ambient conditions until being characterized. Normally, a minimum of 10–15 layers was deposited when fabricating films in order to reduce any substrate effects; ultrathin systems (e.g., PAA/PAH 6.5/6.5, as explained in section 2.3.1) usually were prepared to be at least 40 layers in thickness to ensure a uniform film had been assembled before any measurements were performed. Generally, the TCPS dishes and multiwell plates were additionally dried at  $\sim 90^\circ\text{C}$  for  $\sim 10$  min.

### **2.2.2 Thickness Determination**

The thickness and refractive index of multilayer films deposited onto silicon were measured using a Gaertner ellipsometer, operating at 633 nm. Typically, a minimum of 5 measurements was obtained per sample. Profilometry was used on glass-coated substrates and also on some silicon samples with an applied force of 5 mg.

### **2.2.3 Wettability Measurements**

To determine the film wettability, contact angles with pure water were acquired using the standard sessile drop technique with an Advanced Surface Technology (AST) device and camera. Samples were first blown dry with N<sub>2</sub> gas, and drops ~ 1 μL in size were applied to the surface. Both advancing and receding contact angles were recorded on a minimum of 4 locations per sample. Wettable angles were recorded as < 10°.

### **2.2.4 Methylene Blue and Rose Bengal Dye Staining**

Samples were immersed in either the methylene blue solution (adjusted to pH 7.0) or the rose bengal dye solution (adjusted to pH 5.0) for 15 min followed by 3 successive neutral water rinses with agitation for 2, 1, and 1 minute(s), respectively. UV-visible absorbance spectra were then measured as described in section 2.2.5.

### **2.2.5 Chemical Analysis: UV-visible and FT-IR Spectroscopy**

UV-visible absorbance spectra were obtained at  $\lambda_{\max}$  using an Oriel Intraspec II spectrometer with a grating spacing of 150 nm. Absorbance measurements denote absorption from both sides of the film. A Nicolet Fourier transform infrared (FT-IR) spectrophotometer was used to obtain absorbance spectra after depositing the polyelectrolyte multilayers onto ZnSe substrates. Absorbance values for the COO<sup>-</sup> and COOH peaks of the PAA were estimated by examining the absorbance signal bands at ~1550 cm<sup>-1</sup> and ~1710 cm<sup>-1</sup>, respectively, and assuming approximately equal extinction coefficients. Each peak height was also assumed to be the maximum of a Gaussian absorbance curve for its respective chemical species.

### **2.2.6 Surface Morphology and Roughness: Atomic Force Microscopy (AFM)**

To determine the surface morphology and roughness of the multilayer samples, an atomic force microscope (AFM, Digital Instruments Dimension 3000 Scanning Probe Microscope, Santa Barbara, CA) was used in tapping mode with Si cantilevers. Spring constants for the cantilevers were ~ 40 N/m. Typically, square images of 1 x 1, 5 x 5, or 10 x 10 μm<sup>2</sup> images were obtained for samples using a scanning rate of ~1–1.5 Hz, a setpoint ~1–1.5 V, and a resolution of 512 samples/line. Generally, a “flatten” routine was performed

on most raw images before any additional data processing, such as RMS (root mean square) roughness analysis.

## 2.3 Representative PAA/PAH Polyelectrolyte Multilayer Systems

### 2.3.1 The 6.5/6.5 PAA/PAH System

The simplest PAH/PAA multilayer case to consider is when both weak polyelectrolytes are deposited from solution at pH conditions where they are essentially fully charged. A typical thin film representative of this fully charged situation is the 6.5/6.5 PAA/PAH system. PAH, being below its  $pK_a \sim 8-10$ , and PAA, being above its  $pK_a$  of  $\sim 5$ , are both nearly completely ionized at 6.5/6.5 PAA/PAH conditions into carboxylate ions ( $COO^-$ ) and charged amines ( $NH_3^+$ ), respectively. As previously shown in Figure 1.3(a), such fully charged multilayers adopt numerous stoichiometric, cooperatively paired (i.e., one cation to one anion) “train” conformations. Consequently, these 6.5/6.5 PAA/PAH multilayers are ultrathin and ultra-smooth yet still highly interpenetrated. A typical layer thickness is well under  $5 \text{ \AA}$ , and even films of around 40 layers are  $< 10 \text{ \AA}$  in RMS roughness.

Chemical analysis, via both FT-IR and UV-visible spectroscopy, has helped to elucidate much about the internal and surface bonding character of PAA/PAH thin films. For instance, the absorbance of the cationic dye methylene blue, which binds to unbound carboxylic acids ( $COOH$ ), may easily be measured with UV-visible spectroscopy to identify the fraction of free acids on multilayer film surfaces. Since very little methylene blue binds to the surfaces of 6.5/6.5 PAA/PAH multilayers (regardless of whether PAA or PAH is the outermost layer),<sup>1</sup> nearly all of the carboxylic acids are ionized and paired with the charged amines of PAH. In fact, the 6.5/6.5 PAA/PAH film surface is approximately an equal blending of PAA and PAH. Wettability measurements further confirm this surface mixing; the advancing contact angle,  $\theta_{adv}$ , on a 6.5/6.5 PAA/PAH multilayer with either PAA or PAH as the outermost layer is  $\sim 25^\circ$  and  $\sim 35^\circ$ , respectively,<sup>2</sup> which is between the value of a pure PAA film ( $\theta_{adv} < 10^\circ$ ) and that of a pure PAH film ( $\theta_{adv} \sim 50-55^\circ$ ).<sup>1,3</sup> The internal structure similarly consists of nearly fully charged PAA and PAH chains existing in a densely ionically stitched architecture. Specifically,  $COO^- \cdots NH_3^+$  ionic bonds abound in the film and act to physically crosslink the multilayer.

### 2.3.2 The 3.5/7.5 PAA/PAH System

A less straightforward multilayer case to consider is the 3.5/7.5 PAA/PAH combination. Here, PAH is ~ 90% charged, but the PAA is only partially negatively charged in a solution of pH 3.5. Therefore, the deposition of the weakly ionized PAA onto the preceding highly ionized PAH layer reflects an assembly depicted in Figure 1.3(b), whereby the PAA absorbs in a loopy conformation with many free acid groups on the film surface. However, exposure to the next PAH layer at pH 7.5 (a pH condition at which the PAA would normally be fully charged in solution) then re-ionizes those free acids, and the PAH readily adsorbs to the underlying thick and loopy PAA layer. What results is a thick, loop-rich film that actually possesses a highly ionically paired internal structure, much like the substantially thinner 6.5/6.5 case, yet with a surface rich in uncharged, free acids if PAA is the outermost layer. Correspondingly, if PAH were the surface layer, many charged amines (ionically paired to the carboxylic acids of the preceding PAA layer) and a small number of free, non-ionized amines would be on the surface. In fact, FT-IR reveals that about 80–90% of the carboxylic acids of the PAA chains are ionized within assembled 3.5/7.5 films,<sup>4</sup> a substantially higher percentage than that of a pH 3.5 PAA solution.

The loop-rich nature of 3.5/7.5 PAA/PAH multilayers leads to unusually thick layers of ~ 50–80 Å and RMS roughness values approaching as high as ~ 50 Å or more. Unlike the 6.5/6.5 system with its blended surface composition, 3.5/7.5 PAA/PAH films exhibit discrete surfaces that retain the identity of the last layer deposited. Methylene blue absorbance is high (~ 0.17) when PAA is the outermost layer, since the surface is predominately composed of unpaired carboxylic acids. However, very little absorbance (~ 0.04) is seen when PAH is the last layer deposited. Contact angle data also shows some alternation with respect to the identity of the last layer deposited for the 3.5/7.5 PAA/PAH system. Specifically, a 3.5/7.5 multilayer with PAA as the outermost layer is wettable (advancing contact angle,  $\theta_{adv} < 10^\circ$ ), which is about the same value of a pure PAA film, compared to a value of  $\theta_{adv} \sim 53^\circ$  when PAH is the surface layer, which is approximately the value of pure PAH.<sup>1,3</sup>

Overall, 3.5/7.5 PAA/PAH multilayers exhibit an unusual assembly process with PAA deposited at a low degree of ionization, only to be subsequently “charged up” before the addition of the next PAH layer. Although electrostatic  $\text{COO}^- \cdots \text{NH}_3^+$  crosslinks abound in the multilayer, most probably these bonds exist between many different polymer chains, not in a

more preferable, well-coordinated 1:1 fashion as in the case of 6.5/6.5 multilayers. Furthermore, 3.5/7.5 multilayers are an optimal system for undergoing a large-scale phase separation, simply induced by brief exposure to acidic water, which permits the creation of nano- and/or microporous thin films.<sup>4</sup> This unique pH-induced porosity phenomenon will be treated in depth in Chapter 3.

### **2.3.3 The 2.0/2.0 PAA/PAH System**

Another interesting situation is when both weak polyelectrolytes in PAA/PAH multilayers are deposited at low pH, typified by the 2.0/2.0 PAA/PAH multilayer combination. Here, PAA is deposited at a low pH and thus is only slightly ionized, creating a loopy conformation with many free acids, just like its behavior in the 3.5/7.5 PAA/PAH case. However, the PAA then experiences PAH adsorbing also at a low pH, and therefore, unlike the 3.5/7.5 PAA/PAH system, the PAA does not re-ionize upon exposure to the next PAH bath. Hence, such 2.0/2.0 multilayers are abundant with uncharged carboxylic acids and do not exhibit the high degree of intermolecular ionic pairing as in 6.5/6.5 and 3.5/7.5 PAA/PAH multilayer films.

2.0/2.0 PAA/PAH films have a loop-rich conformation with layers  $\sim 25$  Å thick and RMS roughness values of  $\sim 50$  Å for a typical 20-layer film. This thickness and loopiness results from the fact that less than about 40% of the carboxylic acid groups of PAA exist in an ionized form, as determined via FT-IR measurements. Methylene blue absorbance is quite high ( $\sim 1.29$  or  $\sim 1.18$ ) when either PAA or PAH, respectively, is the outermost layer, further suggesting a surface rich in free carboxylic acids. Contact angles similarly show that the 2.0/2.0 surface is dominated by PAA segments when PAA is the outermost layer ( $\theta_{adv} < 10^\circ$ ). Even when PAH is the outermost layer, the surface is significantly more hydrophilic ( $\theta_{adv} \sim 28^\circ$ ) than a pure PAH-rich surface and thus is mixed with PAA chains. Therefore, 2.0/2.0 PAA/PAH multilayers are overall highly dominated, both internally and on the film surface, by PAA segments, especially in their free, non-ionized acid (COOH) form. More specifically,  $\sim 75\%$  of a typical 2.0/2.0 PAA/PAH film is composed of the PAA fraction. Since the 2.0/2.0 PAA/PAH films are rich with carboxylic acid groups, these multilayers offer numerous reaction sites for subsequent chemistry. In addition, since there is only minimal ionic crosslinking in these films, the 2.0/2.0 PAA/PAH system tends to exhibit a relatively open

and thus more a permeable internal structure<sup>5</sup> compared to the more tightly-stitched 6.5/6.5 and 3.5/7.5 PAA/PAH combinations.

To further illustrate the structural differences among the 6.5/6.5, 3.5/7.5, and 2.0/2.0 PAA/PAH combinations, Figure 2.2 portrays proposed molecular architectures for each system. In addition, Table 2.1 summarizes their average layer thickness, RMS roughness values, the relative ratio of PAA to PAH segments, and the approximate % ionization of PAA (PAH is essentially fully ionized, i.e., ~ 90%, in each case). Figure 2.3 also clearly illustrates how the film thickness for each system increases with an increasing number of deposited layers, yet the magnitude of the thickness in the individual combinations is quite different (as indicated in Table 2.1). Both Table 2.1 and Figures 2.2 and 2.3 reveal how simply adjusting the pH of the polyelectrolyte solutions results in dramatically different multilayer properties, even for a single polycation/polyanion combination.

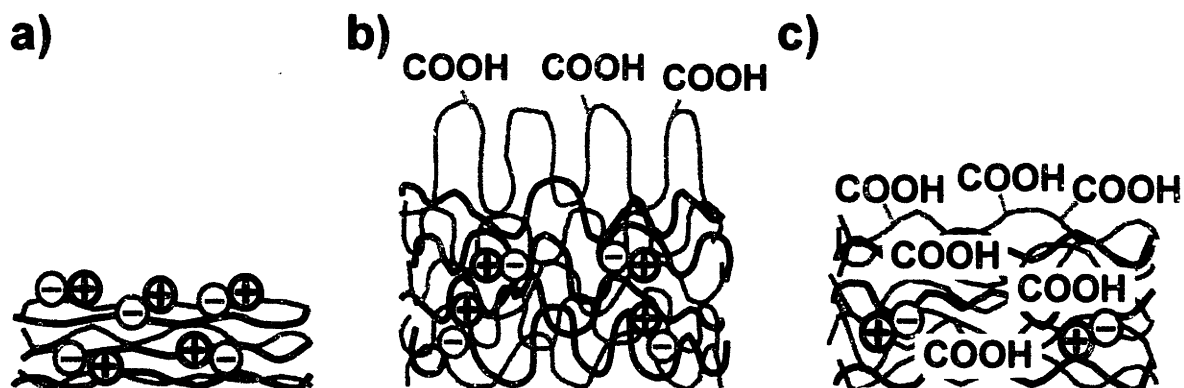


**Figure 2.2:** Schematics of proposed molecular architectures for the: a) 6.5/6.5, b) 3.5/7.5, and c) 2.0/2.0 PAA/PAH multilayer thin films, depicted with PAA as the outermost layer in the assembly. (Adapted from ref. # 2.)

**Table 2.1:** Comparison of important physical and chemical properties of various PAA/PAH multilayers.

	6.5/6.5 PAA/PAH	3.5/7.5 PAA/PAH	2.0/2.0 PAA/PAH
Layer thickness (Å)	< 5	~ 50–80	~ 25
RMS roughness (Å)	< 10	~ 20–50	~ 50
Relative composition (PAA:PAH segments)	~ 50:50	~ 40:60	~ 75:25
% ionization of acids	> 90	> 90	< 40

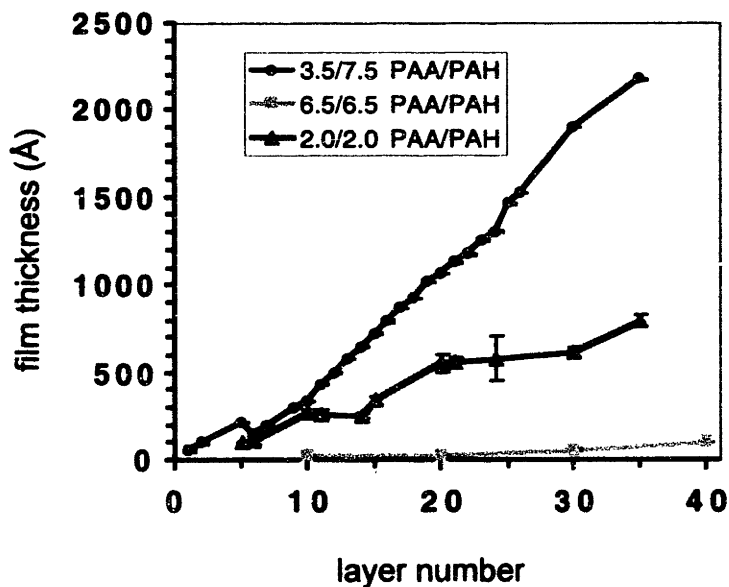


**Figure 2.3:** Graph of the mean total film thickness vs. the number of layers deposited for the 3.5/7.5, 6.5/6.5, and 2.0/2.0 PAA/PAH multilayers. Error bars correspond to  $\pm 1$  standard deviation.

## 2.4 Other Polyelectrolyte Multilayer Systems

### 2.4.1 Introductory Remarks

Besides the weak PAA/PAH multilayer combination, there are numerous other polyelectrolyte systems reported in the literature. This section briefly describes the important features of some other weak and strong polyionic or hydrogen-bonded multilayers, which are discussed later in Chapter 5 with regards to their *in vitro* interactions with mammalian cells. It is worth noting here that it is possible to combine many of these different systems together to form more complicated heterostructured films.

### 2.4.2 Polyacrylamide Systems

Some multilayers may be assembled completely without any electrostatic interactions but rather with only hydrogen bonds between hydrogen bond donors and acceptors. There have been several reports<sup>6-8</sup> in the literature that discuss hydrogen bonding to construct such multilayers, including, for example, films of PAA alternating with poly(ethylene oxide) (PEO).<sup>9</sup> Yet another entirely hydrogen-bonded multilayer system studied in the Rubner group contains polyacrylamide (PAAm), a common non-ionic polymer with a repeat unit structure

shown in Figure 2.1(f). The pendant  $-\text{CONH}_2$  functional group readily hydrogen bonds with the uncharged carboxylic acids of weak polyacids (e.g., PAA and poly(methacrylic acid) (PMA)). PAA/PAAm or PMA/PAAm films are necessarily fabricated at low pH conditions (e.g., pH 3.0) where the carboxylic acid functionalities are relatively uncharged. Higher pH conditions, which ionize the carboxylic acid groups, prevent the PAA from continuing to hydrogen bond with the PAAm, and consequently, the multilayer dissolves.<sup>6</sup> The successful fabrication, stabilization, and micropatterning of PAA/PAAm systems has been reported recently.<sup>6</sup>

### 2.4.3 PMA/PAH Systems

Another common weak polyanion that has been employed in assembling multilayer heterostructures is poly(methacrylic acid) (PMA). As seen in Figure 2.1(b), the repeat unit structure of PMA is identical to that of PAA except for a hydrophobic methyl group rather than just a hydrogen in each repeat unit. PMA can easily be substituted for PAA in the layer-by-layer process and alternate with a polycation such as PAH. Similar to PAA/PAH films, PMA/PAH multilayers assembled at neutral conditions (e.g., at pH 6.5 for both PMA and PAH are ultrathin), whereas the multilayers are thicker and more loop-rich at, for instance, pH conditions of 2.5 for each polyion. Much more detail regarding the fundamental aspects of the properties of PMA/PAH films have been detailed previously.<sup>10</sup>

### 2.4.4 SPS/PAH Systems

Rather than constructing multilayers from PAH and a weak polyanion, such as PAA or PMA, a strong (i.e., always fully charged) polyanion may be used instead. Commonly, poly(styrene sulfonate) (SPS), a strong polyanion with a charged sulfonate group ( $\text{SO}_3^-$ ), whose repeat unit structure is shown in Figure 2.1(c), has been assembled into multilayer films by alternating with PAH, for example. When PAH is essentially fully charged at pH values below its  $\text{pK}_a$ , SPS/PAH films absorb in thin, flat train conformations, analogous to PAA/PAH at 6.5/6.5 deposition conditions. Therefore, SPS/PAH films at, for example, 2.0/2.0 or 6.5/6.5 are both ultrathin with a layer thickness of  $< 5 \text{ \AA}$  and RMS roughness values of  $< 10 \text{ \AA}$ . However, as a weak polycation, PAH, when deposited at pH conditions near and greater than its  $\text{pK}_a$  of  $\sim 9$ , is only partially ionized. At basic pH values, the SPS remains



essentially fully charged. Thus, for instance, an SPS/PAH multilayer at pH 10.0/10.0 consists of a weakly ionized PAH depositing onto a fully charged SPS layer; at this pH of 10.0, the next adsorbing SPS layer does not re-ionize the preceding layer of PAH chains. Thus, a 10.0/10.0 SPS/PAH multilayer is analogous in many ways to the assembly and structure of a 2.0/2.0 PAA/PAH film and possesses a loop-rich, thicker conformation than SPS/PAH films at other fully charged deposition conditions, such as at 6.5/6.5. It should be noted that most multilayer literature using SPS and PAH do not exploit the pH tunability of PAH to adjust film thickness and conformation but rather add salt to control thickness by screening charges.<sup>11</sup>

#### **2.4.5 SPS/PDAC Systems**

Yet another system to consider is one formed by the assembly of two fully-charged macromolecules. Multilayers of the fully-ionized polyanion SPS alternating with the fully-charged polycation poly(diallyldimethylammonium chloride) (PDAC), whose repeat unit structure is shown in Figure 2.1(e), typify such a system. Similar to films of PAA and PAH deposited at neutral pH conditions (e.g., pH 6.5/6.5), whereby both polyions are essentially completely ionized, SPS/PDAC films at neutral conditions are ultrathin ( $< 5 \text{ \AA}/\text{layer}$ ) and smooth (RMS roughness  $< 10 \text{ \AA}$ ). Therefore, researchers generally add salt to the SPS and PDAC solutions in order to generate loopier conformations and thus thicker multilayers, since the salt screens some of the charges.<sup>12,13</sup> One salt-containing SPS/PDAC system is discussed in Chapter 5; this multilayer uses 0.25 M NaCl in each of the polyelectrolyte solutions and results in film thicknesses of  $\sim 25 \text{ \AA}/\text{layer}$  and an RMS roughness of  $\sim 30 \text{ \AA}$  or more. Nonetheless, an advantage of weak polyelectrolytes is the ability to fine-tune the film thickness and structure via pH adjustments alone without any extraneous salt.

### **2.5 Conclusion**

This chapter has introduced many of the common polyelectrolyte multilayer combinations with regards to their salient assembly features and resulting film properties, such as their ionization characteristics, conformation, and thickness. The standard film deposition and analytical techniques used to fabricate and evaluate these common multilayer systems (as well as any multilayers assembled from other polyions) were also discussed. It

should be evident from the description of these various representative weak polyelectrolyte multilayer systems that pH adjustment has a powerful impact in controlling thin film features on the molecular level. By manipulating the deposition pH values, it was shown how the internal film ionic stitching and blending as well as the surface composition may be readily tailored to allow one to control the film thickness, wettability, and fraction of free charges available for subsequent chemistry, among others. To further compare and contrast some of the fundamental attributes of these multilayer systems before discussing them in more detail in later chapters, Table 2.2 summarizes each case's average layer thickness and RMS roughness values; the data clearly reinforces the concept that shifts in pH deposition conditions may lead to significant differences in the resulting multilayers.

**Table 2.2:** Comparison of the average layer thickness and RMS roughness values for some of the various multilayer combinations to be discussed in this thesis.

	<b>Layer thickness (Å)</b>	<b>RMS roughness (Å)</b>
<b>6.5/6.5 PAA/PAH</b>	< 5	< 10
<b>3.5/7.5 PAA/PAH</b>	~ 50–80	~ 20–50
<b>2.0/2.0 PAA/PAH</b>	~ 25	~ 50
<b>6.5/6.5 SPS/PAH</b>	< 5	< 10
<b>2.0/2.0 SPS/PAH</b>	< 5	< 10
<b>10.0/10.0 SPS/PAH</b>	~ 20	> 200
<b>6.5/6.5 SPS/PDAC</b>	< 5	< 10
<b>6.5/6.5 SPS/PDAC (w/ 0.25 M NaCl)</b>	~ 25	~ 20–50
<b>6.5/6.5 PMA/PAH</b>	< 10	< 10

Each representative system addressed in this chapter was composed of the simplest case possible—only two polymers, and each polymer was assembled at one specific pH value throughout the film. However, the versatile layer-by-layer approach enables the construction of much more complex structures. For instance, it is possible to fabricate heterostructured films with the same two polyions deposited at several different pH's (e.g.,  $x$  number of layers

of 6.5/6.5 PAA/PAH followed by  $y$  number of layers of 2.0/2.0 PAA/PAH), multiple polyelectrolyte systems deposited at the same pH's (e.g.,  $w$  number of layers of 6.5/6.5 PAA/PAH followed by  $z$  number of layers of 6.5/6.5 SPS/PAH), or any combination thereof. For the majority of this thesis, however, only binary heterostructures assembled at one pH for each polymer will be discussed.

## 2.6 References

- (1) Shiratori, S. S.; Rubner, M. F. pH-Dependent Thickness Behavior of Sequentially Adsorbed Layers of Weak Polyelectrolytes. *Macromolecules* **2000**, *33*, 4213.
- (2) Choi, J.; Rubner, M. F. Selective Adsorption of Amphiphilic Block Copolymers on Weak Polyelectrolyte Multilayers. *J. Macromol. Sci.—Pure Appl. Chem.* **2001**, *A38*, 1191.
- (3) Yoo, D.; Shiratori, S. S.; Rubner, M. F. Controlling Bilayer Composition and Surface Wettability of Sequentially Adsorbed Multilayers of Weak Polyelectrolytes. *Macromolecules* **1998**, *31*, 4309.
- (4) Mendelsohn, J. D.; Barrett, C. J.; Chan, V. V.; Pal, A. J.; Mayes, A. M.; Rubner, M. F. Fabrication of Microporous Thin Films from Polyelectrolyte Multilayers. *Langmuir* **2000**, *16*, 5017.
- (5) Chung, A. J.; Rubner, M. F. Methods of Loading and Releasing Low Molecular Weight Cationic Molecules in Weak Polyelectrolyte Multilayer Films. *Langmuir* **2002**, *18*, 1176.
- (6) Yang, S. Y.; Rubner, M. F. Micropatterning of Polymer Thin Films with pH-Sensitive and Cross-linkable Hydrogen-Bonded Polyelectrolyte Multilayers. *J. Am. Chem. Soc.* **2002**, *124*, 2100.
- (7) Wang, L.; Fu, Y.; Wang, Z.; Fan, Y.; Zhang, X. Investigation into an Alternating Multilayer Film of Poly(4-Vinylpyridine) and Poly(acrylic acid) Based on Hydrogen Bonding. *Langmuir* **1999**, *15*, 1360.
- (8) Stockton, W. B.; Rubner, M. F. Molecular-Level Processing of Conjugated Polymers. 4. Layer-by-Layer Manipulation of Polyaniline via Hydrogen-Bonding Interactions. *Macromolecules* **1997**, *30*, 2717.
- (9) Sukhishvili, S. A.; Granick, S. Layered, Erasable, Ultrathin Polymer Films. *J. Am. Chem. Soc.* **2000**, *122*, 9550.
- (10) Baur, J. W. *Fabrication and Structural Studies of Sequentially Adsorbed Polyelectrolyte Multilayers*. Ph.D. Thesis, Department of Materials Science and Engineering; MIT, 1997.
- (11) Caruso, F.; Lichtenfeld, H.; Donath, E.; Möhwald, H. Investigation of Electrostatic Interactions in Polyelectrolyte Multilayer Films: Binding of Anionic Fluorescent Probes to Layers Assembled onto Colloids. *Macromolecules*. **1999**, *32*, 2317.
- (12) Gao, C.; Leporatti, S.; Moya, S.; Donath, E.; Möhwald, H. Stability and Mechanical Properties of Polyelectrolyte Capsules Obtained by Stepwise Assembly of

- Poly(styrenesulfonate sodium salt) and Poly(diallyldimethyl ammonium) Chloride onto Melamine Resin Particles. *Langmuir* **2001**, *17*, 3491.
- (13) Clark, S. L.; Montague, M. F.; Hammond, P. T. Ionic Effects of Sodium Chloride on the Templated Deposition of Polyelectrolytes Using Layer-by-Layer Ionic Assembly. *Macromolecules* **1997**, *30*, 7237.

# **Chapter 3:**

## **The Development of Porosity in Polyelectrolyte Multilayers**

### **3.1 Introductory Remarks**

As previously mentioned, multilayers are polyelectrolyte complexes formed one molecular layer at a time, which are necessarily deposited onto a surface to advantageously avoid the precipitation that is typical of the mixing of most oppositely charged polyions in solution. Variables such as salt and pH, which can certainly affect the behavior of polyionic complexes in solution,<sup>1</sup> also could surely impact the construction and subsequent performance of multilayers on a substrate. Chapter 2 showed how varying the pH during the assembly of weak multilayers can dramatically influence the resulting film structure and properties. Similarly, multilayers may be affected by salt or pH conditions *after* the film assembly, including, for example, the tendency of the film to desorb under conditions of high ionic strength (e.g., via exposure to 0.6 M NaCl).<sup>2</sup> It would be expected that polyelectrolyte multilayers could also experience phase separation phenomena similar to that of polyelectrolyte complexes in solution.

In an interesting discovery, PAA/PAH multilayers undergo a unique pH-induced morphological reorganization during a spinodal decomposition<sup>3,4</sup> simply with just acidic water.<sup>5</sup> What results via this rapid, low-pH phase separation are nano- or microporous thin films. Besides dramatic structural changes, the porous multilayers also exhibit increased thicknesses and correspondingly lowered refractive indices relative to the original, denser films. An immediate potential application of these porous ultrathin films would be semipermeable membranes. Previously, several other groups have investigated the transport properties of multilayers, such as the diffusion of gases or other small molecular weight species within the films, and have reported on the permeability and “membrane-like” qualities of multilayers.<sup>6-13</sup> In fact, these groups have demonstrated that multilayers can be quite permselective and thus beneficial for separation applications. This pH-driven phase separation, however, is the first demonstration of the ability to create true microporous, or in some cases, nanoporous multilayers. Consequently, with respect to possible biomedical applications, this pH-induced porosity transition may be used to create porous thin film coatings, biocompatible membranes, and controlled release and drug delivery systems.

This chapter describes this unusual phase separation behavior exhibited by certain multilayer systems. The experimental protocols and all of the processing parameters by which to generate, control, and characterize the resulting pore morphologies are provided. A significant amount of data regarding the porosity transition itself and the optimization of the porous films is presented, followed by some discussion regarding the mechanism of this useful, porosity-creating pH-driven phase separation.

## **3.2 Materials and Methods**

### **3.2.1 General Multilayer Deposition and Assembly**

Nonporous multilayer films of PAA and PAH were first prepared on silicon or glass substrates as previously detailed in section 2.2.1. The pH of the polymer solutions was adjusted to ~3.5 and ~7.5 (or ~3.5 and ~7.75) for PAA and PAH, respectively, although other pH combinations were also examined for their tendency to become porous. Typically, 10 to 40 layers of PAA/PAH films were fabricated, with films of 19–21 layers most commonly studied.

### 3.2.2 The Porosity Process

After the assembly of the precursor PAA/PAH 3.5/7.5 (or 3.5/7.75) multilayer, the film was immersed for some predetermined time, typically 15 sec to 4 min, in acidic water. While many different pH values of the water were initially examined for their effectiveness in inducing phase separation behavior, most studies kept the pH of the water constant at an optimal value of ~ 2.40. The temperature of the acid bath was varied from 15 to 50°C, and the ionic strength was also adjusted by using both monovalent and divalent salt (NaCl vs. MgCl<sub>2</sub>) of varying concentrations ranging from 0 M (i.e., no additional salt) to 1.0 M. After exposure to the initial acidic water treatment, the films were either immediately dried with compressed air (denoted as “no rinse” samples) or rinsed briefly for ~ 15 seconds in neutral water and then dried (referred to as “brief rinse” samples). Occasionally, the time of the post-neutral water rinse was performed for up to 18 hours rather than just a short 15 seconds. A flowchart depicting the various porosity processing paths along with the numerous adjustable parameters in each step (shown italicized) is displayed in Figure 3.1.

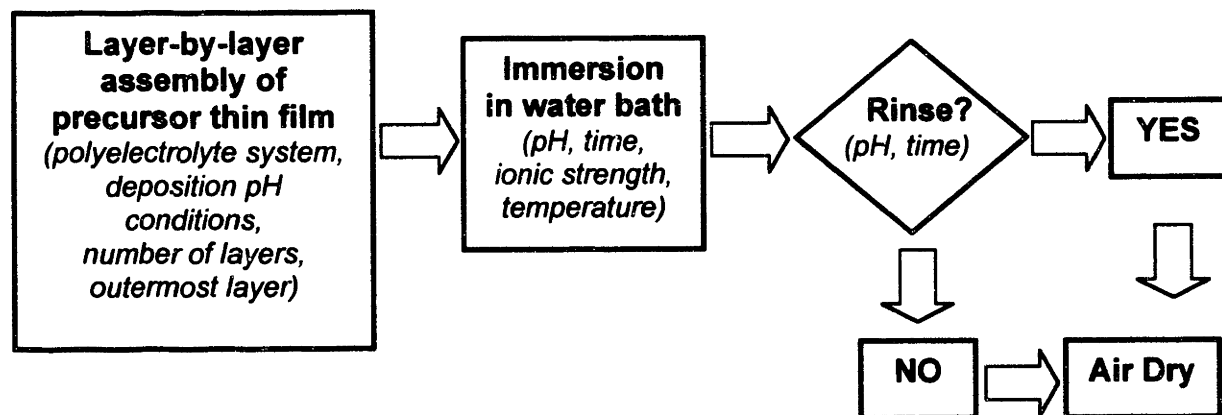


**Figure 3.1:** Flowchart depicting the various processing routes and variables used to fabricate porous polyelectrolyte multilayer thin films. The important variables of each step are shown italicized.

### 3.2.3 Characterization of the Porous Multilayers

Nonporous precursor and porous multilayer thin films were analyzed with several different surface characterization techniques, all as detailed previously in section 2.2. Ellipsometry was used to obtain thickness and refractive index data. Some refractive index measurements were also derived from UV-visible-NIR (near infrared) transmission/reflectivity data on transparent polystyrene or glass substrates, as will be detailed

in a forthcoming publication.<sup>14</sup> AFM imaging was used for surface and morphology profiling and roughness measurements. Image processing using Adobe® Photoshop® Version 5.0 was performed on binarized AFM figures to obtain pore size data. Chemical bonding information was obtained via FT-IR spectroscopy. As described previously,<sup>5</sup> dielectric measurements were performed by assembling PAA/PAH multilayers onto patterned indium tin oxide (ITO)-coated glass substrates and subsequently making the films porous. An aluminum electrode was then thermally evaporated on the film surface prior to taking measurements.

### **3.2.4 Thermal Crosslinking**

In certain cases, PAA/PAH multilayers were additionally thermally crosslinked at temperatures  $> 200$  °C for several hours. This annealing causes an amidization reaction to occur between the carboxylic acids of PAA and the amines of PAH to form stable nylon-like crosslinks within the multilayers.<sup>12,15</sup> The thermal crosslinking was performed on both nonporous and porous PAA/PAH thin films.

## **3.3 Results and Discussion**

### **3.3.1 General Findings**

When certain multilayers, especially that assembled from PAA/PAH at pH 3.5 and 7.5, respectively (referred to hereafter as 3.5/7.5 PAA/PAH), are immersed even just briefly, i.e., a few seconds, in acidic water, those films rapidly undergo a large-scale molecular reorganization to result in nano- or microporous structures. Figure 3.2 reveals typical AFM images of the dramatic transformation of an otherwise fairly dense 3.5/7.5 PAA/PAH precursor thin film prior to (shown in a) and after (b) exposure to acidic water. Concomitant with this drastic change in morphology is a substantial increase in the porous film's thickness and a corresponding decrease in the film's refractive index ( $n$ ). The thickness increase of up to 2–3 times that of the initial film height arises from the swelling associated with the reorganization of the multilayer during the spinodal decomposition. Similarly, the drop in refractive index is a consequence of the film, which initially possesses an  $n_{\text{film}}$  of  $\sim 1.52$ – $1.54$ , becoming porous and filling with air ( $n_{\text{air}} \sim 1.0$ ). The new refractive index of the porous film,  $n_{\text{pore}}$ , exhibits a composite refractive index between that of air and of the original nonporous film and usually has a value of  $\sim 1.2$ – $1.4$ .



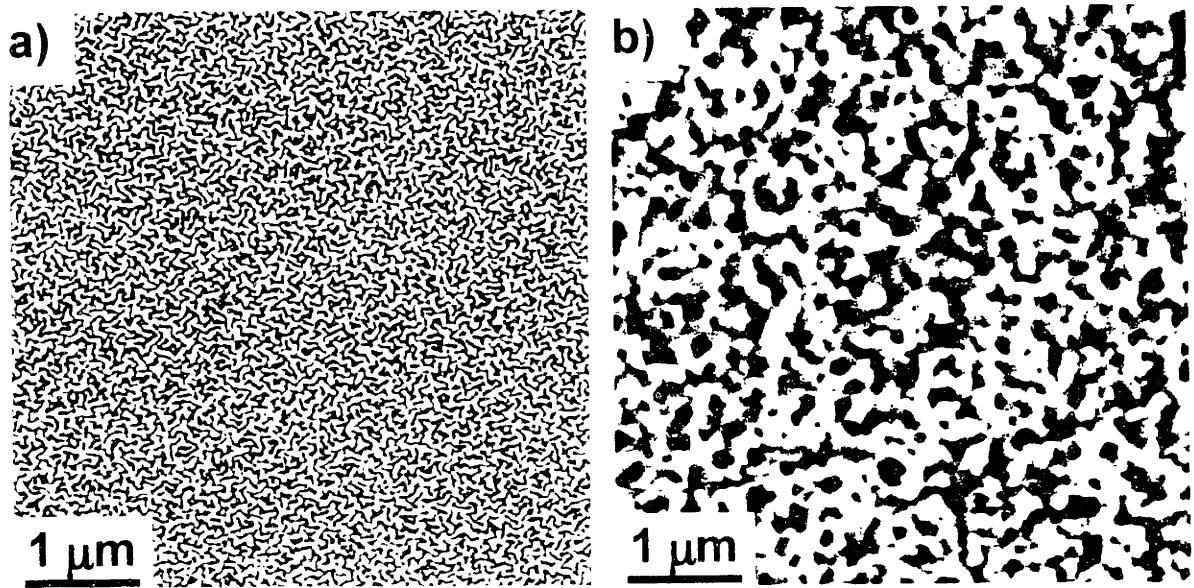


**Figure 3.2:** Representative  $5 \times 5 \mu\text{m}$  AFM images of a) an initially dense, nonporous 3.5:7.5 PAA/PAH precursor film and b) after exposure to pH  $\sim$  2.40 water for  $\sim$  1 minute at room temperature

As seen in Figure 3.1, there are many processing parameters by which to modify this pH-induced phase separation and hence adjust the resulting porous film's properties. Overall, the porosity  $P$  may be expressed as a function of these treatment variables such that

$$P = f(\text{PEM}, \text{pH}_{\text{PEM}}, l, l_{\text{out}}, \text{pH}_{\text{water}}, t, T, I, R) \quad (3.1)$$

where PEM denotes the specific polyelectrolyte multilayer system of the nonporous film,  $\text{pH}_{\text{PEM}}$  is the deposition pH conditions of that film,  $l$  is the number of layers in the film,  $l_{\text{out}}$  is the identity of polymer of the outermost layer,  $\text{pH}_{\text{water}}$  is the pH of the transition water bath,  $t$  is the time of exposure to the water,  $T$  is the water bath temperature,  $I$  is the ionic strength of the water bath, and  $R$  is the post-processing neutral water rinse treatment (i.e., the presence, if any, and time of the rinse). The resulting porosity itself may be defined in terms of several measurable quantities such that

$$P = f(\mathcal{V}_{\text{pore}}, \text{morph}_{\text{pore}}, h_{\text{pore}}, n_{\text{pore}}, \text{RMS}, \text{size}_{\text{pore}}) \quad (3.2)$$

where  $\mathcal{V}_{\text{pore}}$  is the  $\mathcal{V}$  pore volume of the transformed pore-containing film,  $\text{morph}_{\text{pore}}$  refers to the type of porous morphology (e.g., discrete or percolating pores),  $h_{\text{pore}}$  is the final thickness of the porous film,  $n_{\text{pore}}$  is the final refractive index of the porous film, RMS is the root-mean squared roughness of the porous film, and  $\text{size}_{\text{pore}}$  is the mean pore size. Since these

measurable features of the porous multilayer depend on the many tunable processing parameters in the porosity transition, it is therefore clear that:

$$P = f(\text{PEM}, \text{pH}_{\text{PEM}}, l, l_{\text{out}}, \text{pH}_{\text{water}}, t, T, I, R) = f(\%_{\text{pore}}, \text{morph}_{\text{pore}}, h_{\text{pore}}, n_{\text{pore}}, \text{RMS}, \text{size}_{\text{pore}}) \quad (3.3)$$

From equation 3.3, there is obviously a great deal of parameter space by which to modify and optimize the final structure and properties of the porous multilayer. Each of these processing variables will be now addressed with regard to how varying them affects the resulting porous thin film's properties with respect to morphology, thickness, and refractive index.

### 3.3.2 The pH Parameter

The pH of the transition water bath is perhaps the most critical parameter in determining whether or not a nonporous PAA/PAH thin film will be able to undergo this pH-induced porosity development. A nonporous 3.5/7.5 PAA/PAH multilayer is quite stable even for several years under ambient conditions, moderate heat, and extended exposure to water over a wide range of pH conditions. However, when an otherwise dense multilayer is immersed in a more acidic water environment, the film undergoes significant physical and chemical changes, which are manifestations of an unusual pH-driven phase separation that leads to porosity. Specifically, this dramatic morphological transition commences at about pH  $\sim 2.5$ , at which point a multilayer almost instantaneously experiences a substantial swelling of 2–3 times and a corresponding refractive index decrease. As seen in Figure 3.3, there is only a very narrow pH range by which to effect this porosity transformation; over only  $\sim 1/10$  of a pH unit (from pH 2.55 to pH 2.45), acid-exposed multilayers quite abruptly go from little discernable changes in their properties to a substantial morphological transformation with a highly porous structure. Figure 3.3 plots the % pore volume, defined in the simplest terms as:

$$\% \text{ pore volume} = (h_{\text{pore}} - h_{\text{init}}) / h_{\text{pore}} \times 100\% \quad (3.4)$$

where  $h_{\text{init}}$  is the initial nonporous film thickness, and  $h_{\text{pore}}$  is the porous film thickness as mentioned previously. Assuming a conservation of mass during the phase separation, equation 3.4 provides a rough estimation of the fraction of pores in the multilayer, simply based on thickness (i.e., volume) changes alone. For example, a multilayer whose thickness doubles upon becoming porous will have a pore volume equal to 50% and a pore volume equal to 67% if the original thickness triples, and so forth. If assembled onto a reflective substrate such as

silicon, multilayers exposed to the transition acidic water experience a substantial change in their interference color, indicating a significant thickness increase. Overall, the optimal pH condition of the acidic water (i.e., the one that leads to the greatest thickness increase and refractive index decrease) is  $\sim 2.40$ , with pH values  $> 2.6$  having minimal effect, and pH conditions  $< 1.75$  entirely removing the multilayer from the substrate. In fact, as will be discussed in section 3.4, the ability to dissolve polyelectrolyte multilayers from a substrate, particularly in a *regioselected* fashion, will be shown to be a quite useful and unique approach to processing and patterning materials.

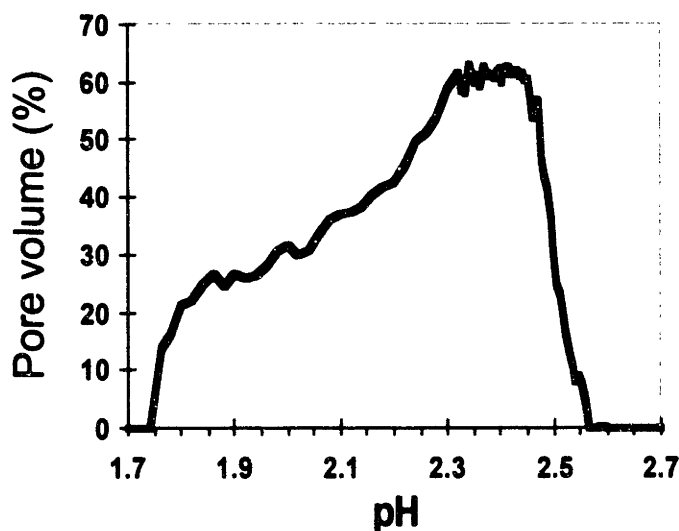


**Figure 3.3:** Graph of the % pore volume vs. pH curve for the 3.5/7.5 PAA/PAH system. The % pore volume is as defined in the text and is based on ellipsometry thickness measurements. As the pH of the water is lowered, the % pore volume, which effectively equals zero for the more dense, initial film abruptly changes to nearly 60% at a pH of  $\sim 2.40$ . However, pH conditions  $< 1.75$  entirely remove the multilayer from the substrate.

### 3.3.3 Multilayer System

Certain polyelectrolyte multilayers tend to be highly favorable precursor candidates for undergoing phase transformations that develop porosity. Many PAA/PAH combinations exhibit the ability to phase separate and become porous, although an optimal system appears to be the 3.5/7.5 PAA/PAH combination. As will be discussed in section 3.3.8, the ability to break the ionic bonds between the oppositely charged PAA and PAH chains and then reform those bonds in presumably more favorable conformations is an integral element of this pH-induced spinodal decomposition. Due to their weak polyelectrolyte nature, PAA/PAH multilayers can easily have their charge densities modified after the film assembly. If the film

is already energetically unstable, then having its internal ionic stitching diminish could consequently enable bond reorganization and phase separation to ensue. Common processing variables of pH and/or salt could be utilized to accomplish such a reduction in the effective ionic crosslink density within an electrostatically-assembled multilayer.

Surveying the PAA/PAH system has revealed that nonporous multilayers deposited at pH conditions of 3.5/7.5, respectively, and at an even further optimized variation, that of PAA/PAH 3.5/7.75, tend to yield some of the most substantial changes upon exposure to the acid transformation bath. Compared to many other PAA/PAH systems, the porous films, initially adsorbed at 3.5/7.5 or 3.5/7.75, present substantial thickness increases, large refractive index decreases, and the most pronounced porous morphologies. For consistency, all of the porosity studies presented hereafter concern the 3.5/7.75 PAA/PAH assembly, although other PAA/PAH systems may be more useful or better candidates for achieving, for example, highly specific refractive indices or other desirable porous features.

In addition, it is hypothesized that other multilayer combinations may similarly undergo pH-induced porosity phase separations. In principle, the spinodal decomposition and ensuing porosity development should not be limited just to weak PAA/PAH systems, and thus there is likely some universality to this phenomenon in polyelectrolyte multilayer thin films in general. For instance, preliminary evidence reveals the emergence of porous structures when multilayers assembled at pH 3.5/7.5 conditions, respectively, from PAA and the polycation PDAC are exposed to pH  $\sim$  2.4 water.<sup>14</sup> This example simply involves substituting the strong polycation PDAC for the weak PAH, but completely different polyelectrolyte systems should also potentially be able to experience porosity transformations. However, the critical transition pH would likely occur not at pH  $\sim$  2.4, for example, but at another specific pH that is dependent on the  $pK_a$  values of the constituent polymers of the multilayer.

As it will be presented in section 3.3.8, approximately half of the ionic bonds physically crosslinking any PAA/PAH multilayers (i.e., the 3.5/7.5 as well as other pH combinations) are cleaved at pH  $\sim$  2.4. In fact, FT-IR analysis reveals that the  $pK_a$  (the pH at which the molecule is half charged) of PAA within these films is not at pH  $\sim$  5, as in solution, but rather at about pH 2.4–2.5, the same pH where the phase separation occurs. By analogy, it is believed that as long as some critical number, e.g., half, of the ionic bonds within a multilayer are broken in order to enable the subsequent bond reorganization necessary for the

porosity process, then many different multilayer systems could be assembled and then “deconstructed” or rearranged in a pH-induced phase separation. As will be discussed in section 3.3.8, these other multilayers should first be constructed in a unique, rather unstable conformation, like the 3.5/7.5 PAA/PAH system, in order to phase separate. Thus, depending on the  $pK_a$  values of the constituent polyelectrolytes in any given multilayer system, a similar spinodal decomposition could potentially occur at other pH values, whether at acidic pH's, as in case of the PAA/PAH combination, or at neutral or basic pH conditions. Furthermore, as it will be shown later in this chapter, the manipulation of ionic strength and/or the inclusion of surfactants to the pH transformation bath could shift that critical transition pH to other values. Again, for the purposes of this thesis, the porosity will only be discussed for the PAA/PAH multilayer system and for the 3.5/7.75 PAA/PAH combination, in particular.

### **3.3.4 Layer Number and the Identity of the Outermost Layer**

Most porosity studies were performed with precursor PAA/PAH 3.5/7.75 samples having about 20 layers. For consistency and to control the total number of variables, the number of layers in the nonporous film was fixed at 19 or 21. These 19 or 21-layer films, which end with the polycation PAH as the outermost layer, would be used for subsequent studies in which the time, temperature, and/or rinsing parameters in the porosity process were varied. It should be noted that all films of 10–30 layers in thickness exhibit a similar pore volume vs. pH curve as in Figure 3.3, with the greatest porosity occurring around pH 2.4. However, there is some apparent pore size dependence on the thickness and thus the number of layers in a precursor film; thinner films (< 10 layers, for instance) yield smaller pores compared to thicker multilayers. The effect of the number of precursor layers (i.e., the initial film thickness) and the influence of the identity of the outermost layer (i.e., PAA vs. PAH) on the resulting porosity are variables certainly worth further investigation.

### **3.3.5 Time, Temperature, and Rinsing Parameters**

The entire pH-induced phase separation and the emergence of a porous structure in the multilayers occur quite rapidly on the timescale of seconds to minutes. To further explore the impact of the variables of time and temperature on the evolution of the porous film properties, identical nonporous precursor multilayers (of 21 layers) were fabricated and subsequently

exposed to the acidic water at a constant, optimal pH of  $\sim 2.4$  for four different times (15 sec, 1 min, 2 min, and 4 min) and at five different temperatures (15, 20, 30, 40, and 50°C). In addition, the post-acid bath neutral water rinse was performed for 0 sec (i.e., denoted as “no rinse”), 15 sec (“brief rinse”), or as long as several hours to overnight (“long rinse”).

Figures 3.4 and 3.5 present representative AFM top-view images of the evolution of the multilayer porosity as a function of time and temperature for both non-rinsed and briefly rinsed samples, respectively. A minimum of three samples for every condition in each time/temperature/porosity array was imaged, and in all cases, similarly-treated samples resembled one another, confirming the reproducibility of this process. Several trends are evident from these porosity arrays in Figures 3.4 and 3.5, including notably: 1) that there tend to be two porous morphological extremes—a) a rough-textured, highly-interconnected, percolating microporous network and b) a surface with discrete rounded pores; 2) the pore size in general increases with longer times and higher temperatures; 3) rinsed samples typically resemble non-rinsed samples only at longer times and higher temperatures but not at shorter times and lower temperatures.

For better clarity and comparison purposes, Figure 3.6(a) presents a larger image of the representative sample for the non-rinsed 15 sec/20°C condition as in Figure 3.4, whereas Figure 3.6(b) displays a larger image of the representative sample for the non-rinsed 4 min/50°C condition as in Figure 4; clearly, Figure 3.6(a) reveals the tortuous, highly-interconnected microporous morphology extreme, while Figure 3.6(b) presents the discrete rounded throughpore extreme. Figures 3.6(c) and (d) display those same morphologies in a 3-D view to better illustrate the overall porous structure of each extreme condition, respectively. In most cases, AFM cross-sectional analysis has revealed that the pores of the interconnected microporous structure do not extend directly downward to the substrate, whereas the discrete pores of Figure 3.6(b) and (d) tend to be true throughpores, reaching the substrate. Furthermore, dielectric measurements performed on porous films sandwiched between conductive indium tin oxide (ITO) and aluminum electrodes similarly reveal that the microporous structure, such as one shown in Figure 3.6(a) and (c) is tortuous without a direct path to the substrate but that the discrete morphology, typified by the one shown in Figure 3.6(b) and (d) shorts out via its true throughpores.

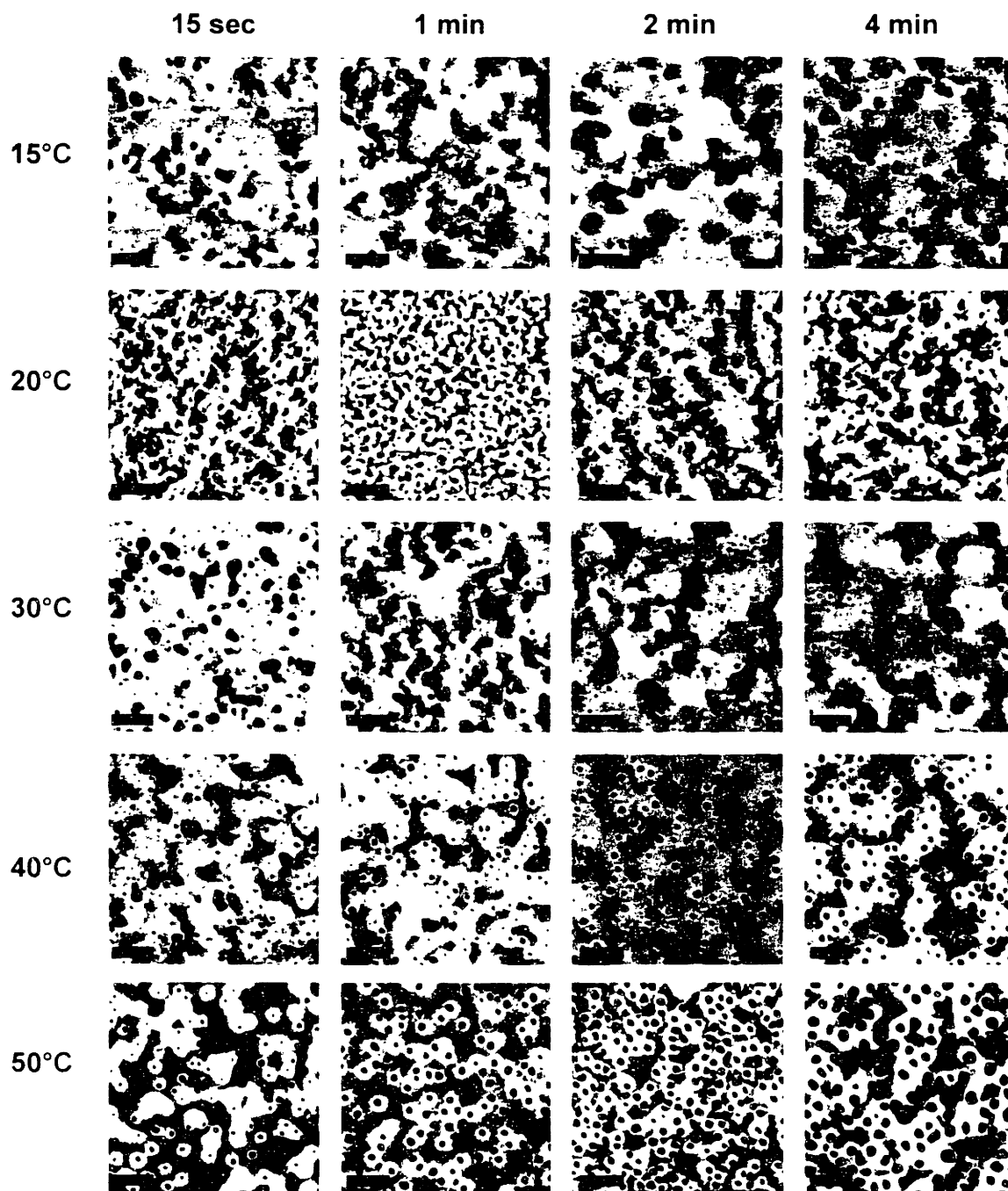


**Figure 3.4:** An array of typical  $5 \times 5 \mu\text{m}^2$  tapping-mode AFM top-view images of porous multilayers conditioned in pH  $\sim$  2.4 water for various exposure times and acid bath temperatures, as indicated. After immersion in the acidic water, the films were then immediately dried with compressed air ( =  $1 \mu\text{m}$  )

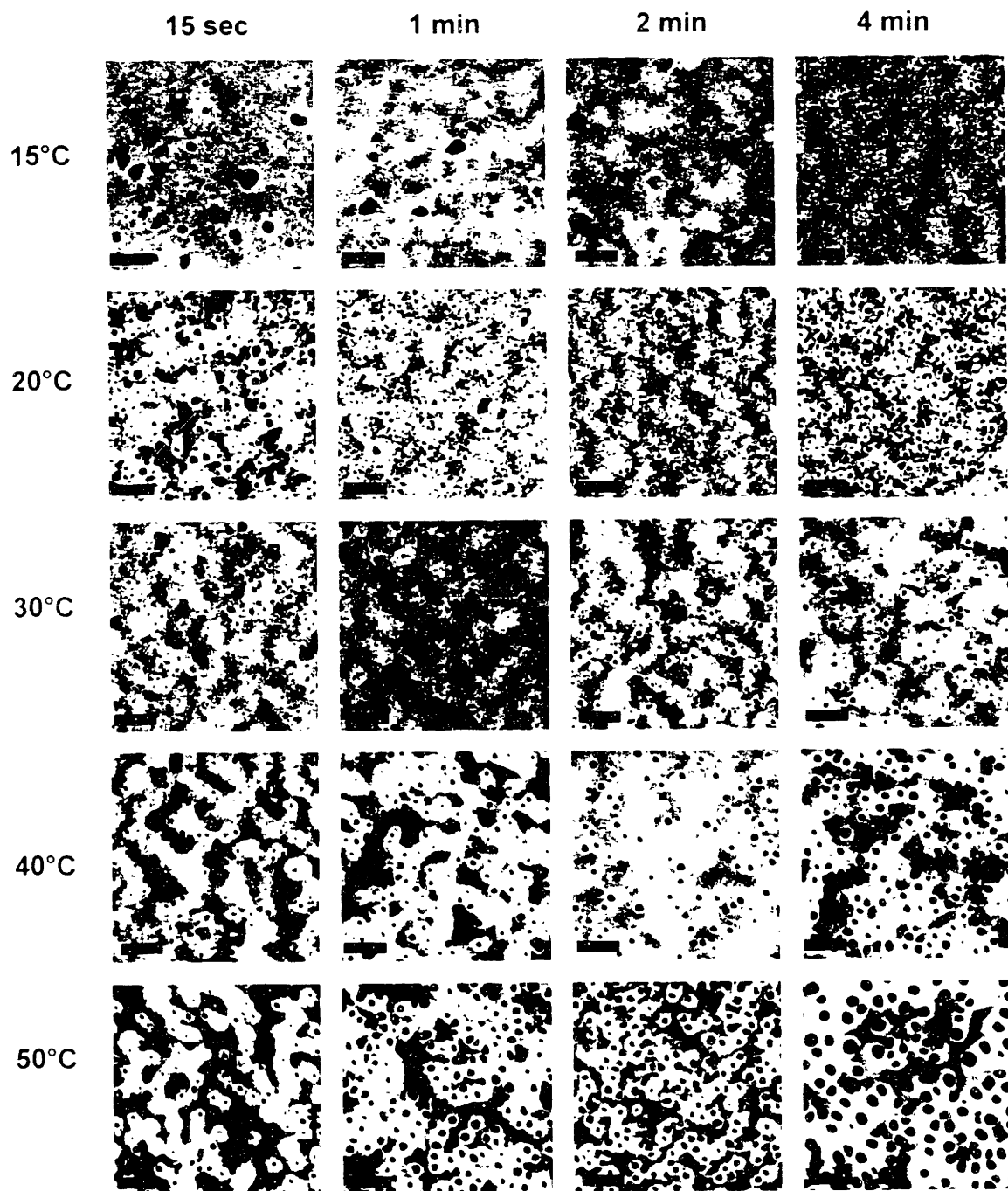


**Figure 3.5:** An array of representative  $5 \times 5 \mu\text{m}$  tapping mode AFM top-view images of porous multilayers conditioned in pH = 2.4 water for various exposure times and acid bath temperatures, as indicated. After immersion in the acidic water, the films were rinsed briefly ( $\approx 15$  sec) in neutral water before being dried with compressed air. (■ =  $1 \mu\text{m}$ )



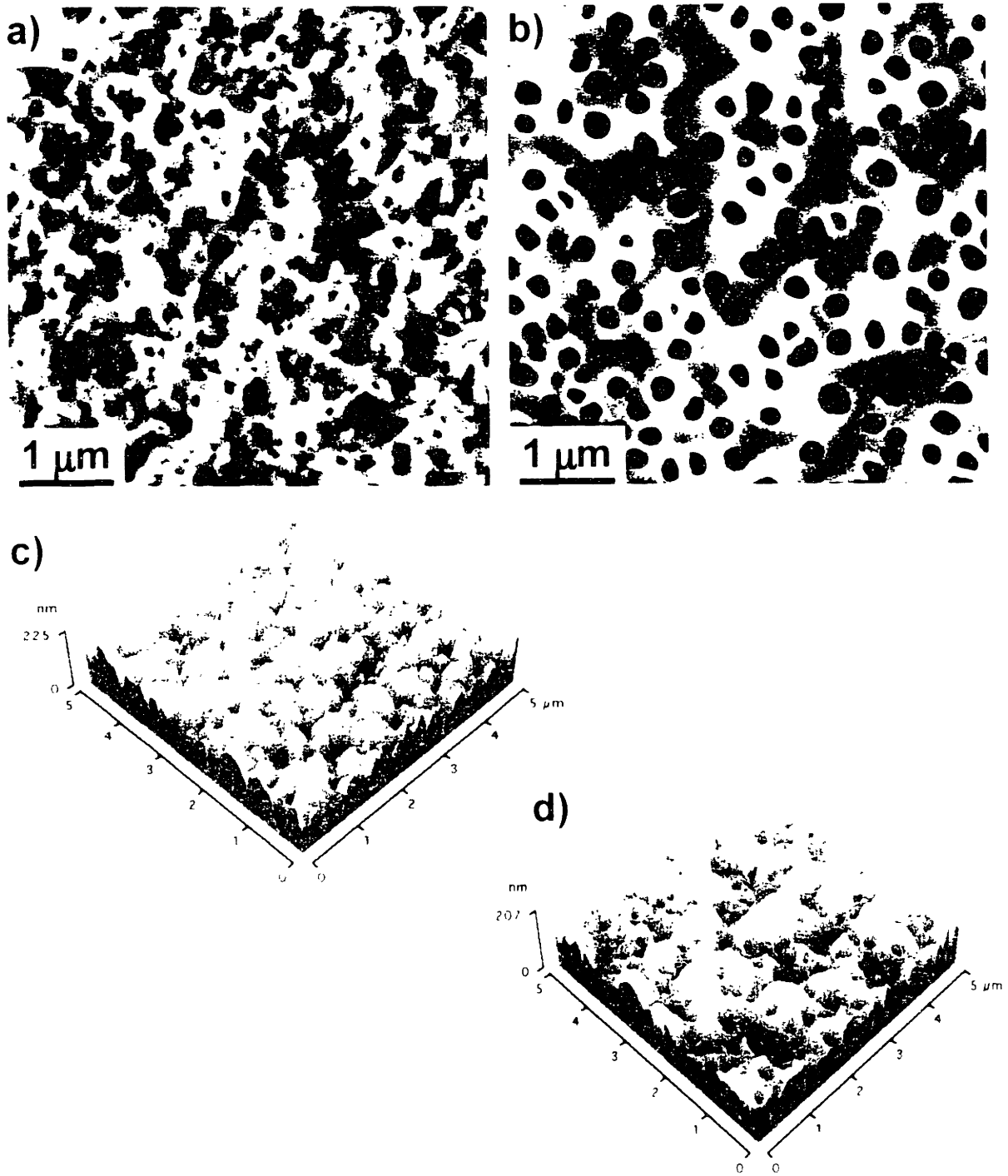
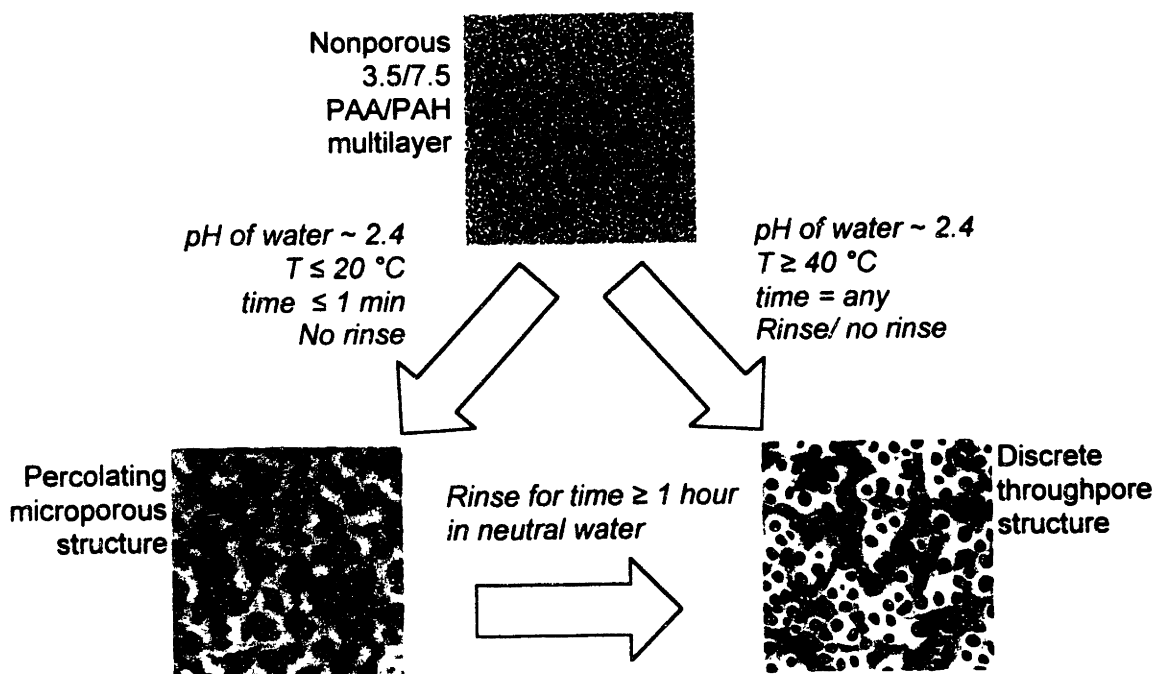


**Figure 3.6:** Larger top view and 3-D AFM images of (a, c) the percolating microporous morphology typified by the 15 sec 20 °C sample and (b, d) the rounded discrete throughpore structure represented by the 4 min 50 °C sample, both as shown previously in Figure 3.4. Neither film was rinsed in neutral water after the acid exposure.

With regard to the rinsing step with neutral water following the acid exposure, rinsed samples generally resemble morphologically, at least, the non-rinsed films at most processing

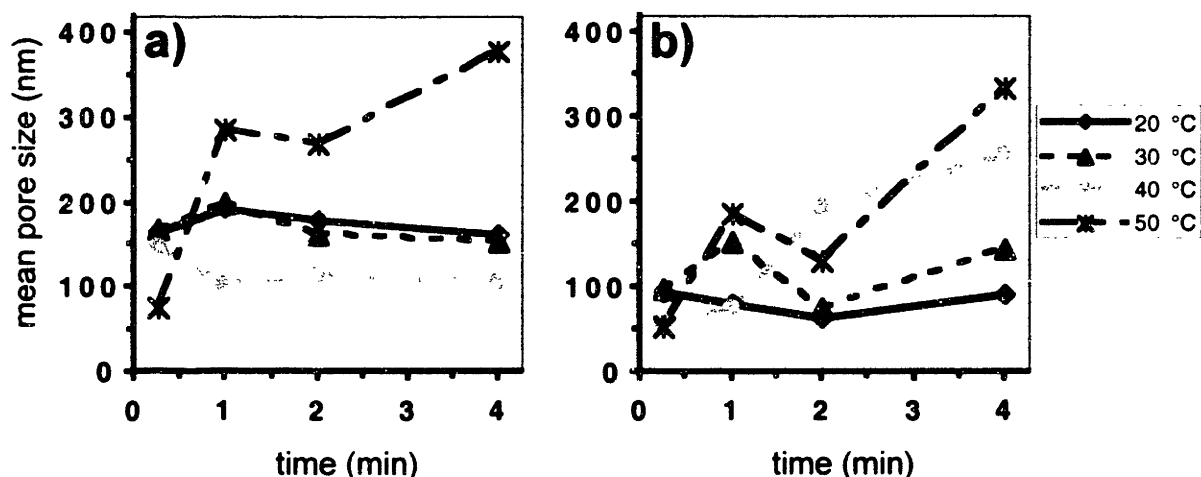
conditions, except for those at shorter times and lower temperatures. To be more specific, the most significant differences are observed at times of  $\leq 2$  min and temperatures  $\leq 20^\circ\text{C}$ ; at those conditions, it can be seen empirically from Figures 3.4 and 3.5 that non-rinsed samples tend to exhibit more pronounced tortuous microporous morphologies, but rinsed films also seem to possess some discrete pore character.

Figure 3.7 provides the simple processing paths necessary to fabricate a range of porous thin films. In general, the end-goal of the porosity procedure would likely be to prepare either the percolating microporous network or the discrete throughpore surface. As discussed herein, the processing conditions needed to achieve the interconnected, microporous network would involve immersing a precursor film into pH  $\sim 2.40$  water at a low temperature for a short time (e.g., 1 min,  $20^\circ\text{C}$ ) without any subsequent neutral water rinse. To obtain the discrete throughpore morphology, one would expose a precursor multilayer to pH  $\sim 2.40$  water at a high temperature for any amount of time (e.g., 2 min,  $50^\circ\text{C}$ ) and could (but need not) rinse the film. In addition, as will be described in section 3.3.6, rinsing for about an hour or longer also results in the discrete throughpore structure.



**Figure 3.7:** Processing paths by which to create from nonporous 3.5/7.5 PAA/PAH multilayers either interconnected microporous structures or discrete, rounded throughpore morphologies. As shown, the discrete structure may be achieved in two ways: 1) by performing the acid treatment at elevated temperatures, or 2) by first fabricating a microporous structure and subsequently immersing it in neutral water for many hours.

As seen in the images presented in Figures 3.4 and 3.5 and as quantified in Figure 3.8, the mean pore size generally tends to increase with longer immersion times, especially in elevated acid bath temperatures. It should be noted that the pore size distribution of these porous multilayers is, in many cases, quite large. Furthermore, the imaging analysis used to binarized AFM pictures to calculate pore sizes becomes quite complex due to the fact that often it is difficult to discern between a true “pore” and simply an indentation or depression on the surface due to the increased surface roughness. For the percolating porous morphology, in particular, the observation that many multiple interconnected pores exist on the surface greatly complicates the analysis. Some discussion regarding the pore size behavior and its relationship to classical spinodal decomposition theory will be addressed further in section 3.3.8.



**Figure 3.8:** Graphs of the mean pore size of the porous multilayers treated in pH ~ 2.4 water for various times and at different temperature conditions. The porous films in graph (a) were not rinsed, whereas the samples in graph (b) were rinsed in neutral water briefly (~ 15 sec) following the acid exposure. For clarity, error bars, corresponding to  $\pm 1$  standard deviation, are not shown, due to the large pore size distribution.

Besides the obvious changes in morphology exhibited by an initially nonporous multilayer upon exposure to the transition acidic water, there are substantial changes in the refractive index and film thickness. As expected, the nonporous film’s initial refractive index,  $n_{\text{film}}$ , having a value of  $\sim 1.52$ – $1.54$ , decreases as the multilayer fill with air ( $n_{\text{air}} \sim 1.0$ ), such that the porous film exhibits a new composite refractive index with a value between that of air and of the nonporous multilayer. Additionally, the porous film thickness,  $h_{\text{pore}}$ , is usually 1.5 times

or more that of the initial nonporous multilayer. For instance, upon exposure to pH ~ 2.40 water for 1 min at 20°C without any brief rinse, a 21-layer 3.5/7.75 PAA/PAH precursor with an initial thickness and refractive index of ~1000 Å and ~1.53, respectively, will swell to a new thickness of ~1500 Å on average and exhibit an associated  $n_{\text{pore}}$  of ~1.3. Similarly, the RMS roughness of the porous multilayer is now ~325 Å, which increased from its nonporous value of < 100 Å. However, if the same 3.5/7.75 PAA/PAH multilayer were subject to the same porosity treatment but simply briefly rinsed in neutral water as well, then the film increases to over 2000 Å in thickness, the  $n_{\text{pore}}$  drops to ~1.2, and the RMS roughness increases to ~170 Å. Thus, different times, temperatures, and rinse conditions may lead to significant changes in these porous multilayer properties.

Figures 3.9–3.11 quantify how the final porous film’s thickness, refractive index, and RMS roughness, respectively, vary depending on the chosen processing conditions for the immersion time, the temperature of the acidic water, and the post-acid rinse step. To normalize for any variances in the initial multilayer thickness, the increase in the porous film height was expressed simply as an expansion or swelling factor, which may be thought of as the porous film thickness relative to the initial nonporous film height. Thus:

$$\text{Expansion factor} = h_{\text{pore}} / h_{\text{init}} \quad (3.5)$$

where  $h_{\text{pore}}$  is the porous film thickness and  $h_{\text{init}}$  is the initial nonporous film thickness, as defined previously. Very simply, for example, a multilayer that doubles in thickness upon becoming porous will have an expansion factor of 2, and so forth. According to Figure 3.9, all porous films increase in thickness due to the porosity transformation, but there is some difference with respect to the post acid neutral water rinsing step. Multilayers briefly rinsed in neutral water tend to swell in a range of ~1.5 to ~2.5 times their initial height on average compared to only ~1.2 to ~2 times for non-rinsed films. These results were observed for all cases regardless of the temperature of the pH ~ 2.4 water bath. To be explained in section 3.3.8, the neutral water rinsing condition serves to recharge many of the temporarily-cleaved ionic bonds within the multilayer and thus further facilitates large-scale intermolecular bond reorganization. The non-rinsed acid-exposed films are simply in a transient state with many bonds still not re-paired, and the overall film mass has not fully rearranged to a more favorable state.

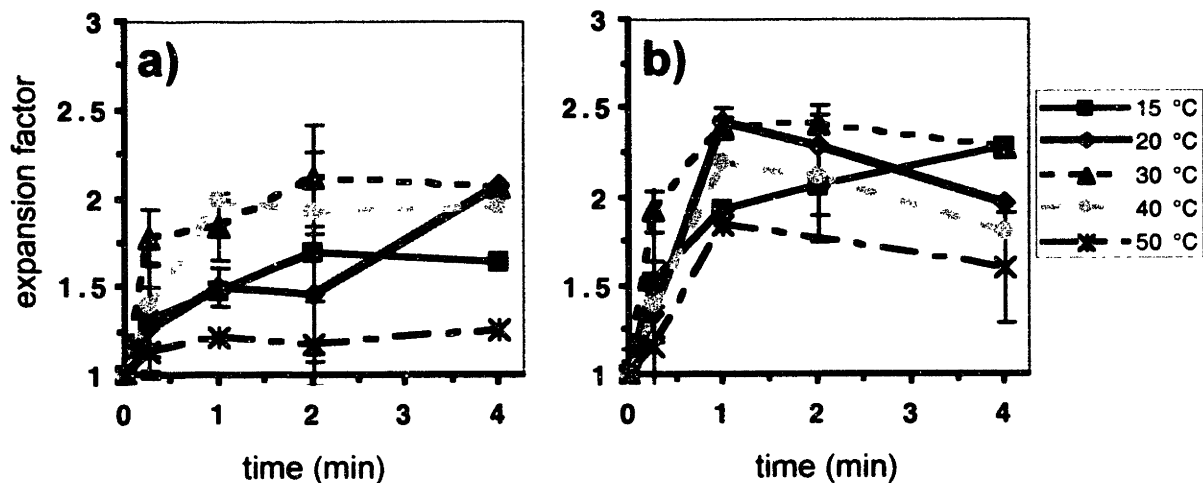


**Figure 3.9:** Graphs of the expansion factor or thickness increase for porous films that were a) not rinsed or b) rinsed in neutral water briefly (~ 15 sec) following the acid exposure at a variety of times and temperature conditions. Error bars correspond to  $\pm 1$  standard deviation. The expansion factor at the time of 0 min (i.e., no treatment, and therefore, no expansion) is simply equal to 1.

In general, both rinsed and non-rinsed films swell more with longer exposure times in the acidic water, but the greatest thickness increase is usually observed in the first minute and in the first 15 seconds, in particular. In addition, films processed at warmer acidic transformation conditions, especially at 30°C and at 40°C (but only for the non-rinsed case), tend to expand more than those treated at relatively cooler conditions (15°C and 20°C). Compared to the porosity processing at 15°C and 20°C, the treatment at the higher temperature of 30°C (and also at 40°C for the non-rinsed situation) should lead to more chain mobility and an associated higher degree of swelling; as described in section 3.3.8, this greater chain mobility enables the film to undergo a more substantial intermolecular bond reorganization. Interestingly, multilayers immersed in acid at 50°C do not exhibit the greatest thickness increases, but rather these 50°C-conditioned films experience the least expansion of any system tested. As will be discussed in section 3.3.6, the discrete throughpore morphology observed in the 50°C films, in particular, resembles similar porous structures seen when any acid-exposed multilayers are rinsed in neutral water for several hours. Moreover, those extended-rinsed films have redensified somewhat as suggested by their reduced thickness values. By analogy, as it will be shown, rapid processing at this elevated acid temperature is similar to longer immersion times in water at room temperatures.

Overall, however, it is difficult to identify, for certain, truly meaningful trends in this swelling data, given the often large error bars (equal to  $\pm 1$  standard deviation) in the

thickness measurements; since the porous films have high surface areas and thus high roughness values, their thickness measurements, from which the expansion factors are then derived, can be misleading. In addition, these thickness measurements were obtained from ellipsometry, which could easily scatter light on the rough-textured porous films. Profilometry, even when performed with minimal applied force, tends to compress the air-filled porous films and therefore underestimates the thickness. UV-visible spectroscopy, which has been used recently to gather transmission and reflectance data on *nanoporous* multilayers,<sup>14</sup> may prove to be a useful alternative way to confirm the thickness and refractive index of these porous films instead of relying solely on ellipsometry or profilometry measurements.

Figures 3.10(a) and (b) present the refractive index data of the non-rinsed and rinsed porous films, respectively. Again, since ellipsometry was used to obtain the refractive index values, the accuracy of the measurements is not necessarily completely valid due to the probable scattering of the light by the pores. Nonetheless, some general trends are evident from the graphs. As seen for both non-rinsed and rinsed multilayers, the porous refractive index,  $n_{\text{pore}}$ , drops considerably from the initial dense film's refractive index,  $n_{\text{film}}$ , of ~1.52–1.54 to values as low as ~1.2 within just a short time, i.e., about one minute, of exposure time to the acidic water. Comparing the rinsed versus non-rinsed case, the rinsed samples exhibit overall lower  $n_{\text{pore}}$  values as a whole than non-rinsed multilayers, meaning that the rinsed porous films are less dense and filled with more air/pore volume; this finding agrees well with Figure 3.9(b), which shows that rinsed multilayers generally have expanded in thickness more than their non-rinsed counterparts. Whereas the rinsed samples all share relatively similar  $n_{\text{pore}}$  values independent of the processing temperature, the non-rinsed multilayers show differences in the  $n_{\text{pore}}$  data with respect to the processing temperature. In fact, the relative ranking of the  $n_{\text{pore}}$  values for the porous samples conditioned at different temperatures follows the same order as that of the degree of film swelling presented in Figure 3.9(b). For instance, the 30 and 40°C non-rinsed samples, which showed the greatest swelling, correspondingly exhibit the lowest  $n_{\text{pore}}$  values, the 15 and 20°C films have intermediate values of both the expansion factor and  $n_{\text{pore}}$ , and the 50°C-treated samples have the least swelling and, similarly, the least decrease in  $n_{\text{pore}}$ .

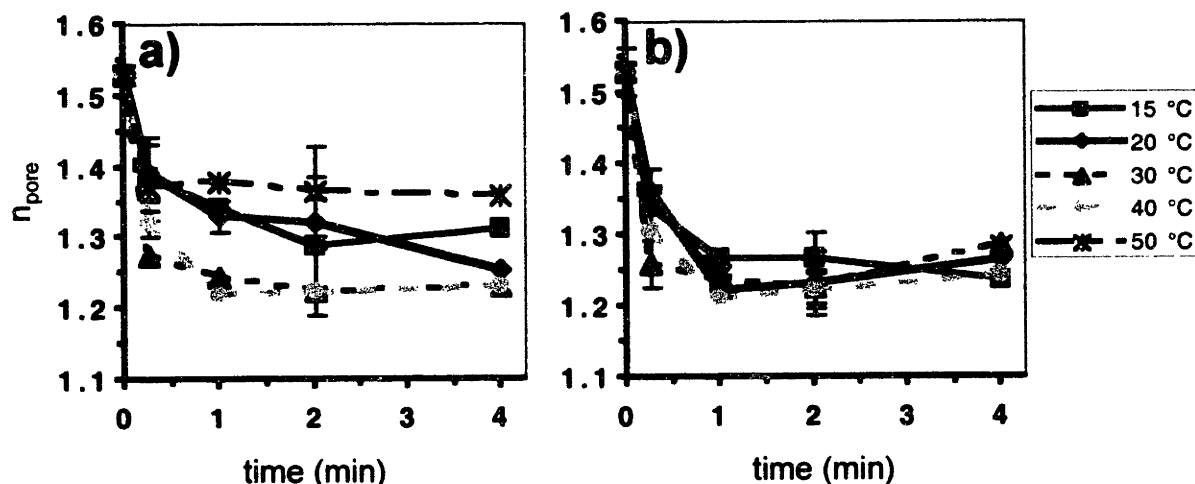


**Figure 3.10:** Graphs of the porous refractive index,  $n_{\text{pore}}$ , for films that were a) not rinsed or b) rinsed in neutral water briefly ( $\sim 15$  sec) following the acid exposure at a variety of times and temperature conditions. Error bars correspond to  $\pm 1$  standard deviation. The  $n_{\text{pore}}$  at the time of 0 min (i.e., no treatment) is equal to initial mean nonporous refractive index of  $\sim 1.53$ .

Figures 3.11(a) and (b) show the RMS roughness data of the non-rinsed and rinsed porous films, respectively. It is evident from both RMS roughness plots that the porous films exhibit substantially rougher surfaces than their nonporous counterparts (having RMS roughness values of  $< 100 \text{ \AA}$ ), which is expected due to the much higher amount of surface area that arises from the porosity. Although usually less thick overall than the rinsed samples, the non-rinsed films generally are rougher ( $\sim 350\text{--}450 \text{ \AA}$  on average) versus the rinsed films that are  $\sim 100\text{--}300 \text{ \AA}$  rough on average. Also, there is some indication that the porous RMS roughness of rinsed multilayers may increase with elevated temperatures. In this case, the  $50^\circ\text{C}$ -processed samples have the most pronounced depth changes and therefore the highest roughness due to their large discrete throughpores. However, since there are often large variances in the roughness values, which are manifested by the large error bars (representing  $\pm 1$  standard deviation), it is again difficult to identify a significant overall trend in the RMS roughness data as a function of the processing time, temperature, or rinsing condition. While the exact values for all of these porous films' properties may be difficult to obtain with high confidence, it is evident that porous films overall exhibit substantially higher thicknesses, associated significantly lowered refractive indices, and much rougher surfaces compared to nonporous multilayers.

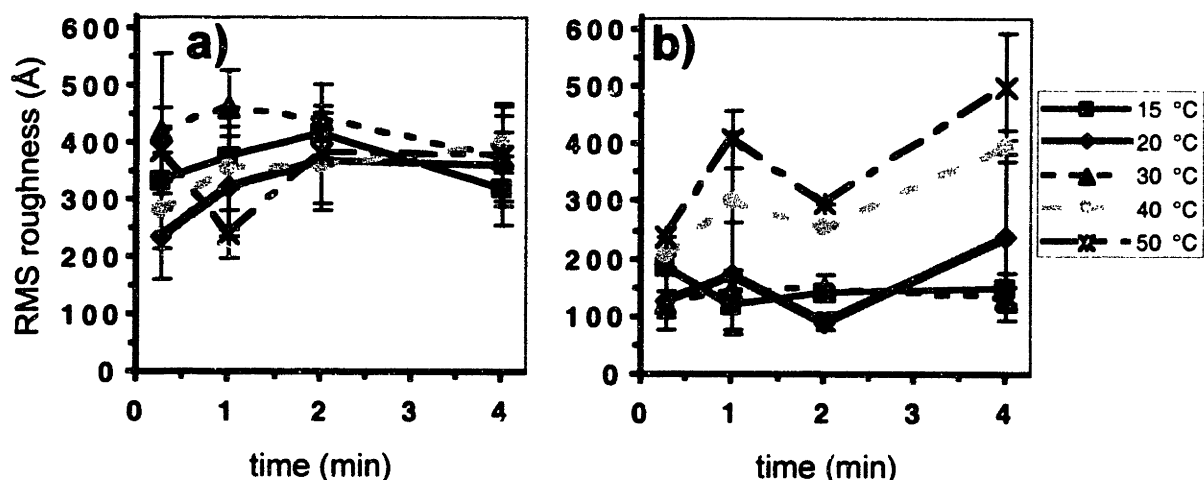


**Figure 3.11:** Graphs of the AFM-derived RMS roughness values for films that were a) not rinsed or b) rinsed in neutral water briefly (~ 15 sec) following the acid exposure at a variety of times and temperature conditions. Error bars correspond to  $\pm 1$  standard deviation.


### 3.3.6 Extended Immersions in Neutral Water

As indicated previously, the time of the post-acid bath neutral water rinse could be increased to several hours rather than just a brief 15 seconds. This longer treatment in neutral water (performed at room temperature) enables a secondary rearrangement to occur that tends to re-densify the porous multilayer. Although the film does remain porous, its refractive index and thickness return to near its original values of  $\sim 1.5$  and  $\sim 1000$  Å, respectively, thus confirming a densification effect. The morphology also resembles the discrete, rounded throughpore structure typical of multilayers processed in acid at higher temperatures, such as in Figure 3.6(b) and (d). Figure 3.12 shows the structure of a film, initially made porous with the standard pH 2.4 water treatment, after immersion in neutral water for over ten hours. In fact, for any initial porosity treatment, i.e., regardless of the porosity time, temperature, or rinsing conditions, all porous films that are exposed to neutral water for at least one hour develop a throughpore morphology, typified by Figure 3.12, with a corresponding decrease in thickness and increase in refractive index. Even films treated in acid at higher temperatures and thus already exhibiting discrete throughpores can still return to a higher refractive index and lower thickness after the longer neutral water conditioning. Therefore, the original non-porous 3.5/7.75 multilayer can ultimately reach the discrete throughpore structure via two very different treatment paths, as previously depicted in Figure 3.7: 1) *rapidly*, upon contact with acidic solutions at elevated temperatures (e.g., 40–50°C) for only a few seconds to



minutes, or 2) *slowly*, by being briefly exposed to the acidic solution for any time, temperature, and rinse condition and then immersed in neutral water for several hours.

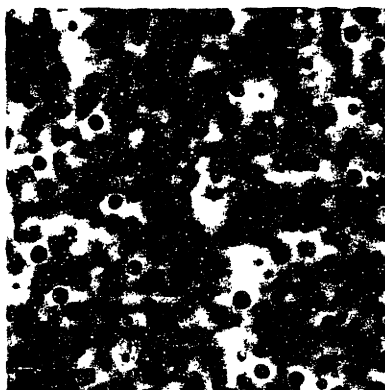


**Figure 3.12:** A representative  $5 \times 5 \mu\text{m}^2$  tapping-mode AFM top-view image of a typical porous multilayer conditioned for several hours in neutral water after the initial acid treatment. Regardless of the time, temperature, or rinsing conditions in the initial acid treatment, long immersions in neutral water result in discrete throughpore morphologies similar to that shown above. (  =  $1 \mu\text{m}$ )

The observation that a multilayer may reach the discrete, rounded throughpore morphology via two very different processing paths suggests how the throughpore structure is energetically favorable. Microporous films, typified by Figure 3.6(a) and (c), retain the integrity of their unique percolating structure for several years under ambient conditions in air. However, exposure to neutral water for even one hour or less induces a secondary morphological reorganization leading to the throughpore structure. This secondary rearrangement in neutral water alone further conveys how the initial microporous film is indeed unstable energetically. Immersion in the water provides, over time, the additional mobility needed for the polymer chains of the porous film to sample more favorable conformations and thus reorganize into the discrete throughpore structure. This rearrangement is accomplished with much faster kinetics by initially treating a nonporous multilayer with warmer porosity-inducing acidic water (e.g., at  $40\text{--}50^\circ\text{C}$ ); the elevated temperature of the acidic water bath similarly provides substantial mobility for the polymer molecules to much more quickly arrive at the discrete morphology. Therefore, it appears that if given enough energy for large-scale mobility—whether via long times at lower temperatures or much faster times at higher temperatures—microporous multilayers all tend to be driven toward creating these discrete throughpore-containing thin films.

### 3.3.7 Ionic Strength

Another processing parameter investigated was the ionic strength of the transition acid bath. The effect of salt during the assembly of polyelectrolyte multilayers has previously been studied, particularly when fabricating films from strong polyelectrolytes.<sup>16</sup> As expected, extraneous salt ions can effectively screen charges in the films. Since the acidic water protonates many of the carboxylate ions of PAA and consequently cleaves many of the electrostatic bonds within the multilayer to ultimately lead to the phase-separated porous film, it was hypothesized that salt could also potentially result in porosity by screening the ionic bonds between PAA and PAH. At neutral pH's, however, no concentration of salt ions was found to be able to disrupt the electrostatic crosslinks in the PAA/PAH multilayer to induce gross phase separation. Moreover, salt concentrations of ~ 3.0 M would entirely strip the film from the substrate, and even lower concentrations have been reported to remove multilayers.<sup>2</sup>

If, however, slightly more acidic water—instead of neutral water—were coupled with additional salt, then some porosity would indeed occur. Specifically, when water at a pH of ~ 3.2–3.5 at ~ 20°C had an ionic strength,  $I$ , of either 1.0 M (when using NaCl) or 0.75 M (using MgCl<sub>2</sub>), the treated samples exhibited substantial film swelling and a refractive index decrease, indicative of the development of porosity. In fact, as demonstrated in Figure 3.13, the addition of either monovalent NaCl or divalent MgCl<sub>2</sub> to moderately acidic water actually shifts the pore volume vs. pH curve of Figure 3.3 towards a higher pH by approximately 1 pH unit. Thus, rather than at pH of ~ 2.2–2.5, porosity occurs at a pH of ~ 3.2–3.5. Moreover, the dissolution of the film from the substrate, which normally occurs at a pH < about 1.7, similarly shifts to a higher pH. Specifically, the addition of salt with an ionic strength of 1.0 M (for NaCl) or 0.75 M (for MgCl<sub>2</sub>) to acid at a pH < ~ 2.7 would remove the multilayer.

In a related study, the ionic strength of the standard acidic water bath of pH ~ 2.4 was varied by the addition of NaCl or MgCl<sub>2</sub>. However, there was only a small range of extraneous salt concentrations that could be included to the normal acidic transition bath. Ionic strength values of ~ 0.15 M for either NaCl or MgCl<sub>2</sub> at pH ~ 2.4 were near the upper limit of salt concentrations; values higher than that would completely remove the film from the substrate. Interestingly, regardless of the time or temperature variables, the coupling of salt with the pH ~ 2.4 water would lead to much smaller-sized nanopores (< 100 nm), compared to the readily-obtainable larger-sized micropores (of ~ 100–400 nm), which would

normally result from the acid exposure alone without any extra salt. Figure 3.14 presents AFM imaging of a representative nanoporous multilayer, which was treated at room temperature for 4 minutes in pH  $\sim$  2.4 water containing MgCl<sub>2</sub> with an ionic strength of 0.1 M. To remove any residual salt from the film, this sample in Figure 3.14, along with all other salt-treated multilayers, were briefly rinsed in neutral water afterwards. A thorough analysis of these nanoporous multilayers, especially with respect to their formation via salt as well as their resultant unique optical properties (i.e., very low refractive indices) is currently underway.<sup>14</sup>

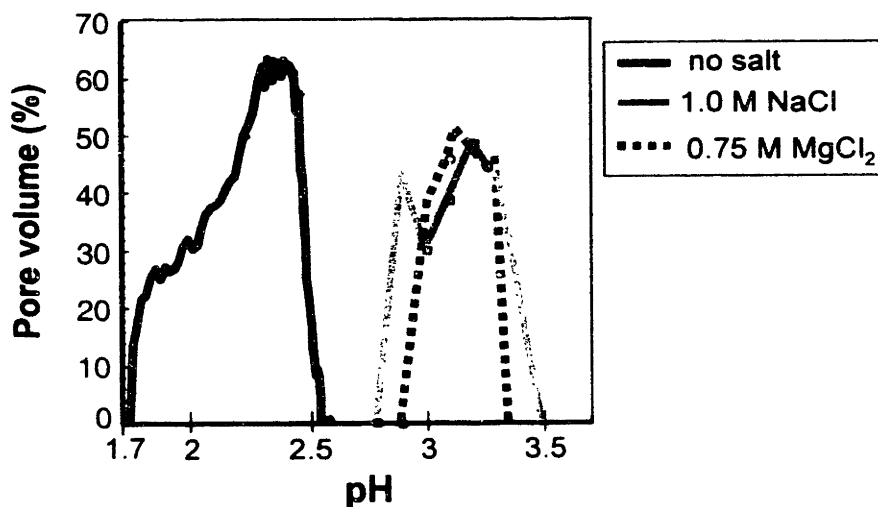


**Figure 3.13:** Graph of the % pore volume vs. pH curve for the 3.5/7.5 PAA/PAH system treated in acidic water of various ionic strengths. The “no salt” curve refers to the same data as previously plotted in Figure 3.3. The addition of NaCl (with an I = 1.0 M) or MgCl<sub>2</sub> (with an I = 0.75 M) effectively shifts the “no salt” curve up by about 1 pH unit.

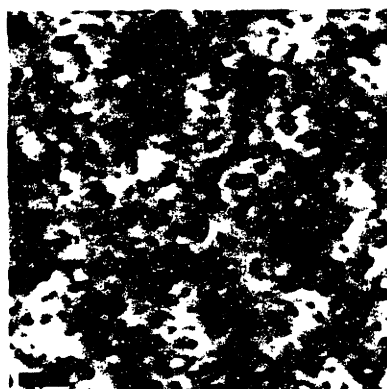


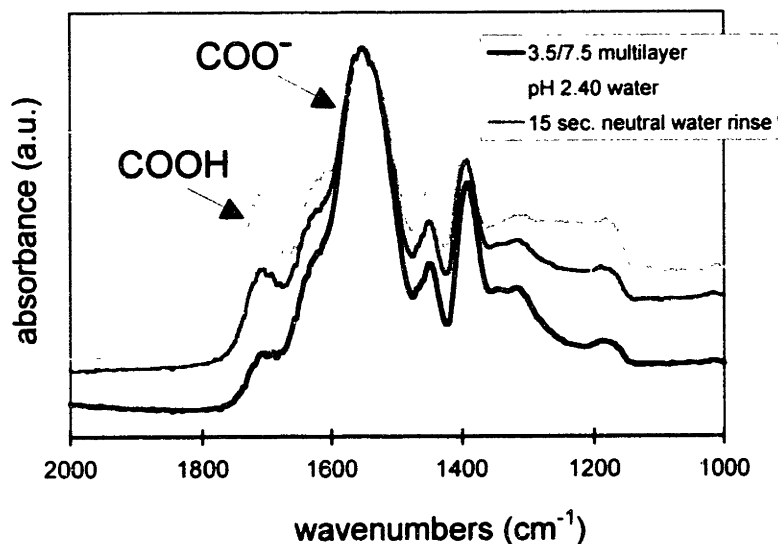
**Figure 3.14:** A representative 2 x 2  $\mu\text{m}^2$  tapping-mode AFM top-view image of a nanoporous multilayer conditioned for 4 min in  $\sim$  20°C, pH  $\sim$  2.4 water having an ionic strength of 0.1 M (using MgCl<sub>2</sub>). The film was rinsed in neutral water afterwards. (  $\blacksquare$  = 250 nm)

### 3.3.8 Mechanism of Porosity Formation in Polyelectrolyte Multilayers

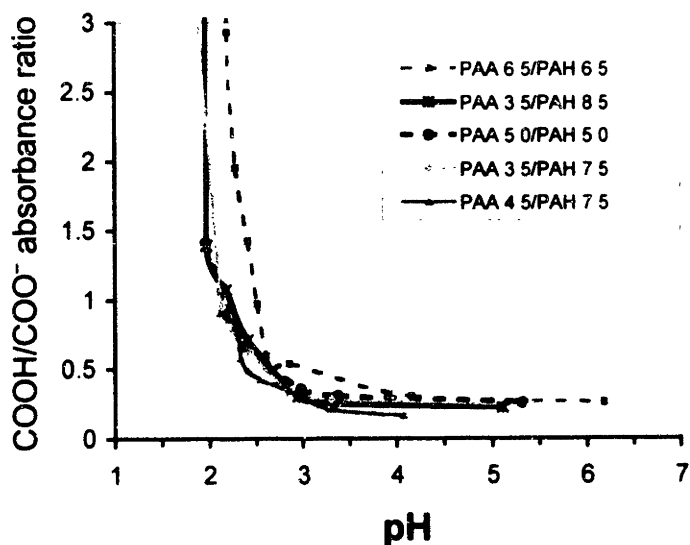
Now that much of the morphological, thickness, and optical data regarding the porosity effect has been presented, it is necessary to further discuss the mechanism of this pH-induced phase separation. Considering just the optimal precursor system for generating porous thin films, PAA/PAH 3.5/7.5 (or 3.5/7.75) multilayers have a highly interpenetrated, loop-rich structure with a high degree of ionic intermolecular crosslinks ( $\text{COO}^- \cdots \text{NH}_3^+$ ) randomly stitching the film together. Central to the large-scale phase separation and molecular rearrangement is a bond breaking and bond reformation mechanism of these electrostatic crosslinks. As presented in Figure 3.15, FT-IR chemical spectroscopy has proven to be quite helpful in elucidating these bonding changes, particularly via measuring the state of ionization of the carboxylic acid functionality of PAA. FT-IR reveals that approximately 80–90% of the carboxylic acids of the PAA molecules are indeed ionized to their carboxylate ion form of  $\text{COO}^-$  (which has a peak absorbance at  $\sim 1540 \text{ cm}^{-1}$ ). After exposure to the pH  $\sim 2.4$  water, however, a significant number of those carboxylate ions become protonated to their unbound acid form ( $\text{COOH}$ , having a peak absorbance at  $\sim 1710 \text{ cm}^{-1}$ ) in the acidic environment, and consequently only about half of the groups remain charged. This cleaving of some of these physical electrostatic crosslinks temporarily frees the structure to enable more chain mobility and the sampling of more energetically favorable conformations and ionic stitching. The subsequent neutral water rinse, if performed, then recharges  $\sim 80\%$  of the protonated groups back to the ionic form. The thickness increases discussed earlier in section 3.3.5 are a consequence of the once tightly-stitched multilayer swelling as the structure becomes more free and mobile.

Figure 3.16 displays further FT-IR-derived data revealing the absorbance ratio of the unbound  $\text{COOH}$  to  $\text{COO}^-$  groups for many different systems, including the 3.5/7.5, 6.5/6.5, 3.5/8.5, 4.5/7.5, and 5.0/5.0 PAA/PAH combinations. It is evident from the plot that there is an abrupt transition in the  $\text{COOH}/\text{COO}^-$  ratio of all of these various multilayers around pH  $\sim 2$ – $2.5$ , which coincides nicely with the sharp transition signifying the onset of the porosity in the pore volume vs. pH curve of Figure 3.3. FT-IR analysis also suggests that PAA's  $\text{pK}_a$ , the pH at which the polymer is half-ionized (i.e., when the  $\text{COOH}/\text{COO}^-$  ratio of Figure 3.15 equals 1), has shifted substantially from its value in aqueous solution of pH  $\sim 5$  to a much lower value of about pH 2–2.5. Such lowering of the effective  $\text{pK}_a$  values of PAA and other

polyelectrolytes within multilayers has previously been reported.<sup>17,18</sup> Therefore, by exposing a PAA/PAH multilayer to acidic conditions sufficient enough to break about half of the ionic crosslinks, the pH-induced porosity transformation can occur.



**Figure 3.15:** FT-IR spectra of the nonporous 3.5/7.5 PAA/PAH multilayer, the porous multilayer after exposure to pH ~ 2.40 acidic water, and the porous multilayer after being briefly rinsed in neutral water.



**Figure 3.16:** Graph of the FT-IR-derived COOH/COO<sup>-</sup> absorbance ratio for the 3.5/7.5, 6.5/6.5, 3.5/8.5, 4.5/7.5, and 5.0/5.0 PAA/PAH combinations. The COOH and COO<sup>-</sup> peaks, as indicated in Figure 3.15, are at ~1710 cm<sup>-1</sup> and ~1540 cm<sup>-1</sup>, respectively.

In this unusual phase separation, the two polyelectrolytes undergo a spinodal decomposition from the nonsolvent acidic water. Phase separation via a spinodal

decomposition process<sup>3</sup> has recently been used to explain the common immersion precipitation process employed to create porous membranes.<sup>19-21</sup> Similarly, the PAA/PAH multilayer, if thermodynamically unstable, could be driven to undergo such a spinodal decomposition process. It has been proposed previously that the 3.5/7.5 PAA/PAH multilayer, in particular, is assembled in a rather unstable and unfavorable ionic conformation and could therefore phase separate in order to achieve more preferable arrangements.<sup>5</sup> In particular, the resulting percolating microporous morphologies, such as that exemplified by Figure 3.6(a) and (c), are consistent with the phase separated structures (here, a porous phase and a nonporous polymer phase) observed in classical spinodal decomposition theory.<sup>4,20,21</sup> The evolution from the percolating, interconnected porosity to the more discrete, circular porous structure with longer acid-immersion times and elevated temperatures also follows the coarsening phenomena demonstrated in such spinodal demixing processes.<sup>3,4,20,21</sup> Moreover, the increase in pore size under conditions of enhanced polymer mobility—longer acid-immersion times and elevated temperatures—similarly coincides with the observed domain coarsening typical in phase transitions involving spinodal decomposition.<sup>4,20,21</sup> Interestingly, studies performed on crosslinked polyelectrolyte gels have revealed significant swelling (volume) changes associated with spinodal decomposition phase transitions in those materials, often induced by pH or other solvent conditions; the pH-driven spinodal decomposition observed in multilayers is perhaps, then, a phenomenon related to some previous findings in polymer gel theory.<sup>22,23</sup>

The complexation of two oppositely charged polyelectrolytes is a highly favorable process, especially when the positive and negative charges can ion-pair in coordinated stitching conformations. In fact, there are numerous examples from the polyelectrolyte complex literature discussing the observation that the mixing of two oppositely charged polymers in solution usually leads to highly cooperatively (1:1) ionic bonding, which is often manifested by the complex precipitating.<sup>24-26</sup> Furthermore, some reports have stated that polyelectrolyte complexes can fit into one of two general categories according to their overall molecular organization—the “ladder-like” and the “scrambled salt” arrangements.<sup>26,27</sup> As the name implies, the “ladder-like” organization consists of highly coordinated ionic pairing between oppositely charged polymer chains, while the more complex “scrambled salt” architecture involves random ionic stitching between opposite charges on many different

chains. A schematic of these two intermolecular architecture extremes is depicted in Figure 3.17.

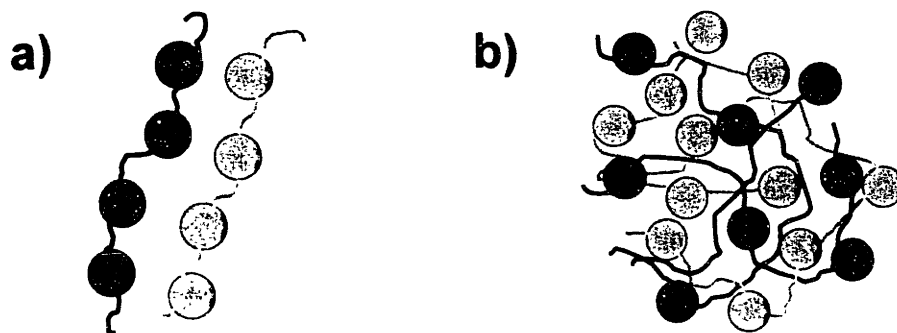


**Figure 3.17:** Schematic of the two main classes of accepted architectures to describe the intermolecular chain organizations of polyelectrolyte complexes. The image in (a) depicts a “ladder conformation,” while (b) portrays a more complex “scrambled salt” arrangement. (Adapted from ref. # 27.) The black and gray circles represent either positive or negative charges.

To reiterate what was presented in Chapter 2 regarding its unique assembly, the 3.5/7.5 (or 3.5/7.75) PAA/PAH multilayer is constructed from weakly ionized PAA molecules depositing onto a highly charged PAH surface, only to be re-ionized in the next immersion in the PAH solution. This act of adsorbing as a slightly charged polymer and then being recharged creates the thick and loop-rich (albeit still highly-internally ionized) structure of the 3.5/7.5 multilayer. Presumably, this unusual assembly process causes the 3.5/7.5 PAA/PAH film to exhibit ionic bonding across many different chains in a rather intermingled, convoluted arrangement, not one of close cooperatively stitched segments. Therefore, the 3.5/7.5 PAA/PAH multilayer would be expected to adopt more of a “scrambled salt” architecture.

If an appropriate path is provided, the 3.5/7.5 multilayer system could potentially reorganize from its apparently frustrated and unstable “scrambled salt” structure into more energetically preferred conformations, such as one where the chain segments are highly coordinated in, for instance, more “ladder-like” arrangements. Therefore, breaking a significant number, e.g., half, of the film’s electrostatic crosslinks in the acidic water enables large-scale chain mobility and the opportunity to reach such architectures. The acid treatment performed at elevated temperatures provides faster kinetics and mobility necessary to rearrange. Upon reorganizing and re-pairing its charges into these more favorable,

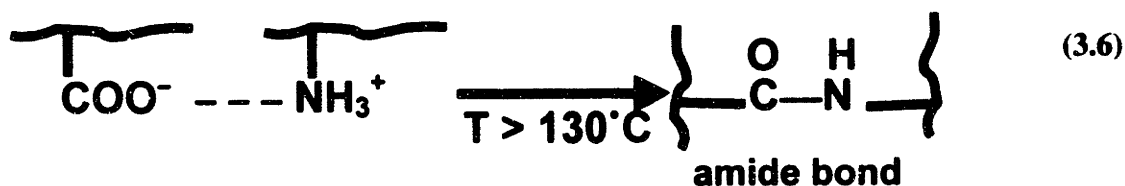
coordinatedly-stitched conformations, the multilayer complex, which displays fewer charges and more hydrophobic hydrocarbon backbones, is now less soluble in the acidic water; what subsequently results is a polyelectrolyte complex that undergoes a spinodal decomposition from the acidic water nonsolvent. The additional act of briefly rinsing an acid-exposed film in neutral water further facilitates the re-ionization of many protonated carboxylic acid groups, thus driving the multilayer to become an even less water-soluble complex. Therefore, these rinsed multilayers undergo a more intense porosity development compared to non-rinsed films, which is consistent with the evidence in section 3.3.5 regarding the thickness increase and refractive index decrease data. Ideally, the transformed 3.5/7.5 PAA/PAH multilayer develops polymeric regions that contain ionically-coordinated chain segments interdispersed among pores, which would have been filled with the water (or air upon drying). In fact, it could be assumed that these richly ionically-coordinated regions of the porous multilayers tend to resemble the stitching demonstrated by the supposedly more energetically favorable, cooperatively paired segments, such as 6.5/6.5 PAA/PAH combination.

The immersion in neutral water for longer than just a rapid 15 second rinse serves to further reorganize the already porous multilayer. During the initial spinodal demixing process, a significant amount of surface area (with high interfacial energy) is generated due to the creation of the numerous pores. In general, as was seen in Figures 3.4 and 3.5, coarsening proceeds on the porous multilayers, causing the pore size to increase. However, given further time and polymer mobility, such as being conditioned for many hours in neutral water, a secondary reorganization occurs as discussed in section 3.3.6. Over time, the system will try to minimize this additional high energy surface area by continuing to rearrange itself.<sup>19</sup> The porosity studies conducted with brief rinses really only capture a transient state, which will ultimately prefer to reduce that surface area while still being porous. The redensification of the long rinsed samples, which is manifested by the film's thickness reverting back to near its original nonporous height and its pores slightly narrowing in size (down to about ~ 100 nm or less),<sup>5</sup> is a consequence of this reduction in the surface area. These films also exhibit overall smoother surfaces in the film regions between the pores, thereby further reducing the high surface tension of the film/pore interface.

Interestingly, if the nonporous 3.5/7.75 PAA/PAH precursor film were thermally crosslinked in an amidization reaction, as shown in equation 3.6, which transforms the ionic



bonds within a multilayer into more stable, nylon-like amide bonds,<sup>15</sup> then the multilayer cannot phase separate at all upon exposure to the acidic water. Essentially, the multilayer is “locked into place,” with a covalently-bonded structure rather than an electrostatically-assembled one. The mobility needed for the polyelectrolyte chains to reorganize is also greatly reduced. Likewise, such amidization reactions may serve the useful purpose of strengthening and stabilizing an already porous multilayer of any morphology; a porous film with the percolating microporous structure such as that of Figure 3.6(a) and (c) or one that exhibits the discrete throughpore structure represented by Figure 3.6(b) and (d) may all easily be crosslinked. Furthermore, as expected, amidization prevents the percolating non-rinsed porous film such as that of Figure 3.6(a) and (c), or any other films for that matter, to undergo any secondary reorganization with long immersions in neutral water.



As indicated in section 3.3.3, the 3.5/7.5 (or 3.5/7.75) PAA/PAH multilayer appears to be an optimal precursor for creating microporous thin films. Other PAA/PAH combinations structurally similar around the 3.5/7.5 system (e.g., the 4.5/7.5 combination) similarly exhibit pH-induced phase separation and porosity transformations in acidic water. Since most of the PAA/PAH matrix consists of thicker, loop-rich films rather than thin, flat multilayers, many other various PAA/PAH combinations (e.g., the 3.5/5.5) also show some tendency to phase separate and become porous. In addition, certain aspects of the porous film, such as the refractive index, may even reach lower values using other loop-rich PAA/PAH systems, for example. Possibly because the 3.5/7.5 system is one of the thickest and most loop-rich films assembled, and could supposedly resemble the intermingled “scrambled salt” conformation more so than other systems, it undergoes some of the richest morphological porosity changes. Again, as discussed in section 3.3.3, there are potentially many other non-PAA/PAH multilayer systems that may be assembled via appropriate pH deposition conditions in randomly ionically stitched architectures, which may experience porosity development. Furthermore, by manipulating simple processing variables, such as the ionic strength or the

presence of surfactants, it is possible to effectively shift the pH regime necessary for the phase separation. In fact, recent preliminary results have indicated that PAA/PAH 3.5/7.75 multilayers may become microporous by simply being exposed to neutral aqueous solutions of the surfactant sodium dodecyl sulfate (SDS). Presumably, the polar, charged head group of the surfactant can screen electrostatic interactions within a film in a manner similar to additional salt and consequently enables the chains to reorganize and become porous.

In addition, there has been a recent publication, based on the microporosity phenomenon in the 3.5/7.5 PAA/PAH system, which reveals that PAA/PAH films assembled under pH 5.0/5.0 conditions could become nanoporous.<sup>28</sup> Similar to the 3.5/7.5 PAA/PAH case, the 5.0/5.0 combination is another example of a loop-rich multilayer with essentially fully charged molecules believed to be arranged in a random organization.<sup>17</sup> By depositing 5.0/5.0 films with added salt in both the dipping and rinsing solutions and then exposing the final multilayer into salt-free neutral water, nanoporous features could develop.<sup>28</sup> Therefore, it is becoming clear that it is possible to fine-tune an appropriate nonporous precursor and control such phase separation processing parameters as ionic strength and pH to lead to a final porous structure with desired film properties.

While a pH-induced spinodal decomposition seems to explain the porosity development, there is also some evidence for minor dewetting at the substrate-multilayer interface. Thickness and refractive index data obtained on nanoporous films (i.e., those processed with salt-containing acidic water) may vary considerably depending on the choice of the substrate (e.g., silicon, glass, or polystyrene) on which the multilayer is assembled. For instance, multilayers deposited onto untreated silicon, which has relatively poor adhesion, behave differently (i.e., the refractive index decreases more rapidly and to a lower final value) than those on chemically silane-treated silicon or plasma-treated tissue culture polystyrene, which have much better adhesive properties. However, even on these much more inherently adhesive substrates or when the substrate-film interaction is greatly improved such that there is no observable dewetting, the multilayers still readily experience the acid-driven phase separation. Therefore, the mechanism of the porosity development in polyelectrolyte multilayers is indeed due primarily to the spinodal decomposition in the acidic water nonsolvent.

### 3.4 Applications of Porous Polyelectrolyte Multilayers

There are certainly many promising applications that may arise from these micro- and nanoporous polyelectrolyte multilayers. First, due to their tunable low refractive indices, the porous films offer many unique strategies for creating useful optical coatings, which, for example, reduce glare and reflections and increase transmission. Often, such antireflection and antiglare coatings are produced by lowering the refractive indices of materials, which may be accomplished by introducing nanoporosity into the material.<sup>29</sup> The nanoporous multilayers mentioned here and further detailed in a future publication would thus be effective candidates for tunable antireflection coatings.<sup>14</sup> Besides having low refractive indices, the porous multilayers also exhibit low dielectric constants,<sup>5</sup> which could be quite valuable for microelectronic applications.

The fact that multilayers may be completely removed from the substrate at pH's < 1.7 (as shown in Figure 3.3) may be useful in selectively patterning relief features in materials. For instance, using a conventional inkjet printer, it is possible to use pH ~ 1.5 water as an "ink" to dissolve multilayers down to the substrate in order to pattern devices with a feature resolution better than 100  $\mu\text{m}$ .<sup>30</sup> For example, already it has been demonstrated that light-emitting devices could be generated simply by dissolving away an electrically-insulating PAA/PAH multilayer and then spin coating a light-emitting ruthenium complex in the voids, which were shaped into any desired design.<sup>30</sup> Furthermore, instead of completely removing the film with very low pH acid, it is possible to print the pH ~ 2.4 acidic water in patterned designs to achieve localized porosity with micrometer-resolution.

A wide range of biomaterial applications could additionally be achieved using these microporous and/or nanoporous multilayers. Membranes for filtration and separations, whether or not for biomedical uses, are certainly just one potential application. The use of these porous films for biomaterial membranes including for cell/protein/drug encapsulation, as an alternative to conventional polyelectrolyte complex coacervation chemistry, is certainly viable. Since researchers have already developed improved capsules from polyelectrolyte multilayers,<sup>31-33</sup> the further introduction of controlled nano- and/or microporosity to those capsule walls should be quite advantageous. Since the multilayers can easily conformally cover substrates of all shapes and sizes, including other synthetic biomaterials, then porous multilayer implant coatings could also be promising. Chapter 5 will address the interactions of

the nano- and microporous 3.5/7.5 PAA/PAH system with living mammalian cells, which is certainly an issue worth investigation for these biomedical applications.

The pH-induced effect of this porosity phenomenon also immediately leads to potential uses as drug and controlled release systems. Again, the PAA/PAH 3.5/7.5 combination, which becomes porous at a pH of  $\sim 2.4$  or at  $\sim 3.4$  with added salt, is simply a model system. Depending on the  $pK_a$  values of other constituent polyelectrolytes in the multilayer assembly, it should be possible to obtain controlled and sustained therapeutic release at more suitable physiologically relevant pH conditions, such as at pH  $\sim 7.4$ . Again, basic surfactant chemistry has already demonstrated the ability for the 3.5/7.5 PAA/PAH system to develop porosity at neutral conditions, and Fery et al.<sup>28</sup> have reported that 5.0/5.0 PAA/PAH multilayers assembled with salt could become nanoporous in neutral water. Moreover, there is recent preliminary evidence showing that under certain processing paths the porosity is reversible in that such pores may repeatedly open and close.<sup>14</sup> If this porosity-reversibility finding is demonstrated at higher physiological pH's, then stimulus-responsive controlled delivery systems using porous multilayer coatings seems quite possible. In addition, as stated in section 1.4.1, some groups have deposited polyelectrolyte multilayers directly onto drug<sup>34</sup> and enzyme crystals<sup>35</sup> and have demonstrated that low molecular weight ( $< 4000$  g/mol)<sup>36</sup> encapsulated substances can permeate through the multilayer film. Certainly the ability of adding controlled nano- and/or microporosity to those polyelectrolyte multilayer coatings could be of great value.

### **3.5 Conclusion and Future Work**

This chapter has presented a unique phase separation process, induced simply by acidic water to yield nano- and/or microporous polyelectrolyte multilayer thin films. While most of the chapter emphasized the 3.5/7.5 (or 3.5/7.75) PAA/PAH combination, specifically samples at  $\sim 20$  layers (i.e.,  $\sim 1000$  Å in thickness), there are many other layer numbers, deposition pH conditions, and even other multilayer systems altogether that could similarly be studied for their behavior to undergo a similar pH-driven spinodal decomposition. This chapter identified many of the various tunable processing parameters in this phase separation and revealed that there is an apparently optimal transformation pH of  $\sim 2.4$  for the 3.5/7.5 PAA/PAH case. Other variables, including the time and temperature of acid exposure, were

discussed, particularly in their influence on the overall porous morphology. The additional step of rinsing an acid-immersed multilayer in neutral water briefly for a few seconds or instead for many hours was also shown to be an important factor. Notably, two distinct porous structural extremes were identified by controlling these time, temperature, and rinsing conditions—1) a percolating, interconnected microporous regime obtainable at short times, cooler temperatures, and without rinsing, and 2) a discrete, rounded throughpore morphology achievable quickly in acid at elevated treatment temperatures or instead developed when any initially acid-exposed porous film was immersed in neutral water for several hours.

FT-IR spectroscopic characterization of the porosity transition has revealed a bond breaking and reformation mechanism, supporting the notion of a large-scale molecular reorganization in the acid treatment. At a pH  $\sim$  2.5, many of the ionized carboxylic acid groups from PAA, electrostatically paired with charged amines from PAH, are protonated to temporarily free and swell the multilayer structure. Based on structures identified in the polyelectrolyte complex literature, one potential argument was made that a porosity-driven, loop-rich film, such as the 3.5/7.5 PAA/PAH system, is arranged in a presumably randomly ionically stitched “scrambled salt” architecture. The acidic water enables the more mobile polymer chains to sample more energetically favorable conformations and thus phase separate. At room temperature and without any subsequent rinsing in neutral water, the multilayer exhibits a percolating microporous morphology. Meanwhile, the neutral water rinsing serves to reform many of the carboxylate ions to re-establish more cooperative charge pairing, resulting in a more insoluble polyelectrolyte complex, which experiences a more substantial phase separation as evident by its greater swelling and lower refractive index, compared to non-rinsed films. Long immersions in the neutral water allow the porous films to undergo a secondary reorganization, leading to a discrete throughpore structure. The observation that all porous films, no matter what the initial porosity treatment, tend to develop this throughpore morphology in neutral water over time (or rapidly in acid at higher temperatures) gives credence to its being an energetically favorable state.

In addition, manipulating the ionic strength of the acidic transformation bath has shown that it is possible to create nanoporous multilayer films (with pore sizes  $<$  100 nm). It is even possible to shift the porosity-pH curve higher by about 1 pH unit by adding more concentrated salt to less acidic water (i.e., at pH  $\sim$  3–3.5 rather than at pH  $\sim$  2–2.5).

Furthermore, crosslinking was discussed as an effective way by which to advantageously stabilize any porous structure and further revealed how chain mobility and cleaved bonds are necessary for the molecular reorganization.

The fundamental findings and analysis on this porosity effect in polyelectrolyte multilayers has been demonstrated, yet there is a great need for further future study. A more rigorous thermodynamic-based analysis that discusses this pH-induced spinodal decomposition in terms of free energy changes should be performed. Relating the findings presented here to other well-known reports on polymer and polyelectrolyte gel theory, which discuss spinodal demixing phase transitions to induce substantial, reversible swelling changes in such gels,<sup>22,23</sup> would be enlightening. This polymer gel theory could also help explain some of the recent results demonstrating how the pores of certain porous multilayer films may open and close in a “reversible” manner.<sup>14</sup> Furthermore, verifying the thickness and refractive index of these porous films using transmission/reflectance measurements from UV-visible spectroscopy, may be a useful alternative method instead of relying solely on ellipsometry or profilometry measurements, which can easily be misleading due to light scattering by the pores.

Many of the processing variables in the porosity development were presented here, but exploring them in more detail and interrelating them together could be useful in order to achieve desired morphologies, pore sizes, thicknesses, and refractive indices on demand. Thus, understanding how each parameter influences the porosity mechanism from a more quantitative thermodynamic point of view would surely be valuable in modifying and optimizing the porosity phenomenon. The combination of salt and temperature variables (each were explored individually) should also be investigated in tandem. The interesting finding that a surfactant alone could induce porosity under neutral aqueous conditions is quite significant and should certainly be explored. Assembling other multilayer systems with ionic stitching analogous to that of the 3.5/7.5 PAA/PAH combination and then identifying specific pH's for phase separation behavior would be useful to confirm the universality of the porosity effect. Ideally, with the appropriate choice of all of these many processing conditions, one could then easily tune the porosity development at will.

From an applications point of view, the study of the transport properties of porous multilayers should be performed. Nonporous multilayers have already been shown to be

suitable for separating gases and small molecules, and micro- and nanoporous multilayers as described here should similarly be useful filtration and membrane systems. Clearly, basic studies on the mass flux and permeability of these porous multilayers is necessary. The recent preliminary data showing that the porosity effect can be reversible under certain circumstances<sup>14</sup> is an important finding and similarly will be addressed in more detail in the future. Ultimately, studying small molecule and/or drug release from porous multilayers will be needed for determining their use as controlled release systems.

Overall, there appears to be a great deal of potential and versatility available from understanding the development of porous polyelectrolyte multilayers using just a simple aqueous-based pH-induced spinodal decomposition. With applications ranging from membranes to antireflection and other optical coatings to a wide variety of biomaterial purposes, these nano- and microporous polyelectrolyte multilayer thin films should provide many interesting opportunities to engineer tunable and functional porous materials.

### 3.6 References

- (1) Tsuchida, E. Formation of Polyelectrolyte Complexes and Their Structures. *J. Macromol. Sci.—Pure Appl. Chem.* **1994**, *A31*, 1.
- (2) Dubas, S. T.; Schlenoff, J. B. Polyelectrolyte Multilayers Containing a Weak Polyacid: Construction and Deconstruction. *Macromolecules* **2001**, *34*, 3736.
- (3) Cahn, J. W. Phase Separation by Spinodal Decomposition in Isotropic Systems. *J. Chem. Phys.* **1965**, *42*, 93.
- (4) Wagner, A. *Theory and Applications of the Lattice Boltzmann Method*. Ph.D. Thesis, Department of Physics; University of Oxford, 1997.
- (5) Mendelsohn, J. D.; Barrett, C. J.; Chan, V. V.; Pal, A. J.; Mayes, A. M.; Rubner, M. F. Fabrication of Microporous Thin Films from Polyelectrolyte Multilayers. *Langmuir* **2000**, *16*, 5017.
- (6) Stroeve, P.; Vasquez, V.; Coelho, M. A. N.; Rabolt, J. F. Gas Transfer in Supported Films Made by Molecular Self-Assembly of Ionic Polymers. *Thin Solid Films* **1996**, *284/285*, 708.
- (7) Krasemann, L.; Tieke, B. Composite Membranes with Ultrathin Separation Layer Prepared by Self-Assembly of Polyelectrolytes. *Mat. Sci. Eng. C* **1999**, *8/9*, 513.
- (8) Krasemann, L.; Tieke, B. Selective Ion Transport across Self-Assembled Alternating Multilayers of Cationic and Anionic Polyelectrolytes. *Langmuir* **2000**, *16*, 287.
- (9) Krasemann, L.; Toutianoush, A.; Tieke, B. Self-Assembled Polyelectrolyte Multilayer Membranes with Highly Improved Pervaporation Separation of Ethanol/Water Mixtures. *J. Membrane Sci.* **2001**, *181*, 221.

- (10) Tieke, B.; van Ackern, F.; Krasemann, L.; Toutianoush, A. Ultrathin Self-Assembled Polyelectrolyte Multilayer Membranes. *Eur. Phys. J. E* **2001**, *5*, 29.
- (11) Harris, J. J.; Stair, J. L.; Bruening, M. L. Layered Polyelectrolyte Films as Selective, Ultrathin Barriers for Anion Transport. *Chem. Mater.* **2000**, *12*, 1941.
- (12) Dai, J. H.; Jensen, A. W.; Mohanty, D. K.; Erndt, J.; Bruening, M. L. Controlling the Permeability of Multilayered Polyelectrolyte Films through Derivatization, Cross-linking, and Hydrolysis. *Langmuir* **2001**, *17*, 931.
- (13) Dubas, S. T.; Farhat, T. R.; Schlenoff, J. B. Multiple Membranes from "True" Polyelectrolyte Multilayers. *J. Am. Chem. Soc.* **2001**, *123*, 5368.
- (14) Hiller, J.; Mendelsohn, J. D.; Rubner, M. F., to be submitted, **2002**.
- (15) Harris, J. J.; DeRose, P. M.; Bruening, M. L. Synthesis of Passivating, Nylon-Like Coatings through Cross-Linking of Ultrathin Polyelectrolyte Films. *J. Am. Chem. Soc.* **1999**, *112*, 1978.
- (16) Clark, S. L.; Montague, M. F.; Hammond, P. T. Ionic Effects of Sodium Chloride on the Templated Deposition of Polyelectrolytes Using Layer-by-Layer Ionic Assembly. *Macromolecules* **1997**, *30*, 7237.
- (17) Shiratori, S. S.; Rubner, M. F. pH-Dependent Thickness Behavior of Sequentially Adsorbed Layers of Weak Polyelectrolytes. *Macromolecules* **2000**, *33*, 4213.
- (18) Klitzing, R. v.; Möhwald, H. Proton Concentration Profile in Ultrathin Polyelectrolyte Films. *Langmuir* **1995**, *11*, 3554.
- (19) Akthakul, A.; McDonald, W. F.; Mayes, A. M. Noncircular Pores on the Surface of Asymmetric Polymer Membranes: Evidence of Pore Formation via Spinodal Demixing. *J. Membrane Sci.* **2002**, in press.
- (20) Nunes, S. P.; Inoue, T. Evidence for Spinodal Decomposition and Nucleation and Growth Mechanisms During Membrane Formation. *J. Membrane Sci.* **1996**, *111*, 93.
- (21) Barton, B. F.; McHugh, A. J. Kinetics of Thermally Induced Phase Separation in Ternary Polymer Solutions. I. Modeling of Phase Separation Dynamics. *J. Polym. Sci. B* **1999**, *37*, 1449.
- (22) Shibayama, M.; Tanaka, T.; Han, C. C. Small-Angle Neutron Scattering Study on Weakly Charged Temperature Sensitive Polymer Gels. *J. Chem. Phys.* **1992**, *97*, 6842.
- (23) Mafé, S.; Manzanares, J. A.; English, A. E.; Tanaka, T. Multiple Phases in Ionic Copolymer Gels. *Phys. Rev. Lett.* **1997**, *79*, 3086.
- (24) Fuoss, R. M.; Hussein, S. Mutual Interaction of Polyelectrolytes. *Science* **1949**, *110*, 552.
- (25) Tsuchida, E.; Osada, Y.; Abe, K. Formation of Polyion Complexes between Polycarboxylic Acids and Polycations Carrying Charges in the Chain Backbone. *Die Macromolek. Chemie* **1974**, *175*, 583.
- (26) Kötz, J. Polyelectrolyte Complexes (Overview), in *Polymeric Materials Encyclopedia*; CRC Press, Inc.: Boca Raton, FL, 1996; p 5762.
- (27) Michaels, A. S. Polyelectrolyte Complexes. *Ind. Eng. Chem.* **1965**, *57*, 32.
- (28) Fery, A.; Schöler, B.; Cassagneau, T.; Caruso, F. Nanoporous Thin Films Formed by Salt-Induced Structural Changes in Multilayers of Poly(acrylic acid) and Poly(allylamine). *Langmuir* **2001**, *17*, 3779.
- (29) Hattori, H. Anti-Reflection Surface with Particle Coating Deposited by Electrostatic Attraction. *Adv. Mater.* **2001**, *13*, 51.
- (30) Rudmann, H.; Mendelsohn, J. D.; Yang, S. Y.; Rubner, M. F., to be submitted, **2002**.



- (31) Pommersheim, R.; Schrezenmeir, J.; Vogt, W. Immobilization of Enzymes by Multilayer Microcapsules. *Macromol. Chem. Phys.* **1994**, *195*, 1557.
- (32) Rilling, P.; Walter, T.; Pommersheim, R.; Vogt, W. Encapsulation of Cytochrome C by Multilayer Microcapsules. A Model for Improved Enzyme Immobilization. *J. Membrane Sci.* **1997**, *129*, 283.
- (33) Schneider, S.; Feilen, P. J.; Sloty, V.; Kampfner, D.; Preuss, S.; Berger, S.; Beyer, J.; Pommersheim, R. Multilayer Capsules: A Promising Microencapsulation System for Transplantation of Pancreatic Islets. *Biomaterials* **2001**, *22*, 1961.
- (34) Qui, X.; Leporatti, S.; Donath, E.; Möhwald, H. Studies on the Drug Release Properties of Polysaccharide Multilayers Encapsulated Ibuprofen Microparticles. *Langmuir* **2001**, *17*, 5375.
- (35) Caruso, F.; Trau, D.; Möhwald, H.; Renneberg, R. Enzyme Encapsulation in Layer-by-Layer Engineered Polymer Multilayer Capsules. *Langmuir* **2000**, *16*, 1485.
- (36) Sukhorukov, G. B.; Brumen, M.; Donath, E.; Möhwald, H. Hollow Polyelectrolyte Shells: Exclusion of Polymers and Donnan Equilibrium. *J. Phys. Chem. B* **1999**, *103*, 6434.



# **Chapter 4:**

## **Protein Interactions with Polyelectrolyte Multilayers**

### **4.1 Introductory Remarks**

Chapter 1 introduced some of the previous biomedical applications of polyelectrolyte multilayers and emphasized the fact that many groups have already manipulated such layer-by-layer processing schemes to assemble hybrid protein-containing thin films.<sup>1-12</sup> A wide range of proteins with many different physiological functions have been successfully incorporated into multilayer films, particularly for biosensing applications. Due to their multifaceted chemical nature, including notably their ionic, hydrogen bonding, van der Waals, and hydrophobic character, proteins can be assembled into multilayer films via potentially many different chemical interactions. Some researchers have even demonstrated the use of more sophisticated specific molecular binding, such as avidin-biotin chemistry, to fabricate protein multilayer films.<sup>13,14</sup>

Usually, however, researchers have exploited ionic bonding to assemble proteins with synthetic polyelectrolytes, in a similar fashion to entirely synthetic-based polymer systems. By depositing a protein at a pH value above or below its isoelectric point (pI, the point at

which the number of positive charges equals the number of negative charges), the protein can be “tuned” to be either predominantly positively or negatively ionized; the protein can then be alternated with an oppositely charged polyelectrolyte to enable the multilayer assembly. Nevertheless, regardless of the charge of the previous polyelectrolyte layer and of that of an adsorbing protein, Ladam et al.<sup>7,8</sup> have recently revealed that the protein still readily binds to the underlying polyion layer. For instance, if a protein were deposited at a pH such that it is predominantly negatively charged, it would bind strongly to a polycationic layer, as expected, yet still interact with a polyanionic layer as well. As an example, Ladam et al. have demonstrated that many different proteins, such as human serum albumin (HSA), lysozyme, and myoglobin, among others, could easily bind to both negatively and positively charged polymer layers when the proteins are either negatively or positively charged themselves.<sup>7,8</sup> Generally, however, the amount of adsorbed protein (determined by its layer thickness) on a similarly ionized polymer layer is less than that which deposits on an oppositely charged polymer surface.<sup>7,8</sup> Therefore, while overall electrostatic effects are important, other secondary bonding interactions also influence the adsorption of proteins to polymer layers.

In preparation for Chapter 5, which discusses the interactions of mammalian cells with various multilayer thin films previously introduced, this chapter investigates the adsorption of proteins to the surfaces of two distinct systems: the 2.0/2.0 and the 3.5/7.5 PAA/PAH combinations. To reiterate, cells interact with their environment (i.e., other cells, the extracellular matrix, and synthetic biomaterial surfaces) via their transmembrane proteins, such as integrins. Thus, studying if and how proteins bind to polyelectrolyte multilayer surfaces is an important issue related to ultimately understanding how living cells behave, i.e., attach, spread, and proliferate, on the thin films.

The technique used to analyze protein adsorption herein is known as surface plasmon resonance (SPR), an optical method based on the concept of total internal reflection. SPR concerns the reflection of incident light off a thin metal (e.g., gold or silver) film at the interface between two optically different media, such as glass and a liquid. Although the incident light is entirely internally reflected, an evanescent (short-lived) wave component of the light still propagates across the metal interface into the less dense medium (e.g., the liquid) and excites freely oscillating electrons, known as plasmons.<sup>15,16</sup> At a certain incident angle, called the surface plasmon resonance angle, the evanescent wave resonates with the

plasmons. Since this SPR angle is a function of the refractive index adjacent to the metal film, any change in the refractive index will consequently shift the SPR angle.<sup>15,16</sup> In a typical experimental set-up, a buffer is flowed over an optical sensing cell, followed by the flow of a buffered solution of interest (e.g., one that contains proteins). The adsorption of proteins and its associated mass (density) change near the metal interface will cause the local refractive index to change and thus the SPR angle to shift. This shifting is detected in real-time by the SPR instrument, and the amount of protein adsorbed may easily be quantified. Figure 4.1 depicts a schematic of the surface plasmon resonance experimental set-up and how changes in the refractive index are converted to profiles of the angle shifts with time.

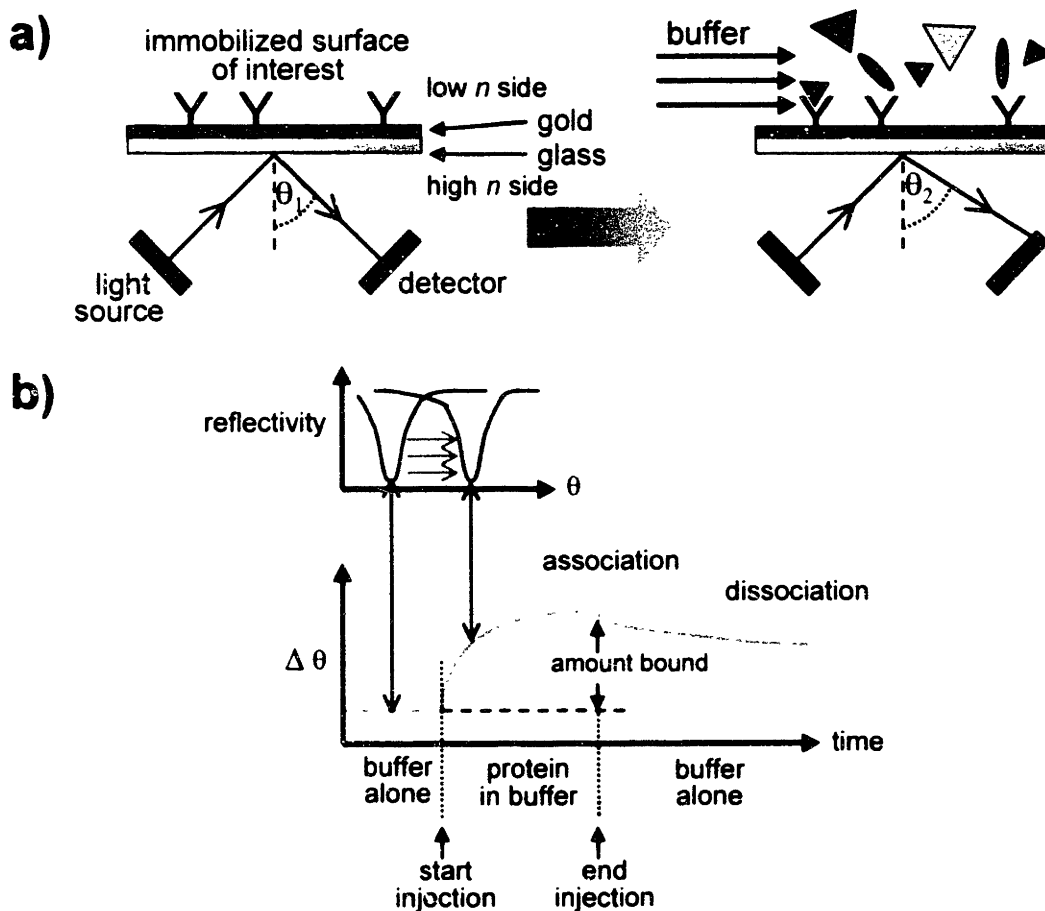


**Figure 4.1:** a) A schematic of the experimental flow cell used in SPR detection. A sensing chip consisting of a thin layer of gold on glass is modified with a surface of interest (in this case, sequentially-adsorbed polyions to form multilayers); proteins in a buffer are flowed over the surface, and any protein-surface binding is detected via refractive index changes, as shown in (b). Adsorption of protein influences the local refractive index and thus the reflectivity of the light, shifting the SPR angle  $\theta$ . Continuous monitoring of the angle shifts over time leads to the creation of adsorption profiles, as depicted in (b). (Adapted from ref. # 16.)

Previously, SPR has been employed to study real-time biological interactions, including, for example, antigen-antibody binding,<sup>15</sup> ligand-receptor binding, enzyme kinetics, and DNA hybridization,<sup>17</sup> among others. Recently, SPR has been used quite frequently to monitor protein adhesion to self-assembled monolayers (SAMs), which are composed of alkanethiols on gold, terminated with a variety of chemical functional groups.<sup>18-26</sup> Researchers anticipate that using SAMs can provide a systematic way to investigate the interactions of proteins with numerous different chemical features, with the hope that it is possible to correlate protein adhesion with cell attachment.<sup>24,25</sup> This chapter details the results regarding using the SPR technique to monitor the adsorption of two different proteins, lysozyme and fibrinogen, to the 2.0/2.0 and 3.5/7.5 PAA/PAH multilayers. Chapter 5 will then review these findings in trying to explain the interactions of these multilayers with living mammalian cells.

## **4.2 Materials and Methods**

### **4.2.1 Materials**

For the 2.0/2.0 multilayers, both PAA and PAH were prepared as  $5 \times 10^{-3}$  M solutions in ultrapure 18 M $\Omega$ -cm Millipore water, prior to pH adjustment. For the 3.5/7.5 case, the PAA and PAH were prepared as  $1 \times 10^{-3}$  M solutions in Millipore water and then pH adjusted. All polymer solutions were filtered through a 0.2  $\mu$ m Acrodisc filter. Lysozyme (from chicken egg white) and fibrinogen (from bovine plasma) were obtained from Sigma. The lysozyme and fibrinogen were prepared as 1 g/L and 0.2 g/L solutions, respectively, in Dulbecco's phosphate buffered saline (PBS) (pH ~ 7.4, with calcium and magnesium).

### **4.2.2 Surface Plasmon Resonance**

**Multilayer thin film deposition.** Gold-coated glass sensing substrates (Biacore, Inc.) were used for all experiments without any additional surface preparation. Using a BIAcore™ 2000 SPR instrument from Biacore, Inc., polyelectrolyte multilayers were assembled in situ with continuous monitoring of the refractive index changes adjacent to the gold substrate. The temperature for the deposition and subsequent protein studies was maintained at 25°C. Neutral Millipore water was used as the buffer in all multilayer assembly procedures and was flowed over a new gold chip for a minimum of 1 hour prior to polymer deposition. Beginning with PAH as the first layer, PAA and PAH were injected (injection volume = 100  $\mu$ L) one at a

time with a flow rate of 20  $\mu\text{L}/\text{min}$  over the gold surface. After injection, the flow cell was washed for 2 minutes with neutral water, before the introduction of the next polyelectrolyte. This process was repeated until 10 or 11 layers were assembled for the 3.5/7.5 system or 14 or 15 layers for the 2.0/2.0 PAA/PAH case, with odd and even layer numbers referring to a PAH and a PAA film surface, respectively.

**Protein adsorption.** After the appropriate number of layers had been adsorbed onto the gold chip, the buffer was changed from water to Dulbecco's PBS. The PBS was flowed over the multilayer-coated gold sensor substrate for at least 1 hour at a flow rate of 10  $\mu\text{L}/\text{min}$ . Then 100  $\mu\text{L}$  of lysozyme and fibrinogen were injected with a flow rate of 10  $\mu\text{L}/\text{min}$  over separate parts of the multilayer film (i.e., there was no competition between the proteins in binding to the film). PBS was then used again to flow over multilayer and wash it of any excess or poorly bound protein. The magnitude of the adsorption of lysozyme and fibrinogen to each multilayer surface was then quantified graphically with the Biacore software.

## 4.3 Results and Discussion

### 4.3.1 Assembly of Polyelectrolyte Multilayers

In this study, PAA/PAH films were deposited directly onto gold substrates in the SPR instrument by flowing the individual polymers over the gold chip one at a time. With this technique, the in situ growth of a multilayer film was therefore monitored continuously over time. To compare the effect of the charge of the outermost layer, multilayers ending in both PAA and PAH were created for each system. Normally, SPR experiments involve the injection of proteins or other analytes over a surface of interest immobilized on the gold chip; any protein-surface interaction or binding is observed via the refractive index changes, manifested in the resulting SPR signal. By analogy, in this case, the polyions were "injected" repeatedly and alternately in order to deposit the different multilayers.

Figure 4.2 presents representative graphs of the layer-by-layer deposition of both the 2.0/2.0 and 3.5/7.5 PAA/PAH multilayers, as fabricated in the SPR instrument. It is evident from the plots that the thin films do indeed build successfully in a stepwise, incremental fashion on the gold sensor chip. The association and dissociation phases of the adsorption are also clearly visible, particularly in Figure 4.2(b), which shows a larger view of three

sequential layers from the graph in (a). It should be noted that the y-axis is in terms of measured response units (RU), which are simply linearly related to the amount of angle shifting detected. The SPR instrument used in these studies defines the relation that 1000 RU is equivalent to a shift of  $0.1^\circ$ . The absolute value of the response units is arbitrary; what is significant is only the change in the response units, which corresponds to a change in the SPR angle and thus indicates material adsorption. Other groups have observed similar stepwise deposition in monitoring the layer-by-layer adsorption process. For instance, Pei et al.<sup>27</sup> investigated the assembly of negatively charged DNA and the positively charged poly(diallyldimethylammonium chloride) (PDAC), revealing an incremental layer growth resembling that of Figure 4.2.

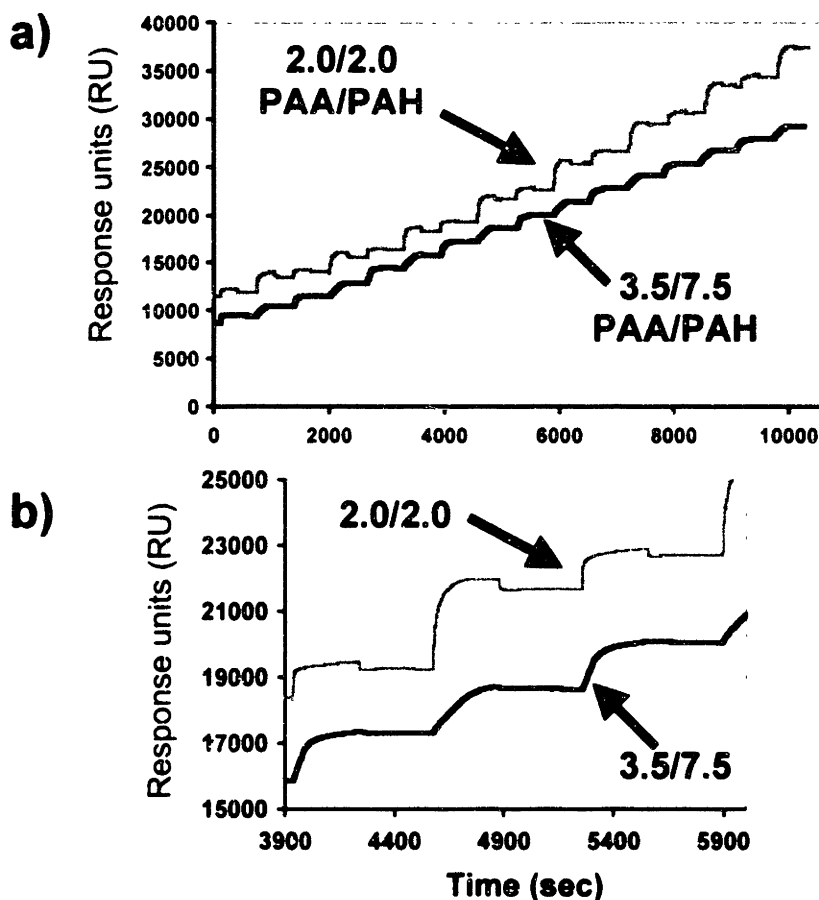


**Figure 4.2:** a) Representative response units vs. time graph obtained from SPR data, displaying stepwise growth of 16 polymer layers for the PAA/PAH 2.0/2.0 and 3.5/7.5 systems as assembled on the plain gold sensor chips. The absolute values of the response units are unimportant, and only the relative change is meaningful. b) A larger image of the time region from 3900 sec to 6000 sec from graph (a), which more clearly shows the increase in the SPR signal, exhibiting both associative and dissociative adsorption phases.



### 4.3.2 Protein Adsorption to Polyelectrolyte Multilayers

After the PAA/PAH multilayers were successfully assembled in situ on the gold sensor chips in the SPR instrument, protein adsorption experiments were performed. Usually, buffered salt-containing solutions are used in all SPR studies, as is typical of most experiments with proteins. However, the buffer used during the fabrication of the films was simply pure Millipore water, thereby creating an aqueous-based process similar to that of how multilayers are assembled outside of the SPR apparatus. Of necessity, the buffer was then changed to physiological saline, PBS, (pH ~ 7.4, I ~ 0.15 M) for the subsequent protein studies. In general, it is normal to allow the buffer to flow over the surface of interest (here, the various multilayers) for some time in order to achieve a stable, flat baseline prior to protein injection. In fact, there was at least 1 hour maintained between the time of incubation of the PBS solution and the injection of any protein. Such time allowed for the baseline to stabilize, since there were significant decreases in the value of the response units; interestingly, this reduction in the SPR response units reflects that fact that the films are swelling, as expected, in the buffer.

Previously, other groups have employed SPR experiments to observe the swelling of materials by water or buffers. For instance, Green et al.<sup>28</sup> researched the hydration behavior of various poly(ethylene oxide) (PEO) hydrogels using SPR analysis. The well-known swelling and hydration of PEO-based materials is offered as an explanation for their protein and cell resistance.<sup>29</sup> Green et al.<sup>28</sup> reported that these PEO-containing hydrogels exhibited characteristic negative SPR angle shifts, which were indicative of the polymers swelling in the water. As the polymers became hydrated in the water, the net refractive index of the swollen hydrogel would decrease, thereby resulting in a negative shift in the SPR angle.<sup>28</sup> Thus, the substantial reduction in the SPR response units observed after the incubation with the PBS buffer (as well as with water to a lesser extent) in these multilayer studies clearly suggests the films are swelling. The relationship of this film swelling to the cell culture experiments performed on these multilayers will be addressed further in Chapter 5.

After ~ 1 hour of swelling in the PBS buffer (which is a longer time needed for the baseline to stabilize), two proteins—lysozyme and fibrinogen—were injected independently over the film surface. Both of these proteins have frequently been used in SPR studies as model proteins for investigating the adhesiveness of various surfaces. A large (MW ~ 340 kD)

blood plasma protein, fibrinogen is representative of “sticky” serum proteins, since it readily binds to hydrophobic surfaces.<sup>19</sup> The pI of fibrinogen is ~ 5.5,<sup>26</sup> rendering it predominantly negatively charged under physiological buffer conditions. Lysozyme is a much smaller (MW ~ 14 kD) enzymatic protein, which is highly positively ionized at pH ~ 7.4 conditions, since its pI is ~ 11.<sup>19,26</sup> Consequently, lysozyme is a good indicator of electrostatic interactions involved in protein adhesion, particularly to anionic surfaces.

Figure 4.3 displays the amount of each protein adsorbed to the different PAA/PAH multilayer films, prepared with both PAA and PAH as the last layer deposited. For comparison purposes, the adsorption of both proteins to the plain gold chip, without any polymer coating, is also provided. The absorbed amount was simply derived from the SPR manufacturer’s guidelines that, regardless of the size and molecular weight of the protein, 1000 response units is equivalent to ~ 1 ng/mm<sup>2</sup> of adsorbed protein. The change in response units was obtained simply from the SPR software computing the relative difference between the SPR signal at the baseline prior to the protein injection and the signal after the injection was completed, as illustrated in Figure 4.1(b).

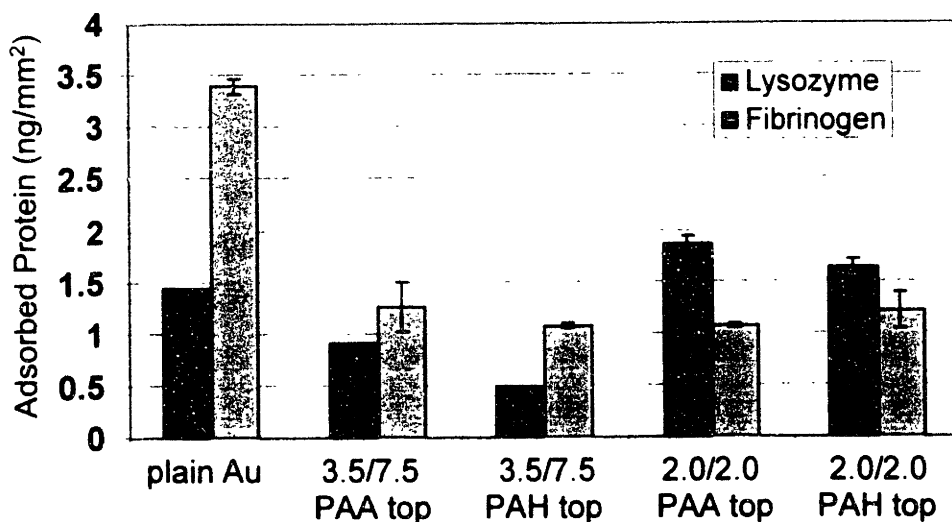


**Figure 4.3:** SPR-derived adsorption data for lysozyme and fibrinogen on an uncoated gold surface and gold coated with 3.5/7.5 or 2.0/2.0 PAA/PAH multilayers.

As expected, both proteins bind nonspecifically to the relatively hydrophobic gold surface, with about twice as much of the more hydrophobic fibrinogen adhering compared to the lysozyme. All PAA/PAH multilayer surfaces also exhibited some protein adhesion, irrespective of the identity and charge characteristics of the outermost layer. However, in

many cases, the amount of adsorbed lysozyme was less than that on the gold control, and the adsorbed fibrinogen was always consistently less than that on gold. In addition, there are interesting results observed on the specific multilayer surfaces. With the 3.5/7.5 PAA/PAH films,  $\sim 0.91 \text{ ng/mm}^2$  of lysozyme adsorbed when PAA was the last deposited layer, compared to only  $\sim 0.48 \text{ ng/mm}^2$  when PAH was the outermost layer. Such results are consistent with the fact that in pH  $\sim 7.4$  buffer conditions the numerous uncharged carboxylic acid groups (COOH) on a PAA-topped film would necessarily ionize to carboxylate groups (COO<sup>-</sup>), which would strongly attract highly cationic lysozyme molecules. Meanwhile, an overall cationic PAH outermost surface, with a few unbound amines and many positively charges (although mainly already bound to the preceding PAA layer) would not be expected to attract as much lysozyme. Of course, some positively charged lysozyme molecules can still bind even to a similarly charged PAH surface via negative charged domains on the protein, other secondary interactions, and binding to any PAA chain segments penetrating into the surface. Likewise, the anionic fibrinogen binds to either a PAA or PAH outermost layer of the 3.5/7.5 system about equally well.

For the 2.0/2.0 PAA/PAH multilayers, the fact that the films are overall dominated by PAA segments, especially in the form of unbound acid groups, is evident in the protein adhesion findings. As discussed in section 2.3, both a PAA and a PAH outermost layer are highly rich in free acids, which readily ionize in the PBS buffer to become negatively charged (COO<sup>-</sup>); this high degree of negative charges on both PAA and PAH surfaces attracts a significant amount of the cationic lysozyme. Compared to the 3.5/7.5 system, the 2.0/2.0 PAA/PAH case overall possesses much more free acid character, which is also independent of the identity of the outermost layer. As Figure 4.3 shows, the COO<sup>-</sup> surface-rich 2.0/2.0 PAA/PAH films bind more cationic lysozyme than in the 3.5/7.5 case. In addition, these 2.0/2.0 films attract more oppositely charged lysozyme than the anionic fibrinogen. All of these results confirm earlier work<sup>7,8</sup> showing that similarly charged proteins and multilayer surfaces may easily attract each other due to electrostatic binding between the surface and other oppositely charged parts of the protein, secondary interactions, and the mixed, interpenetrated nature of many multilayer surfaces.

From these results, it may be concluded that the polyelectrolyte multilayers examined here bind the cationic lysozyme roughly the same amount or less on average compared to an

uncoated gold substrate. However, fibrinogen binds to gold about 3 times more than to both the 3.5/7.5 and 2.0/2.0 PAA/PAH films, irrespective of the identity of the outermost layer. Thus, compared to gold, multilayers somewhat resist, although certainly not completely, the adsorption of a hydrophobic protein such as fibrinogen. Overall, the multilayers do indeed adhere proteins to some degree, which is not surprising due to the many demonstrations in the polyelectrolyte multilayer literature of all types of proteins being able to adsorb to previous polymeric layers to fabricate alternating polymer-protein films.

It should be noted that any protein adsorption on the gold and on the multilayer coatings is occurring through nonspecific interactions, since there are no peptide adhesive ligands (e.g., the amino acid RGD tripeptide) to precisely bind only certain proteins. Of course, as mentioned in section 1.1, eliminating nonspecific protein and cell interactions is an emerging theme in biomaterials engineering, which demands the creation of effective bioinert materials. According to the data presented here, the 3.5/7.5 and 2.0/2.0 PAA/PAH films are not protein resistant materials, a finding which would certainly impact their use as biomaterials. Nevertheless, as will be presented in Chapter 5, the correlation between protein and cell adhesion is relatively poor and still not well understood,<sup>24</sup> although many groups have tried to elucidate what determines the protein resistance or adhesiveness of a given surface. In fact, many routinely measurable surface properties, such as wettability, conformation aspects, and polarity do not seem to correlate well with how the surface will interact with proteins.<sup>19</sup> A recent conclusion has been that suitable protein resistant materials possess polar functionalities, are net electrically neutral, and contain hydrogen bond acceptors but not hydrogen bond donors, such as COOH or NH<sub>2</sub> groups.<sup>19,23</sup> However, most of these studies were performed with self-assembled monolayers (SAMs) on gold, terminated with a variety of chemical functional groups; such general rules may not necessarily apply to the interactions of proteins with the more complex nature of highly interpenetrated polyelectrolyte multilayers. Obviously, according to these general findings, the functional groups of neither PAA nor PAH would be considered protein resistant but would rather be inherently adhesive. Recently, for instance, it has been reported that SAMs grafted with PAH chains were found to be protein adhesive.<sup>18</sup>

## 4.4 Conclusion and Future Work

This chapter has introduced an investigation into the interaction of proteins with two typical weak polyelectrolyte multilayer systems. The technique of surface plasmon resonance has been demonstrated to be an effective way by which to explore: 1) the in situ assembly of multilayers, showing a characteristic stepwise growth of the individual layers, and 2) the ability of proteins to nonspecifically interact with such fabricated multilayers. Consistent with recent findings in the literature, the outermost layer easily attracted both oppositely and similarly charged proteins. There was also some dependence on the nature of the multilayer system; for instance, a COOH-rich 2.0/2.0 film attracted a substantial amount of the cationic lysozyme to either a PAA or PAH outermost layer, confirming the fact that, in either case, the film is dominated by PAA chains and its surface becomes highly ionized to  $\text{COO}^-$ , which readily binds the oppositely charged protein.

In the future, it would be interesting to examine more types of proteins, including ones with different molecular weights, isoelectric points, and other characteristics. For example, the common protein serum albumin is considered to be a nonadhesive protein compared with fibronectin, for instance, which readily adheres cells.<sup>30</sup> Thus, one must be careful in saying that a surface found to be protein adhesive would correspondingly be cell adhesive, if, for instance, it binds the protein albumin, which is nonadhesive to cells.<sup>30</sup> Ultimately, it would be advantageous to relate these and other more extensive protein adhesion studies with in vitro cell culture experiments, although researchers investigating both protein and cells studies on SAMs with identical materials found no obvious correlation. It would also be useful to measure, alongside the protein adsorption experiments with these multilayers, the response to known protein resistant ethylene glycol SAMs<sup>21-23</sup> or other ethylene glycol-rich materials, such as poly(oxyethylene) methacrylate (POEM) comb polymers<sup>31</sup> for comparison purposes. Furthermore, confirming the protein adhesion results via another complimentary technique, such as quartz crystal microbalance (QCM) gravimetric analysis to measure the uptake of proteins to polymer films through mass/frequency changes could prove valuable.

Besides studying protein adhesion, the use of SPR techniques to investigate the assembly of polyelectrolyte multilayers would be quite informative, as well. Other groups researching multilayers have recently realized the utility of SPR for monitoring the in situ film growth as the layers are built in solution. Overall, SPR seems to be an especially useful

method to compliment dry (in air) measurements on thin films, which do not necessarily reflect the actual dynamic adsorption process of the aqueous-based layer assembly. Such in situ characterization methods will surely prove useful in elucidating the swelling and related behavior of multilayers in fluids, which is of great importance in understanding their potential role as biomaterials.

## 4.5 References

- (1) Onda, M.; Lvov, Y.; Ariga, K.; Kunitake, T. Sequential Reaction and Product Separation on Molecular Films of Glucoamylose and Glucose Oxidase Assembled on an Ultrafilter. *J. Ferment. Bioeng.* **1996**, *82*, 502.
- (2) Caruso, F.; Niikura, K.; Furlong, D. N.; Okahata, Y. 2. Assembly of Alternating Polyelectrolyte and Protein Multilayer Films for Immunosensing. *Langmuir* **1997**, *13*, 3427.
- (3) Caruso, F.; Möhwald, H. Protein Multilayer Formation on Colloids Through a Stepwise Self-Assembly Technique. *J. Am. Chem. Soc.* **1999**, *121*, 6039.
- (4) Caruso, F.; Schüler, C. Enzyme Multilayers on Colloid Particles: Assembly, Stability, and Enzymatic Activity. *Langmuir* **2000**, *16*, 9595.
- (5) Caruso, F.; Fiedler, H.; Haage, K. Assembly of  $\beta$ -glucosidase Multilayers on Spherical Colloidal Particles and Their Use as Active Catalysts. *Colloids Surf. A* **2000**, *169*, 287.
- (6) Decher, G.; Lehr, B.; Lowack, K.; Lvov, Y.; Schmitt, J. New Nanocomposite Films for Biosensors: Layer-by-Layer Adsorbed Films of Polyelectrolytes, Proteins or DNA. *Biosens. Bioelect.* **1994**, *9*, 677.
- (7) Ladam, G.; Gergely, C.; Senger, B.; Decher, G.; Voegel, J.-C.; Schaaf, P.; Cuisinier, F. J. G. Protein Interactions with Polyelectrolyte Multilayers: Interactions between Human Serum Albumin and Polystyrene Sulfonate/Polyallylamine Multilayers. *Biomacromolecules* **2000**, *1*, 674.
- (8) Ladam, G.; Schaaf, P.; Cuisinier, F. J. G.; Decher, G.; Voegel, J.-C. Protein Adsorption onto Auto-Assembled Polyelectrolyte Films. *Langmuir* **2001**, *17*, 878.
- (9) Lvov, Y.; Ariga, K.; Kunitake, T. Layer-by-Layer Assembly of Alternate Protein/Polyion Ultrathin Films. *Chem. Lett* **1994**, 2323.
- (10) Lvov, Y.; Ariga, K.; Ichinose, I.; Kunitake, T. Assembly of Multicomponent Protein Films by Means of Electrostatic Layer-by-Layer Adsorption. *J. Am. Chem. Soc.* **1995**, *117*, 6117.
- (11) Lvov, Y.; Munge, B.; Giraldo, O.; Ichinose, I.; Suib, S. L.; Rusling, J. F. Films of Manganese Oxide Nanoparticles with Polycations or Myoglobin from Alternate-Layer Adsorption. *Langmuir* **2000**, *16*, 8850.
- (12) Onda, M.; Lvov, Y.; Ariga, K.; Kunitake, T. Sequential Actions of Glucose Oxidase and Peroxidase in Molecular Films Assembled by Layer-by-Layer Alternate Adsorption. *Biotech. Bioeng.* **1996**, *51*, 163.

- (13) Anicet, N.; Bourdillon, C.; Moiroux, J.; Savéant, J.-M. Step-by-Step Avidin-Biotin Construction of Bienzyme Electrodes. Kinetic Analysis of the Coupling between the Catalytic Activities of Immobilized Monomolecular Layers of Glucose Oxidase and Hexokinase. *Langmuir* **1999**, *15*, 6527.
- (14) Anzai, J.; Nishimura, M. Layer-by-Layer Deposition of Avidin and Polymers on a Solid Surface to Prepare Thin Films: Significant Effects of Molecular Geometry of the Polymers on the Deposition Behaviour. *J. Chem. Soc. Perkin Trans. 2* **1997**, 1887.
- (15) Caruso, F.; Vukusic, P. S.; Matsuura, K.; Urquhart, R. S.; Furlong, D. N.; Okahata, Y. Investigation of Immuno-Reactions in a Flow-Injection System Using Surface Plasmon Resonance. *Colloids Surf. A* **1995**, *103*, 147.
- (16) Green, R. J.; Frazier, R. A.; Shakesheff, K. M.; Davies, M. C.; Roberts, C. J.; Tendler, S. J. B. Surface Plasmon Resonance Analysis of Dynamic Biological Interactions with Biomaterials. *Biomaterials* **2000**, *21*, 1823.
- (17) Jordan, C. E.; Frutos, A. G.; Thiel, A. J.; Corn, R. M. Surface Plasmon Resonance Imaging Measurements of DNA Hybridization Adsorption and Streptavidin/DNA Multilayer Formation at Chemically Modified Gold Surfaces. *Anal. Chem.* **1997**, *69*, 4939.
- (18) Chapman, R. G.; Ostuni, E.; Liang, M. N.; Meluleni, G.; Kim, E.; Yan, L.; Pier, G.; Warren, H. S.; Whitesides, G. M. Polymeric Thin Films That Resist the Adsorption of Proteins and the Adhesion of Bacteria. *Langmuir* **2001**, *17*, 1225.
- (19) Chapman, R. G.; Ostuni, E.; Takayama, S.; Holmlin, R. E.; Yan, L.; Whitesides, G. M. Surveying for Surfaces that Resist the Adsorption of Proteins. *J. Am. Chem. Soc.* **2000**, *122*, 8303.
- (20) Silin, V.; Weetall, H.; Vanderah, D. V. SPR Studies of the Nonspecific Adsorption Kinetics of Human IgG and BSA on Gold Surfaces Modified by Self-Assembled Monolayers (SAMs). *J. Colloid Interface Sci.* **1997**, *185*, 94.
- (21) Chapman, R. G.; Ostuni, E.; Yan, L.; Whitesides, G. M. Preparation of Mixed Self-Assembled Monolayers (SAMs) That Resist Adsorption of Proteins Using the Reaction of Amines with a SAM That Presents Interchain Carboxylic Anhydride Groups. *Langmuir* **2000**, *16*, 6927.
- (22) Holmlin, R. E.; Chen, X.; Chapman, R. G.; Takayama, S.; Whitesides, G. M. Zwitterionic SAMs that Resist Nonspecific Adsorption of Protein from Aqueous Buffer. *Langmuir* **2001**, *17*, 2841.
- (23) Ostuni, E.; Chapman, R. G.; Holmlin, R. E.; Takayama, S.; Whitesides, G. M. A Survey of Structure-Property Relationships of Surfaces that Resist the Adsorption of Protein. *Langmuir* **2001**, *17*, 5605.
- (24) Ostuni, E.; Chapman, R. G.; Liang, M. N.; Meluleni, G.; Pier, G.; Ingber, D. E.; Whitesides, G. M. Self-Assembled Monolayers That Resist the Adsorption of Proteins and the Adhesion of Bacterial and Mammalian Cells. *Langmuir* **2001**, *17*, 6336.
- (25) Luk, Y.-Y.; Kato, M.; Mrksich, M. Self-Assembled Monolayers of Alkanethiols Presenting Mannitol Groups Are Inert to Protein Adsorption and Cell Attachment. *Langmuir* **2000**, *16*, 9604.
- (26) Sigal, G. B.; Mrksich, M.; Whitesides, G. M. Effect of Surface Wettability on the Adsorption of Proteins and Detergents. *J. Am. Chem. Soc.* **1998**, *120*, 3464.

- (27) Pei, R.; Cui, X.; Yang, X.; Wang, E. Assembly of Alternating Polycation and DNA Multilayer Films by Electrostatic Layer-by-Layer Adsorption. *Biomacromolecules* **2001**, *2*, 463.
- (28) Green, R. J.; Corneillie, S.; Davies, J.; Davies, M. C.; Roberts, C. J.; Schacht, E.; Tandler, S. J. B.; Williams, P. M. Investigation of the Hydration Kinetics of Novel Poly(ethylene oxide) Containing Polyurethanes. *Langmuir* **2000**, *16*, 2744.
- (29) Wang, R. L. C.; Kreuzer, H. J.; Grunze, M. Molecular Conformation and Solvation of Oligo(ethylene glycol)-Terminated Self-Assembled Monolayers and Their Resistance to Protein Adsorption. *J. Phys. Chem. B* **1997**, *101*, 9767.
- (30) Tidwell, C. D.; Ertel, S. I.; Ratner, B. D.; Tarasevich, B. J.; Arte, S.; Allara, D. L. Endothelial Cell Growth and Protein Adsorption on Terminally Functionalized, Self-Assembled Monolayers of Alkanethiols on Gold. *Langmuir* **1997**, *13*, 3404.
- (31) Irvine, D. J.; Mayes, A. M.; Griffith, L. G. Nanoscale Clustering of RGD Peptides at Surfaces Using Comb Polymers. 1. Synthesis and Characterization of Comb Thin Films. *Biomacromolecules* **2001**, *2*, 85.



# **Chapter 5: Cell Interactions with Polyelectrolyte Multilayers**

## **5.1 Introductory Remarks**

As the field of polyelectrolyte multilayers continues to expand, it is becoming apparent that these versatile, nanostructured thin film coatings could have significant potential as biomaterials. Already, numerous studies have examined multilayers for biosensor applications<sup>1-3</sup> and controlled release and drug delivery systems.<sup>4-8</sup> In a logical extension of that work, researchers are beginning to explore polyelectrolyte multilayers as bio-interactive materials,<sup>9-12</sup> as discussed earlier in section 1.4.2. Central to those investigations is the need to elucidate the biocompatibility of polyelectrolyte multilayers, particularly their interaction with living cells. However, few studies to date have examined cell behavior on multilayers, especially with regard to relating the resultant cell attachment and growth with the underlying molecular architecture of the thin films.

One noteworthy study, that of Elbert et al., revealed how multilayers assembled from the biopolymers polylysine and alginate, were resistant to the attachment of human fibroblast cells.<sup>9</sup> Moreover, the multilayers could block these highly adhesive cells from interacting with

extracellular matrix (ECM), collagen, and tissue culture polystyrene (TCPS) surfaces.<sup>9</sup> Again, as explained in section 1.1.2, finding materials to create a bioinert background, which first resists nonspecific protein and cell attachment and then which could be functionalized to bind only desired cells and/or proteins, is an important, emerging theme in designing biomaterials. This chapter surveys the cell response of mouse fibroblasts to a wide range of multilayer combinations, consisting of different constituent polyelectrolytes and deposition pH's, as previously identified in Chapter 2. As it will be presented, there are many other cell-resistant multilayer systems besides the one reported by Elbert et al. Quite significantly, this chapter furthermore describes that by manipulating the pH deposition conditions to thus control the underlying molecular architecture, it is possible to fine-tune a single multilayer combination to be either cell adhesive or cell resistant. For example, the PAA/PAH system, already discussed throughout this thesis, can be readily directed via its molecular assembly to be either adherent (e.g., the 6.5/6.5 case) or completely bioinert (e.g., the 2.0/2.0 case) to the fibroblasts.

## **5.2 Materials and Methods**

### **5.2.1 General Multilayer Deposition and Assembly**

Multilayer thin films, as described previously in section 2.2.1, were directly deposited onto tissue culture polystyrene (TCPS) petri dishes and multiwell plates (Falcon) for in vitro cell studies. Other substrates, including polished <100> silicon wafers (Wafernet), glass slides (VWR Scientific), ZnSe crystals (SpectraTech), and TCPS slides (Nalgene) were used for complimentary multilayer characterization studies. The specific multilayer systems assembled for surveying their interaction with living mammalian cells were (as described previously in Chapter 2): 1) PAA/PAH at pH 3.5/7.5, 6.5/6.5, and 2.0/2.0; 2) PMA/PAH at pH 6.5/6.5 and 2.5/2.5; 3) PAA/PAAm at pH 3.0/3.0; 4) PMA/PAAm at pH 3.0/3.0; 5) SPS/PAH at pH 6.5/6.5, 2.0/2.0, and 10.0/10.0; and 6) SPS/PDAC at pH 6.5/6.5 with and without salt (0.25 M NaCl).

### **5.2.2 Cell Culture**

Unless stated otherwise, all cell culture reagents were purchased from Gibco/Invitrogen/Life Technologies. Murine NR6WT fibroblasts, a cell line derived from

mouse NIH 3T3 cells, were obtained from the laboratory of Prof. Linda Griffith at MIT. Standard sterile cell culture techniques were used for all cell experiments. After the TCPS substrates were coated with the desired multilayer system and with the appropriate number of layers, the substrates were spray sterilized with 70% (v/v) ethanol (VWR Scientific). The NR6WT fibroblasts were cultured in a humid 37°C/ 5% CO<sub>2</sub> incubator in complete pH ~ 7.4 growth media consisting of Modified Eagles Medium- $\alpha$  (MEM- $\alpha$ ) supplemented with 7.5% (v/v) fetal bovine serum (FBS), 1% (v/v) nonessential amino acids (10 mM), 1% (v/v) sodium pyruvate (100 mM), 1% (v/v) L-glutamine (200 mM), 1% (v/v) penicillin (10,000 U/ml, Sigma), 1% (v/v) streptomycin (10 mg/ml, Sigma), and 1% (v/v) Geneticin (G418) antibiotic (350  $\mu$ m/mg). Serum free media was prepared identically to the complete serum-containing media except that the FBS was replaced by 1 g/L bovine serum albumin (Sigma, Fraction V). For normal cell maintenance, cells were grown near confluence in Falcon T75 TCPS flasks or dishes, washed once with warm Dulbecco's phosphate buffered saline (PBS) (pH ~ 7.4), detached with trypsin (1X) (Sigma), and passaged semiweekly.

For quantitative attachment and proliferation assays, the cells were resuspended in normal serum-containing media after the trypsinization and then spun down in a centrifuge at ~1000 rpm for ~5 minutes. The cells were then resuspended in fresh media, mixed in a 1:1 ratio with 0.4% trypan blue (Sigma) and counted with a hemocytometer with trypan blue exclusion to determine cell viability prior to seeding. The NR6WT fibroblasts were seeded at ~10,000 cells/cm<sup>2</sup> onto the sterilized multilayer-coated substrates (day 0), and their population was counted daily with a hemocytometer with trypan blue exclusion. A Nikon inverted phase contrast microscope with Openlab 3.0 software was used for all experiments to capture images of the cell density, spreading, and population growth on the various multilayer surfaces over a minimum of 5 days. In the cell attachment and proliferation assays, the media was usually changed daily, except for cases where cells did not adhere to the multilayers, when media was instead changed at most every other day.

### **5.2.3 Characterization Methods**

Multilayers assembled for studies to compliment the in vitro cell experiments were analyzed using the surface characterization techniques detailed previously in section 2.2. Profilometry and ellipsometry were used to obtain thickness data. AFM imaging was

employed for surface morphology profiling and roughness measurements. FT-IR spectroscopy provided chemical bonding information. Complimentary wettability studies on various multilayers were performed on TCPS slides (Nalgene) preconditioned in various solutions to mimic the treatment seen by multilayer-coated TCPS substrates used for the cell experiments. Specifically, the TCPS slides were immersed in: 1) 70% ethanol, 2) Dulbecco's phosphate buffered saline (PBS) with calcium and magnesium (pH ~ 7.4), 3) complete nutrient media (pH ~ 7.4, with 7.5% FBS), or 4) serum-free media (pH ~ 7.4) for a minimum of 7 days in a humid 37°C/ 5% CO<sub>2</sub> incubator. The samples were removed from the incubator, rinsed briefly with pure Millipore water, and flushed dried with N<sub>2</sub> gas before the advancing and receding contact angles were obtained.

#### **5.2.4 In Situ Swelling Experiments**

The in situ swelling of representative multilayer thin film samples was obtained by using a Digital Instruments Multimode Scanning Probe Microscope in contact mode, both in air and under fluid (Dulbecco's PBS with calcium and magnesium (pH ~ 7.4)). First, films assembled onto silicon substrates were scored down to the bare silicon. A single one dimensional line was imaged repeatedly by first positioning the tip over this scratch, resulting in a clean cross-sectional profile of the film thickness relative to the scratch depth. After obtaining such a profile in air, the same sample was imaged in a fluid cell injected with enough PBS to form a uniform droplet over the tip. The score was again imaged repeatedly to achieve a cross-sectional profile under fluid. Any swelling information could then easily be derived by comparing the differences in film thicknesses during the "in air" and the "under fluid" experiments.

### **5.3 Results**

#### **5.3.1 General Findings: PAA/PAH Multilayers**

To investigate the adhesion and growth of mammalian cells to different multilayer surfaces, NR6WT fibroblasts were seeded at ~10,000 cells/cm<sup>2</sup> onto sterilized cell culture plates that had been directly, conformally coated with the appropriate multilayer system and number of layers (without any additional priming steps). As fibroblasts, the NR6WT cells are responsible for aiding in wound healing and synthesizing the extracellular matrix (ECM), the

supporting scaffold on which many cells anchor. Furthermore, as an anchorage-dependent cell line, NR6WT fibroblasts must be attached to a substrate for survival and are well known to be highly adherent to many biological and synthetic surfaces. These cells also secrete their own adhesion molecules, such as fibronectin, a common protein used to bind cells. Consequently, NR6WT fibroblasts are a strong indicator of the degree of adhesiveness of a surface.

Many studies were performed on the PAA/PAH multilayer combination, in particular the 6.5/6.5, 3.5/7.5, and 2.0/2.0 PAA/PAH systems, whose important film characteristics were compared and contrasted in section 2.3. Figure 5.1 presents the number of attached NR6WT cells on a TCPS control surface and on each of these PAA/PAH multilayer surfaces over several days. As expected, the population of cells increases with time on the highly cell-adhesive TCPS control. Similarly, the cell population increases on the 6.5/6.5 and 3.5/7.5 PAA/PAH multilayers with little difference with respect to whether the outermost layer was cationic (PAH) or anionic (PAA) in either multilayer system. This observation is quite intriguing, since, for example, the surface of a 3.5/7.5 PAA/PAH multilayer under pH ~ 7.4 buffer conditions is essentially fully negatively charged and dominated by carboxylate ions ( $\text{COO}^-$ ), when PAA is the outermost layer, whereas an outermost PAH layer is rich in ion-paired charged amines ( $\text{NH}_3^+$ ).

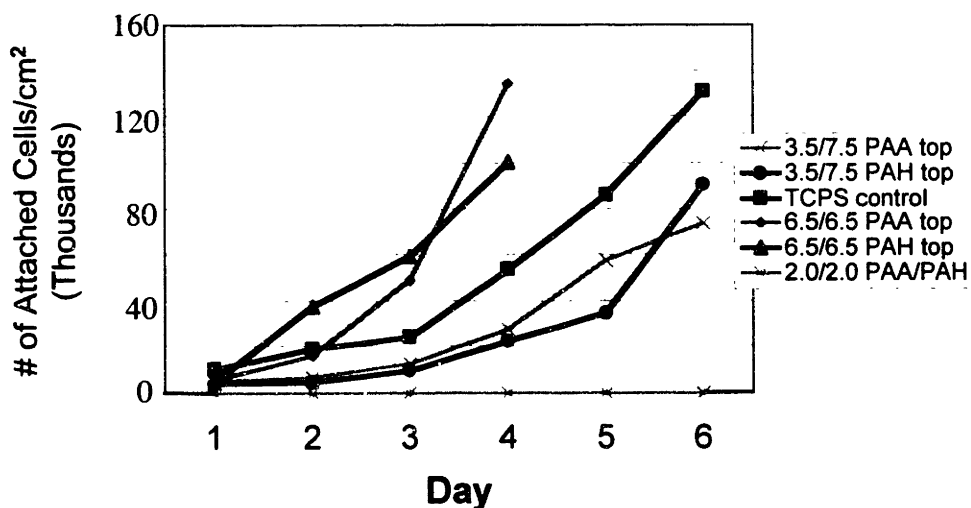


**Figure 5.1:** Graph of the number of fibroblasts attached on various PAA/PAH multilayers and on a TCPS control. The initial seeding density on day 0 was ~10,000 cells/cm<sup>2</sup>. 20- and 21-layer films (corresponding to PAA- and PAH-topped, respectively) were deposited for the 3.5/7.5 and 2.0/2.0 systems; 40 and 41 layers were assembled for the 6.5/6.5 system. Both PAA and PAH-topped 2.0/2.0 films are completely resistant to cell attachment. The same number of layers for each multilayer condition was used for the samples displayed in Figure 5.2.


Phase contrast micrographs of representative fields of the fibroblasts cells on these different multilayers over several days are shown in Figure 5.2. The cell density clearly increases in the TCPS, 6.5/6.5, and 3.5/7.5 PAA/PAH samples, with the cells becoming confluent on the TCPS control by late day 3 and onwards. The images reveal that the fibroblasts exhibit substantial attachment, good spreading into their characteristic elongated morphologies, and noticeable proliferation onto both 6.5/6.5 and 3.5/7.5 PAA/PAH multilayers, similar to that on the TCPS control. Viability analysis with the dye trypan blue has also revealed high cell viability (> 95 %) on all of these adhesive multilayer surfaces.

However, in stark contrast to the TCPS control and the 3.5/7.5 and 6.5/6.5 PAA/PAH systems, fibroblasts seeded onto 2.0/2.0 PAA/PAH multilayers show essentially no attachment and spreading on those surfaces but rather simply remain suspended in the cell culture media, as shown in Figure 5.2(d). The question arises as to whether any cells ever did initially attach to *and then subsequently detached from* these seemingly highly cell-resistant 2.0/2.0 multilayers. Such behavior—cells adhering and subsequently becoming non-adherent and simply floating—would suggest that the multilayers are potentially cytotoxic. However, microscopic examination performed 2 to 5 hours post-seeding revealed no cells ever attaching to the 2.0/2.0 PAA/PAH films. Therefore, it may be concluded that PAA/PAH multilayers assembled at pH conditions of 2.0/2.0 are bioinert; the 3.5/7.5 and 6.5/6.5 PAA/PAH systems are, in contrast, cell adhesive.


All of these in vitro experiments were performed in pH ~ 7.4 serum-containing media, consisting of many essential factors and adhesion proteins, such as fibronectin and vitronectin, necessary for proper cell adhesion and growth. Therefore, the cells were never exposed to the rather harsh acidic conditions *during the assembly* of the 2.0/2.0 system, which could lead to cell death. Even with this highly adhesive cell line and the additional adhesion proteins plentiful in the serum media, 2.0/2.0 PAA/PAH multilayers prevent all noticeable fibroblast attachment. If the suspended cells from the 2.0/2.0 films were also transplanted to fresh TCPS surfaces, even after 2 days of floating, many cells readily attached on the adhesive TCPS, as presented in Figure 5.3. In fact, the transplanted cell population would increase as usual over several days as it would on any TCPS control. The observation that once non-adherent cells could attach and grow as normal, healthy cells on a fresh adhesive surface again validates the concept that the bioinert 2.0/2.0 multilayers are not overtly cytotoxic.

Rather, such materials would be suitable candidates for the cell-resistant backgrounds for engineering biomaterial interfaces that eliminate undesirable, nonspecific cell adhesion.

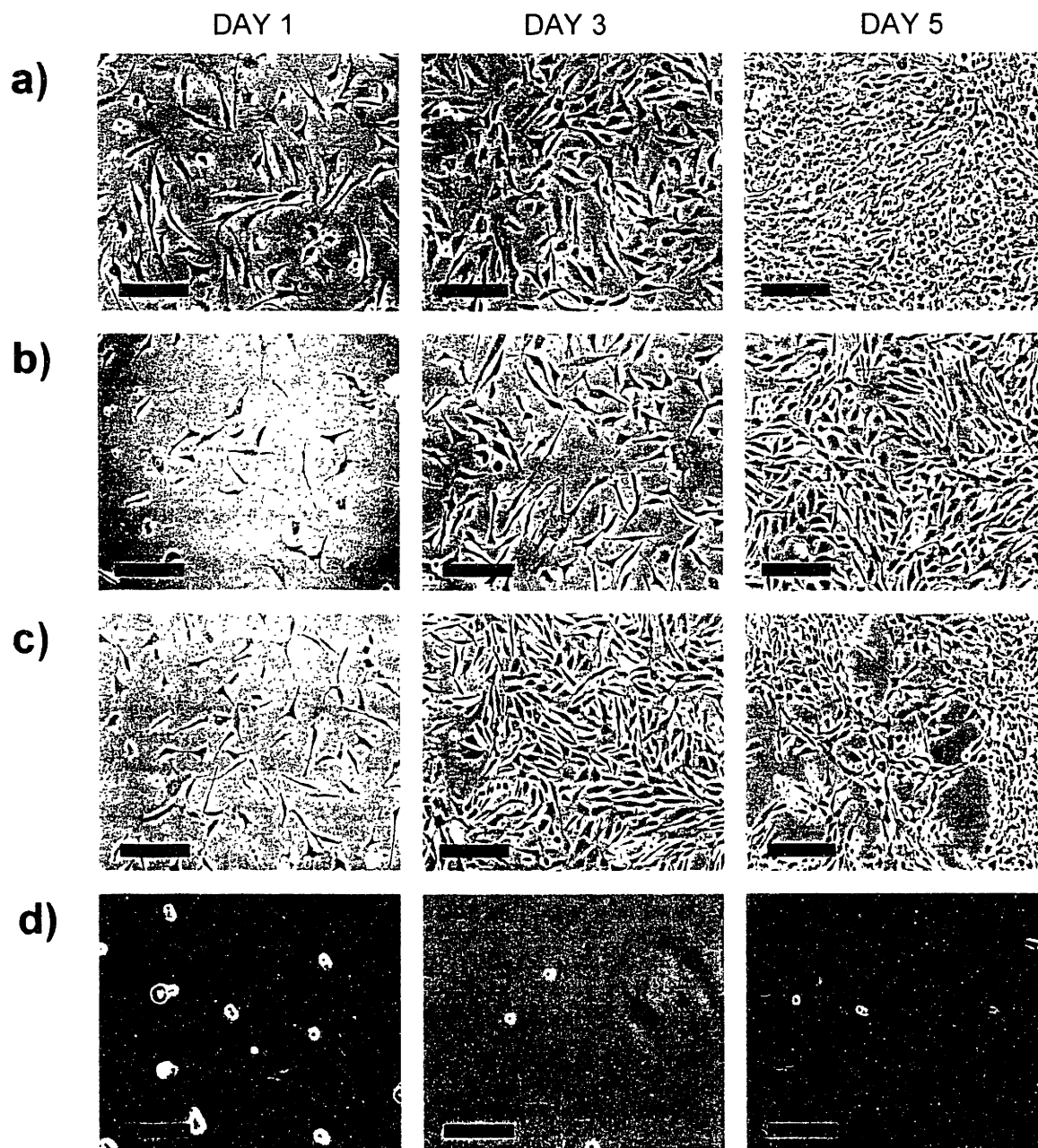


**Figure 5.2:** Phase contrast photographs over several days of NR6WT fibroblasts seeded onto various PAA/PAH multilayers and a TCPS control. The cells readily attach, spread, and proliferate on: a) the TCPS control surface, b) the 3.5/7.5 PAA/PAH multilayer, with either polymer as the last layer deposited, and c) the 6.5/6.5 PAA/PAH system, again with either polymer as the outermost layer. By day 3 and onwards, the cells on these surfaces become fairly confluent. However, the 2.0/2.0 PAA/PAH multilayer, shown in (d), is completely cell resistant, as suggested by the floating, nonadherent cells. (  = 200  $\mu\text{m}$ )



**Figure 5.3:** A phase contrast photograph, taken on day 3, of attached cells on a TCPS surface. The cells were transferred from an initially bioinert 2.0/2.0 PAA/PAH multilayer and remained floating for 2 days in the culture media, resembling what is observed in Figure 5.2(d). Once transplanted, the fibroblasts attach, spread, and proliferate as normal, suggesting that the 2.0/2.0 material was not overtly toxic to the cells. A truly cytotoxic surface would leave few, if any, living cells behind to continue to behave as normal on a fresh TCPS or other adhesive surface. (  = 200  $\mu\text{m}$ )


To reiterate the descriptions from section 2.3 regarding these various PAA/PAH systems, the 6.5/6.5 combination is ultrathin due to the high degree of ionization on both the PAA and PAH molecules. The 3.5/7.5 system, although much thicker and loop-rich, still exhibits a significant degree ( $> 80\%$ ) of charged groups on the PAA and PAH chains. On the contrary, the 2.0/2.0 PAA/PAH system predominantly consists of PAA segments and is quite rich in unpaired carboxylic acids (COOH) (as assembled, not in the cell experimental conditions, when the groups would ionize to  $\text{COO}^-$ ). Based only on these cell findings and the underlying molecular structure (i.e., the degree of ionization), it was hypothesized that multilayer thin films composed of other polyelectrolytes could similarly be bioinert; if these other thin films were fabricated in such a way that the final assembled structure consists of one or both of the polymer(s) with many free, unpaired groups, then perhaps those films could also be cell resistant. The next few sections address other polyelectrolyte multilayer combinations, which are analogous to the 2.0/2.0 PAA/PAH condition with regards to having one polymer with a low degree of ionization (as assembled); it will be shown that these other systems are similarly bioinert. Finally, section 5.4 explains more in depth the chemical and structural issues regarding the cell adhesiveness or resistance of multilayer thin films and tries to provide a more rigorous approach to identifying the source of the bioinertness exhibited by certain multilayers.



### 5.3.2 General Findings: PMA/PAH, SPS/PAH, and SPS/PDAC Multilayers

Chapter 2 identified several other polyelectrolyte multilayer systems, including the poly(methacrylic acid) (PMA)/PAH combination. (Most PMA/PAH thin film samples were prepared by Postdoctoral Associate Sung Yun Yang in the Rubner group at MIT.) Except for the additional methyl group in each repeat unit (as seen in Figure 2.1(b)), PMA is a weak polyanion identical to PAA with ionizable carboxylic acid groups. By substituting PMA for PAA in multilayers with PAH still remaining as the polycation, it was found that these PMA/PAH films yielded similar results with cells as PAA/PAH ones. Specifically, as shown in Figure 5.4, PMA/PAH multilayers assembled at pH 6.5/6.5 exhibited significant cell adhesion, yet PMA/PAH films constructed at pH 2.5/2.5 demonstrated substantially reduced cell attachment, as indicated by the rounded morphology of many floating, non-adherent cells. This latter system resembles the 2.0/2.0 PAA/PAH combination in terms of having a high degree of free acids, while the former system, having both polymers stitched in essentially fully charged, ultrathin conformations, is analogous to the 6.5/6.5 PAA/PAH condition.

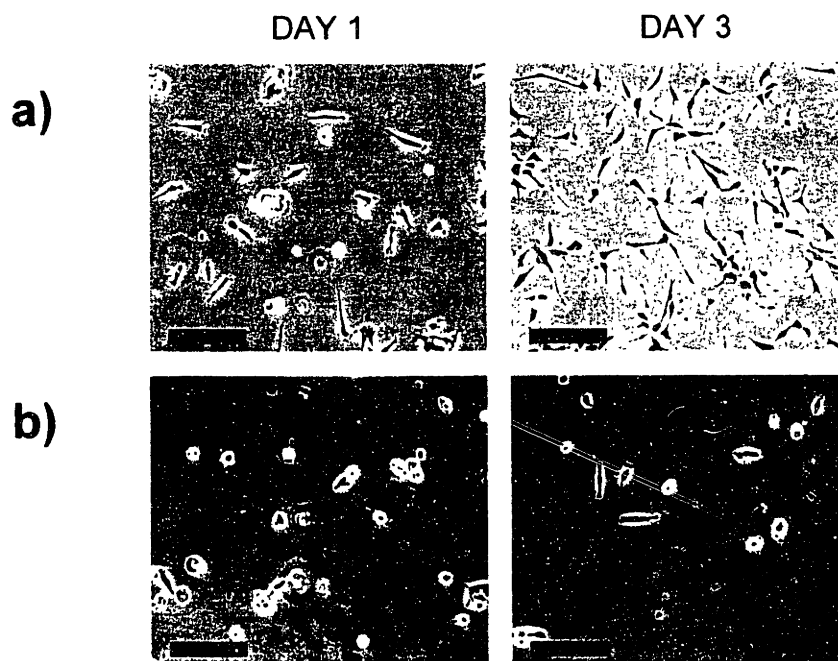


**Figure 5.4:** Phase contrast photographs of the in vitro behavior of NR6WT fibroblasts seeded onto PMA/PAH multilayers at: a) pH 6.5/6.5 deposition conditions and b) pH 2.5/2.5 conditions. These PMA/PAH films evoke similar cell responses as that observed on PAA/PAH films assembled at closely corresponding pH values. 47 and 48 layers (PAH and PAA outermost layers, respectively) were deposited for the 6.5/6.5 PMA/PAH system, while 25 and 26 layers (PAH and PAA outermost layers, respectively) were deposited for the 2.5/2.5 PMA/PAH condition. (  = 200  $\mu\text{m}$ )


Instead of using a structurally-similar weak polyanion for PAA to form alternating layers with PAH, it is possible to replace the PAA or PMA with a strong (i.e., always fully charged) polyanion, poly(styrene sulfonate) (SPS). Figure 5.5 presents cell morphology pictures over several days obtained with various SPS/PAH multilayers. As stated in section 2.4.4, the SPS/PAH combination forms fully charged, ultrathin multilayers under *both* 6.5/6.5 and 2.0/2.0 pH deposition conditions. Analogous to the fully ionized, tightly stitched PAA- and PMA-/PAH 6.5/6.5 systems, Figures 5.5(a) and (b) show how SPS/PAH thin films were highly cell adhesive at both pH 6.5/6.5 *and* at 2.0/2.0 conditions.

However, it is also possible to manipulate the pH-dependent charged density of the weak PAH molecules. With a  $pK_a \sim 9$ , PAH is only slightly ionized at basic pH's, while the SPS remains fully charged. Adsorption measurements with the anionic dye rose bengal, which binds to unpaired, charged amines, confirms the low degree of ionization of PAH in multilayers assembled at high pH's but not at neutral ones (e.g., 6.5/6.5 SPS/PAH). Therefore, it is possible to fabricate multilayers containing an essentially fully ionized SPS polyanion and a slightly charged PAH by depositing the films at high pH's. Section 2.4.4 identified the SPS/PAH 10.0/10.0 combination as an example of such a system, and, as seen in Figure 5.5(c), this condition is also cell resistant. Again, the 10.0/10.0 SPS/PAH system is analogous both structurally as well as in terms of cell interactions to the PAA/PAH and PMA/PAH combinations fabricated at low pH's. These results confirm how simple adjustments in the deposition pH conditions or of the constituent polyions assembling the multilayers may lead to powerful differences in cell response.

Just as a strong, fully charged SPS was substituted for PAA or PMA, it is possible to replace PAH with a fully ionized polycation, such as poly(diallyldimethylammonium chloride) or PDAC. An example of two alternating strong polyelectrolytes, SPS/PDAC thin films assembled without additional salt are tightly stitched and thus ultrathin at all pH values, as stated earlier in section 2.4.5. Furthermore, similar to the thin, fully charged SPS/PAH, PAA/PAH, or PMA/PAH systems, the SPS/PDAC multilayers are also quite cell adhesive, as shown in Figure 5.6(a). However, when the ionic strength of the PDAC and SPS solutions was increased (which is usually how these strong polyions are processed in the literature), the screening of charges by the salt ions yielded thicker, loop-rich films, resembling multilayers formed when weak polyelectrolytes are assembled at pH conditions to leave a low degree of

ionization of one polymer. Figure 5.6(b) displays that when 0.25 M NaCl was added to the solutions, these salt-containing SPS/PDAC multilayers were cell resistant.

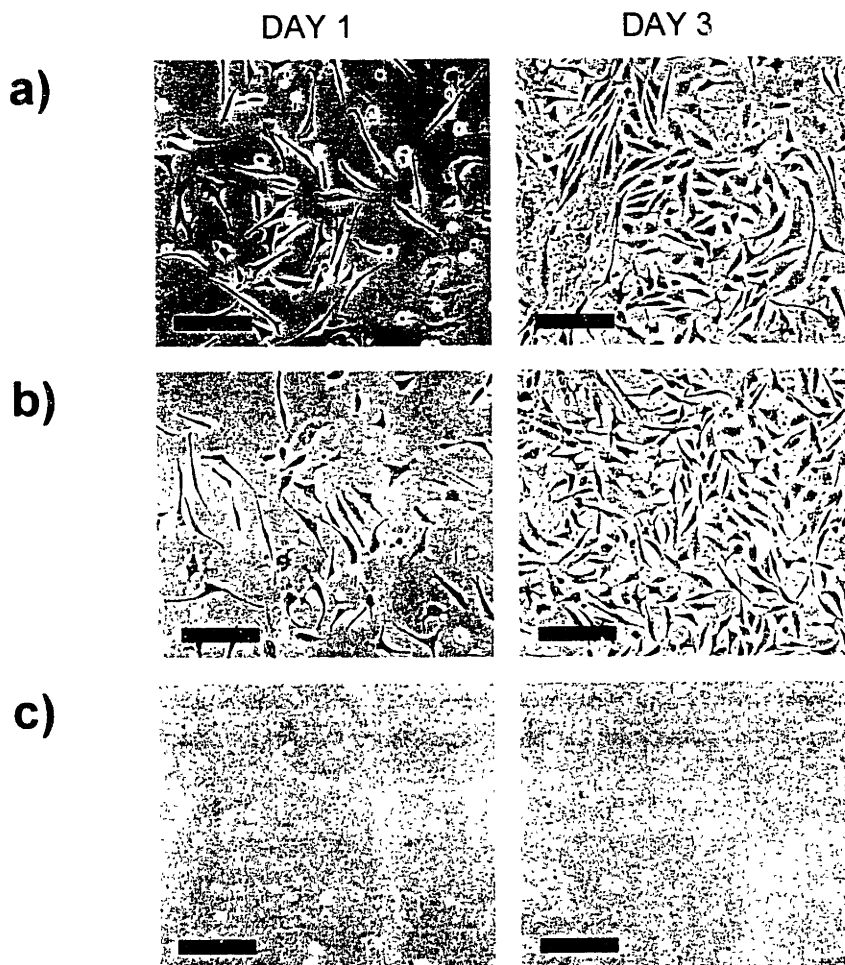



**Figure 5.5:** Phase contrast photographs of NR6WT fibroblasts seeded onto SPS/PAH multilayers at: a) 6.5/6.5, b) 2.0/2.0, and c) 10.0/10.0 assembly conditions, exhibiting cell adhesiveness for the first two systems but inertness for the latter. 40- and 41-layer films (PAA- and PAH-topped films, respectively) were deposited for the 6.5/6.5 and 2.0/2.0 systems; 20 and 21 layers (PAA and PAH outermost layers, respectively) were assembled for the 10.0/10.0 condition. (  = 200  $\mu\text{m}$ )

### 5.3.3 General Findings: PAA/PAAm and PMA/PAAm Multilayers


Besides the electrostatically constructed multilayers, Chapter 2 discussed how completely hydrogen-bonded systems also exist, such as between polyacrylamide (PAAm) and PAA or PMA. (Postdoctoral Associate Sung Yun Yang fabricated all of these hydrogen-bonded multilayer samples for the cell studies.) A well-known bioinert (protein resistant polymer),<sup>13,14</sup> PAAm is often employed in the form of a crosslinked gel for protein

electrophoresis experiments in biochemistry. Figure 5.7 reveals how PAA/PAAm and PMA/PAAm thin films are cell resistant, with all the cells floating in the media.

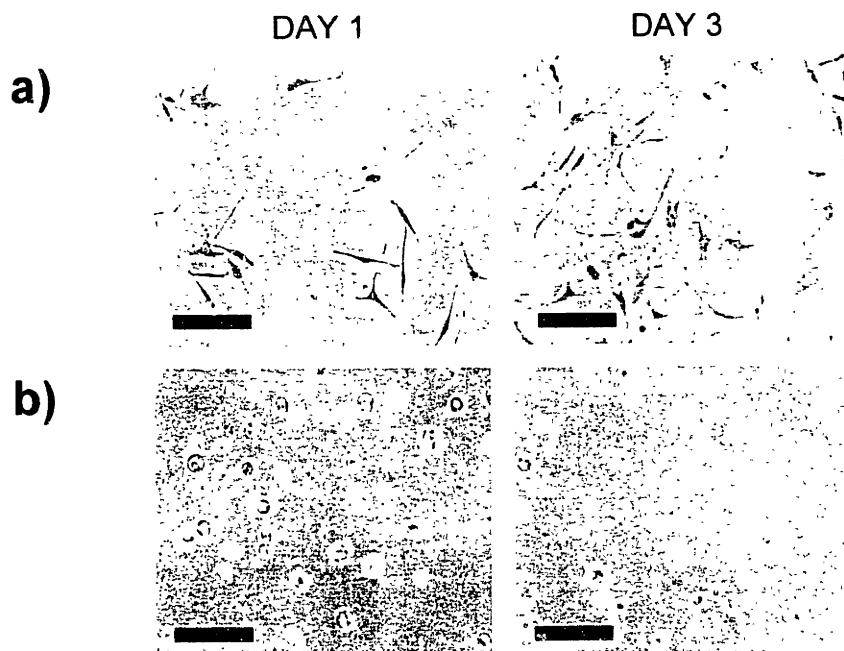


**Figure 5.6:** Phase contrast photographs of NR6WT fibroblasts seeded onto SPS/PDAC multilayers at pH 6.5/6.5 conditions a) without and b) with additional salt of 0.25 M NaCl. Samples prepared without salt were 40 or 41 layers; salt-containing samples were 20 or 21 layers. (  = 200  $\mu$ m)

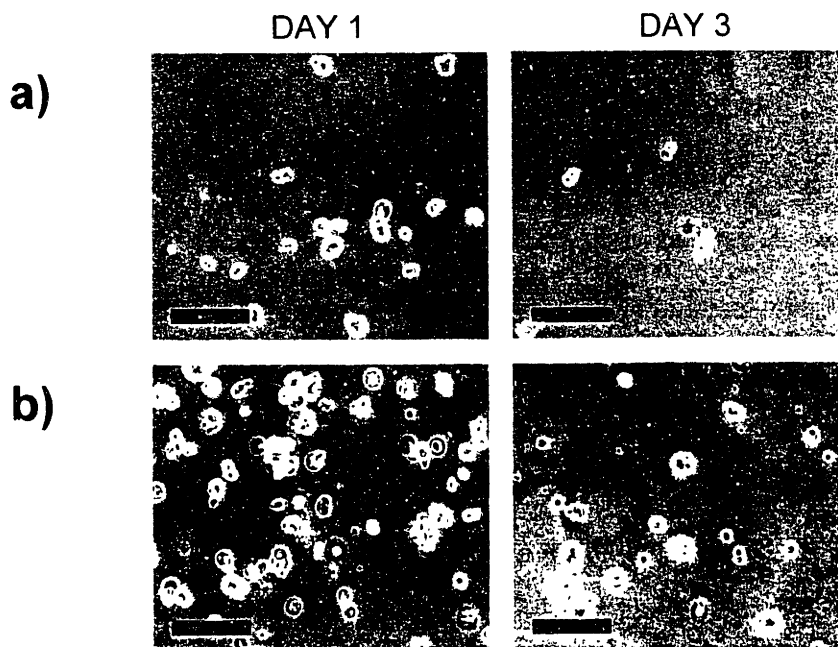


**Figure 5.7:** Phase contrast photographs of NR6WT fibroblasts seeded onto hydrogen-bonded multilayers assembled from: a) PAA/PAAm at pH 3.0/3.0 conditions and b) PMA/PAAm at pH 3.0/3.0 conditions; these polyacrylamide-containing multilayers are highly cell resistant, even with only a few (e.g., 3) layers. (  = 200  $\mu$ m)

## 5.4 Discussion

### 5.4.1 General Remarks

It is not surprising that a highly adhesive cell line such as the NR6WT fibroblasts are able to attach, via *nonspecific* interactions, to TCPS substrates and many multilayer surfaces, especially in the presence of serum proteins. However, it is quite intriguing that many different multilayer assemblies identified in section 5.3 are actually highly cell resistant. More remarkable is the observation that a single polyion multilayer combination can be engineered to be either cell adhesive or cell resistant by simply adjusting the pH deposition conditions or increasing the ionic strength, as in the case of SPS/PDAC films. Thus, it is worth trying to elucidate what underlying themes govern whether or not a multilayer thin film will be bioinert.

As stated in section 5.3, every example of a cell resistant multilayer had one of its constituent polymers in only a slightly ionized state (or uncharged altogether as in the case of the hydrogen-bonded films) usually due to pH control or, in the bioinert case of SPS/PDAC, due to salt effects. It is important to emphasize that this low degree of ionization only concerns the films *as assembled*, since exposure to the pH ~ 7.4 cell media would cause many of those initially uncharged functional groups to ionize. For instance, the abundant number of non-charged carboxylic acids (COOH) on a surface and within a typical 2.0/2.0 PAA/PAH film would readily ionize to COO<sup>-</sup>; this ionization is confirmed by FT-IR spectroscopy as well as UV-vis absorbance measurements, which show the COO<sup>-</sup>-rich 2.0/2.0 films bind high amounts of the cationic dye methylene blue. Thus, there may be some correlation between having many non-ionized, unpaired groups in the as-prepared multilayer, which consequently encourages cell resistance. Chapters 1 and 2 showed that films possessing a polyion with a low degree of charged groups correspondingly led to loop-rich layer conformations, thicker films overall, and generally rougher surfaces. Additionally, polyelectrolyte multilayers are inherently hydrated structures<sup>9</sup>; being highly hydrated and having favorable interactions with water, which is one explanation for the protein and cell resistance of polymeric or oligomeric ethylene glycol (PEO, PEG, or o-EG),<sup>15,16</sup> could help to explain the bioinertness manifested by some multilayers. In fact, the reason provided by Elbert et al. regarding the bioinertness of their alginate/polylysine multilayers is because of the high degree of hydration and overall

hydrogel character of the films.<sup>9</sup> Furthermore, the authors also report that alginate and polylysine have already displayed some bioinertness in their history as biomaterials, particularly in their use as complex coacervates. Such an explanation, presenting a highly hydrated surface that appears to be just water rather than a surface able to promote cell attachment, would certainly justify the bioinertness exhibited by multilayers containing PAAm, a polymer whose inertness and low toxicity are already well established.<sup>13,14</sup>

Interestingly, many of the polymers (and their individual functional groups) discussed here are naturally cell adhesive. It should be noted that several literature reports state that PAH and its amine group are quite protein and cell adhesive.<sup>17</sup> The carboxylic acid group (COOH), the chemical functionality found in PAA and PMA, is similarly often employed to encourage cell binding to hydrogels, e.g., poly(hydroxyethyl methacrylate), which do not generally support cell attachment.<sup>18-20</sup> In fact, Ghosh et. al have reported that hyperbranched PAA films were cell adhesive due to their carboxylic acids, but that grafting PEG to the PAA was required in order to render the surface cell resistant.<sup>21</sup> Modifying surfaces with SAMs of alkanethiols with COOH terminus groups has also frequently been used to enhance cell adhesion.<sup>22,23</sup> In addition, PAA is well known as a bioadhesive and, specifically, a mucoadhesive polymer,<sup>24,25</sup> since its carboxylic acid groups can readily bind with divalent ions (e.g., Ca<sup>2+</sup>) in mucus linings within the body; drug delivery applications have resulted from this unique characteristic of PAA.<sup>24</sup>

On the contrary, there has been at least one report in which highly hydrated PAA grafted chains were able to significantly reduce, but not completely eliminate, the attachment of endothelial cells.<sup>26</sup> Of course, as stated previously, most studies employing PAA have instead shown that the polymer and its carboxylic acid groups encouraged cell attachment. Thus, whereas PAH and carboxylic-acid rich polymers and their respective functional groups, when processed via conventional grafting or self-assembly methods are often reported to be cell-adhesive, multilayers provide an alternative route by which to blend them together into specific molecular architectures. Ultimately, one may importantly direct the resulting thin films generated from a single multilayer combination to be either cell-adhesive or cell-resistant. At this point, it is worth understanding more the observed interactions of these various multilayers with the fibroblasts, with special attention being paid to explaining the their unique feature of tunable bioinertness.

## 5.4.2 Wettability Studies

Many surface features of a biomaterial are believed to have role in determining its overall biocompatibility with the body. For instance, the wettability of a biomaterial's surface is often examined to help explain cell-materials observations. However, there has been no general consensus as to what degree of hydrophilicity or hydrophobicity is best suited to prevent or encourage cell attachment and growth. For example, Altankov et al. found that human fibroblasts interacted more favorably, adhered better, and proliferated more on hydrophilic surfaces, such as glass ( $\theta \sim 25^\circ$ ), than on more hydrophobic materials, e.g., polylactate ( $\theta \sim 70^\circ$ ) and silicone ( $\theta \sim 111^\circ$ ).<sup>27</sup> Horbett et al.<sup>28</sup> similarly reported that glass and other more hydrophilic surfaces attracted more cells than hydrophobic ones, since the ionic groups, e.g., carboxylic acids, usually found on wettable materials can interact better with the charges on the cells' surface proteins compared to nonpolar, hydrophobic materials. Other ionic groups, such as sulfonate and hydroxyl functionalities, also tend to enhance cell adhesion.<sup>21</sup> On the contrary, there have been many reports that highly wettable surfaces (e.g.,  $\theta < 20^\circ$ ) do not attract as many cells as less hydrophilic ones (e.g.,  $\theta \sim 40\text{--}60^\circ$ ).<sup>29</sup>

While wettability may be insufficient as the only factor in determining whether or not a biomaterial is cell adhesive or resistant, it is still worth examining. To investigate the issue of wettability, samples from two different multilayer systems—the resistant 2.0/2.0 and the adhesive 3.5/7.5 PAA/PAH combinations—were first treated in various solutions, including ethanol, normal and serum-free media, and PBS, in order to simulate the effects of the cell experimental conditions. After being incubated in the solutions at  $37^\circ\text{C}$  for at least 7 days, the samples from each multilayer set were rinsed with water and dried with compressed air, prior to measuring their contact angles with water. Since a typical multilayer-coated TCPS plate used for in vitro cell experiments is exposed to a range of solutions—ethanol for sterilization, nutrient media, and PBS for washing cells during media changes—it was deemed necessary to determine how each different solution affected the wettability of the multilayer systems.

Figure 5.8 displays the advancing and receding contact angles with water for each multilayer system after treatment in the various solution conditions. Several trends are evident from these graphs, notably that: 1) usually regardless of the solution treatment, the advancing contact angle of either multilayer with PAA as the outermost layer is less than that of one ending with PAH, 2) the receding contact angles (indicative of molecular rearrangement at the

surface) are always hydrophilic, considerably more than the advancing angles, and 3) in general, the 2.0/2.0 PAA/PAH system has overall more wettable surfaces compared to the 3.5/7.5 PAA/PAH combination. Furthermore, it is apparent that different solutions used in the cell experiments do indeed affect the wettability of the multilayers. The multilayers are only exposed briefly to the ethanol and PBS (and never to the serum-free media in these studies with living cells, because the cells require serum proteins for proper growth). Therefore, most of the time the cells are exposed to the nutrient media, so the contact angles with the media are likely the most appropriate criteria for judging the wettability of the films. While the advancing angles are different, the receding contact angles on the films after the media exposure are not too different between the two multilayer systems. Therefore, as expected, wettability alone cannot explain the bioinertness of the 2.0/2.0 PAA/PAH combination.

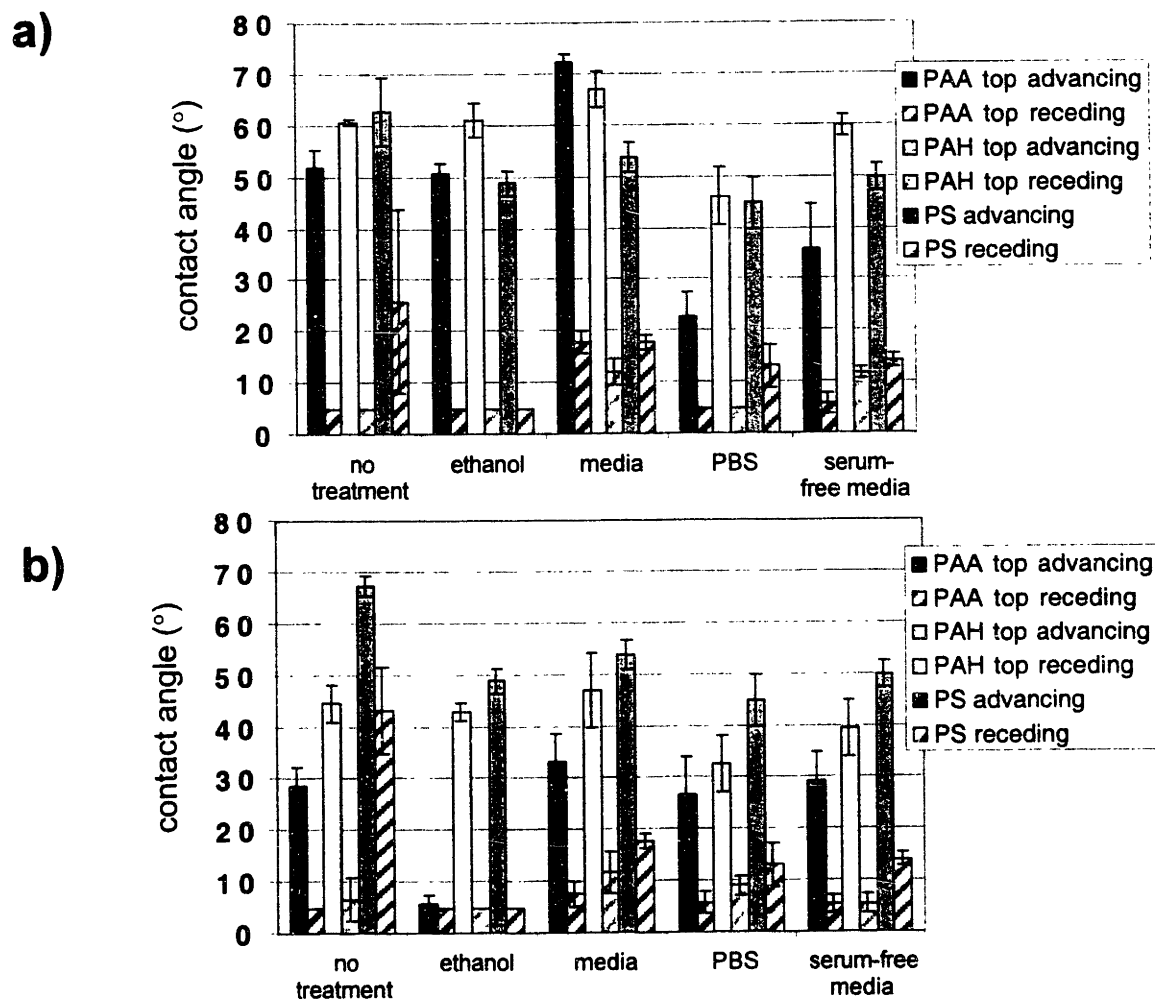


**Figure 5.8:** Advancing and receding contact angles with water on: a) 3.5/7.5 and b) 2.0/2.0 PAA/PAH multilayer films, treated in various solutions used in cell culture.



While a single multilayer combination may exhibit different wettabilities depending on whether PAA and PAH is the last layer deposited, the cells still generally behave the same, although there may be some slight differences in the cell population. In fact, for all of these cell studies, it has been observed that, regardless of the identity of the outermost layer for any given PAA/PAH or other multilayer system, the NR6WT fibroblasts behave the same with respect to cell attachment. For instance, there has not been any evidence of a PAH outermost surface of a film being able to attract cells, while a PAA outermost layer was, on the contrary, resistant to cell adhesion or vice versa. This result is quite intriguing, since the surface of a multilayer can be enriched to be either predominantly cationic or anionic, more hydrophilic or less hydrophilic, and possess different chemical groups altogether. As discussed in section 2.3, both a 3.5/7.5 and a 2.0/2.0 PAA/PAH film with a PAA surface are rich in unbound carboxylic acids (COOH), as assembled. However, in buffered media at pH ~ 7.4, those groups on each film would ionize to COO<sup>-</sup>. If cell attachment were simply based on surface charges, then it would be conceivable that cells would interact similarly on both of the multilayer systems. On the contrary, the cell behavior could not be more different—the NR6WT fibroblasts are clearly adhesive to either PAA or PAH surfaces of 3.5/7.5 multilayers yet are unable to attach to either outermost surface in 2.0/2.0 films. Thus, these cell adhesion studies suggest that it is apparently not simply a surface charge or wettability effect of polyelectrolyte multilayers that governs cell attachment, but that the cell interactions are also dependent on the additional features of the multilayer film as a whole. Such properties would include the roughness and topography, swellability, and the protein adhesiveness of the multilayers.

#### **5.4.3 Roughness and Topography**

Another important issue related to biocompatibility is the surface roughness and overall topography of the multilayer thin films. Like wettability, the role of roughness in promoting or preventing cell attachment is inconclusive and subject to much debate. However, it is well known that, for orthopedic applications, using metallic implants with roughened or textured surfaces helps induce bone cells to adhere to the device; such bony ingrowth beneficially anchors the implant into place with the existing tissue.<sup>30</sup> Furthermore, there have been numerous investigations into how cells respond to a variety of different

topography in the form of grooves, channels, pits, ridges, steps, and so forth.<sup>31-33</sup> These features were usually made via plasma processing, etching, or other photolithographic processes on generally hard materials (e.g., quartz, glass, metals, and sometimes plastics) but only rarely on softer hydrogel or implantable-type polymers. Although many different cell types have been used for these studies, thus complicating the analysis, cells generally tend to clearly detect and respond to these topological features, by, for example, showing preference in aligning with grooves or ridges and modifying their migration according to such features.<sup>31,33</sup> Of all of these different studies, there really has not been any evidence of cells being prevented from attaching at all simply due to “synthetic” topography and geometry. Moreover, the roughness in all of these cases is on the order of microns, which is substantially more than what is observed even for the roughest polyelectrolyte multilayers (which is hundreds of angstroms at most, since most films are usually  $< 1000 \text{ \AA}$  as prepared). Therefore, the ability to draw conclusions from research conducted with significantly rougher and harder materials in predicting the role of roughness in the cell response for multilayers is limited.

It should still be noted, however, that roughness may still have some role when just comparing the cell response between different multilayer systems. Interestingly, all of the bioinert cases (e.g., 2.0/2.0 PAA/PAH, 10.0/10.0 SPS/PAH, and SPS/PDAC with added salt) possessed higher *dry* RMS roughness values than their cell adhesive counterparts assembled from the same polyions under conditions that yielded fully ionized layers. According to Table 2.2, which presented many of the different multilayer assemblies whose cell responses have now been presented, the highest dry roughness values stated there are associated with those multilayer systems exhibiting bioinertness. Not surprisingly, the cell adhesive systems (except for the case of the 3.5/7.5 PAA/PAH) all possess ultrathin layer conformations, due to their high cooperative ionic stitching and thus relatively smoother surfaces. One notable study concerning the inflammatory fibrous encapsulation response (as discussed in section 1.1) to the common polymeric implant material polyethylene revealed that the fibrous capsule was significantly thinner on the roughest surfaces compared to on the smoothest ones.<sup>34</sup> However, even the roughest surfaces still promoted the inflammatory cell response to some degree and displayed numerous attached cells but usually fewer than on smoother surfaces. It should also be emphasized that the “high roughness” samples in this study had RMS roughness values of

10–50  $\mu\text{m}$ , while smooth samples had values  $< 10 \mu\text{m}$ .<sup>34</sup> Hence, since the order of magnitude of the roughness in this and many other studies is considerably higher than that exhibited by even the roughest multilayers, direct comparisons of the results are difficult. Setting the order of magnitude differences aside, the roughest polyethylene and the roughest multilayer samples were agreeable in reducing or eliminating altogether cell attachment.

The pH-induced porosity phenomenon detailed in Chapter 3 furthermore provides intriguing results related to the issue of roughness. In fact, once made porous into either type of morphology (i.e., percolating nano/microporous or discrete structures), 3.5/7.5 PAA/PAH films actually change from being cell adhesive to being cell resistant. Figure 5.9(a) presents an image of a nonporous 3.5/7.5 PAA/PAH film, which as also previously seen in Figure 5.2 is cell adhesive, while Figure 5.9(b) shows a cell resistant 3.5/7.5 film after undergoing the porosity transformation. In general, any porosity treatment discussed in Chapter 3, independent of time or temperature, tends to yield relatively bioinert films.

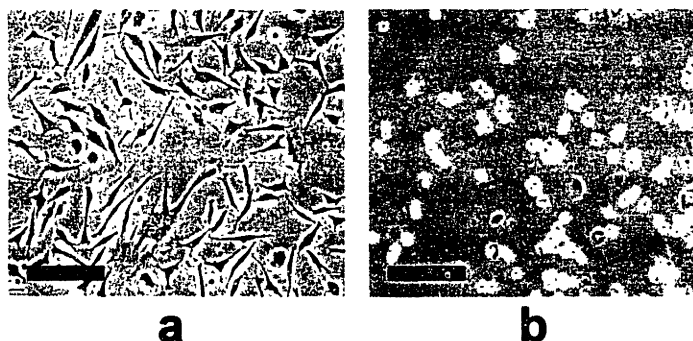


**Figure 5.9:** Phase contrast photographs of NR6WT fibroblasts seeded onto: a) nonporous and b) porous 3.5/7.5 PAA/PAH multilayers. Nonporous films readily attract cells, whereas porous films, which presumably swell much more, resist cell attachment. (  $\blacksquare$  = 200  $\mu\text{m}$ )

While there are some chemical changes associated with the bond breaking and reformation during the spinodal decomposition, a major difference between a nonporous and a porous 3.5/7.5 PAA/PAH multilayer is its overall surface roughness. Nonporous films exhibit *dry* RMS roughness values generally in a broad range of  $\sim 20\text{--}50 \text{ \AA}$ , compared to porous films having *dry* roughnesses of several hundred angstroms, as seen in section 3.3.5. Of course, it should be emphasized that what truly matters in terms of cell adhesion is not so much the *dry* RMS roughness values of a surface in air but rather the film's topology in the cell media; this issue is captured by the swellability and hydration of the multilayer. Thus,

discussing “dry” roughness, in terms of RMS values and feature topography, is much less meaningful than investigating the amount of swelling in a buffered fluid environment. Thus, since all of the in vitro cell experiments were performed under physiological buffer conditions (pH ~ 7.4, with an ionic strength ~ 0.15 M), the swelling of the multilayers in such environments is quite important for understanding cell adhesion behavior. Section 5.4.5 will address this issue in more detail and reveals that multilayers with higher degrees of swelling and hydration are cell resistant. By analogy, porous multilayers, which would be expected to swell more in fluid than their nonporous counterparts, are similarly bioinert. Quite advantageously, this observation that nano/microporous films are resistant to the attachment of this highly adhesive fibroblast cell line would certainly prove valuable in creating bioinert membranes and other porous coatings, which would therefore not succumb to undesirable, nonspecific cell attachment.

#### **5.4.4 Protein Adhesiveness**

From section 4.3, it was presented that both the cell-resistant 2.0/2.0 and the nonporous adhesive 3.5/7.5 PAA/PAH multilayers attracted two model proteins, lysozyme and fibrinogen. Again, it was argued—based on the many other previous investigations in the multilayer literature, which demonstrated how virtually any protein could adsorb onto many different types of synthetic polyelectrolytes to assemble films—that the 2.0/2.0 and 3.5/7.5 PAA/PAH systems would be predicted to be protein adhesive, as well. Usually, however, since cell attachment is mediated via proteins (e.g., integrins and adhesion molecules),<sup>35</sup> conclusions are drawn between a material’s ability to be protein resistant and potential to be cell resistant, and vice versa. Nevertheless, this correlation tends to be much more complicated than just a direct implication of one type of resistance or adhesiveness necessitating the other. Recent studies examining SAMs of alkanethiols terminated with a variety of chemical groups, some of which were protein resistant, showed no obvious correlation with subsequent cell experiments.<sup>36</sup>

Several factors including the type and amount of proteins adsorbed, competition between serum proteins, the strength of protein binding, and the conformation of the adsorbed proteins, all impact the ability of a surface to either prevent or encourage cell attachment. Thus, the fact that 2.0/2.0 PAA/PAH films are apparently protein adhesive yet cell resistant is

not necessarily contradictory. Instead, any attached proteins in the cell culture media presumably may adsorb to the 2.0/2.0 films in conformations not preferable for promoting subsequent cell adhesion. In fact, some modified SAMs have been reported to bind significant amounts of fibrinogen yet remain essentially cell resistant,<sup>36</sup> an observation found with the 2.0/2.0 PAA/PAH combination as well.

#### **5.4.5 Swelling Studies**

As stated in section 5.4.3, the issues of film swelling and hydration are more meaningful in understanding cell adhesion than just dry RMS roughness values. It was noted in section 4.3 that both 2.0/2.0 and 3.5/7.5 PAA/PAH multilayers exhibited swelling in the PBS buffer during the SPR analysis. In fact, 2.0/2.0 films displayed a larger SPR angle decrease, indicative of a larger refractive index lowering and thus more swelling, compared to that of the 3.5/7.5 films. A more quantitative swelling analysis was then performed on similar samples by studying the films with fluid-cell AFM measurements. By profiling the depth of a scored line made in the film from its surface down to the hard silicon substrate, it was possible to profile the changes in film thickness both in dry conditions in air and in fluid conditions under the same PBS buffer used in cell experiments. A 20-layer 3.5/7.5 film, representative of what is typically used in the cell culture experiments, swelled from its original thickness of  $\sim 1200$  Å to just  $\sim 1350$  Å. In contrast, a 20-layer 2.0/2.0 PAA/PAH multilayer, with an initial thickness of  $\sim 500$  Å immediately swelled to  $\sim 2000$  Å, a swelling of 4 times, which is substantially more than the marginal swelling observed in the 3.5/7.5 case. Thus, it appears its overall hydrophilic, loop-rich, swellable, and highly non-ionized (as assembled) attributes may govern the bioinertness of the 2.0/2.0 films. Neutron reflectivity analysis has also been performed on a variety of PAA/PAH multilayers, including the 6.5/6.5 PAA/PAH system as well as the 3.5/7.5 and 2.0/2.0 cases. Preliminary results also seem to support the notion that the cell resistant 2.0/2.0 system swells more than the other adhesive PAA/PAH films.

While multilayers are often considered to be highly hydrated films, the degree of that hydration and swellability is certainly variable. Thus, upon exposure to buffered physiological saline (PBS at pH  $\sim 7.4$ ), the 2.0/2.0 PAA/PAH combination experiences a much greater degree of hydration and swelling. As stated previously and as confirmed from FT-IR and

methylene blue adsorption experiments, the COOH-rich (both internally and on the surface) 2.0/2.0 films become highly ionized. Since the overall structure of 2.0/2.0 films would then be dominated by a high density of COO<sup>-</sup> groups, presumably these ions would start to repel each other and rapidly drive the structure to swell in an attempt to separate those abundant repulsive charges. Clearly, the AFM swelling results confirm the concept that highly ionically crosslinked structures (e.g., the 3.5/7.5 case) would not swell as much as lightly crosslinked structures (e.g., the 2.0/2.0 case) that possess many free ionizable groups, which could then repel one another under highly charged conditions.

By analogy, the other bioinert multilayers have one polymer with a low charge density as assembled; upon exposure to a buffered physiological environment, the numerous similarly charged groups (e.g., charged amines in the case of SPS/PAH 10.0/10.0) would likewise repel each other and induce substantial film swelling. Such significant hydration and swellability could then resemble the inherent characteristics of the well-known protein and cell resistant material PEO.<sup>15,16</sup> Interestingly, unlike many other multilayers, the 3.5/7.5 PAA/PAH system, which swells substantially at acidic conditions of pH ~ 2.4 during the porosity-inducing phase separation, is cell resistant only after becoming porous. The much increased roughness and potentially greater ability to swell renders the porous 3.5/7.5 films bioinert as compared to their nonporous precursor films, as shown in section 5.4.3.

Although bioinert multilayers, as measured by the representative 2.0/2.0 PAA/PAH system, do allow some protein adsorption, the high hydration of such films does not enable the attached proteins from the cell culture media to exist in conformations that encourage subsequent cell adhesion. Having such a swellable, water-rich surface would likely not allow proteins to denature in order to support cell adhesion. From the cells' perspective, the proteins essentially appear to be dissolved in the buffer rather than be anchored and denatured on a surface, which would be necessary for promoting cell attachment. Consequently, while the cell resistant multilayers do attract proteins to some degree, their highly hydrated films are still able to prevent noticeable mammalian cell attachment.

## **5.5 Conclusion and Future Work**

This chapter has surveyed the interaction of a model highly adhesive fibroblast cell line to a wide range of polyelectrolyte multilayers, assembled under many different deposition

conditions. The resulting thin films exhibit varying thicknesses, roughness values, layer conformations, wettability, and the number and fraction of free/unbound and paired ionic groups. Correspondingly, the cells display different behavior in terms of attachment, spreading, and population growth depending on the multilayer surfaces. In general, the cells readily attach, spread in area, and proliferate on the multilayer assemblies, similar to that which is observed on a known adhesive TCPS control. However, as presented in this chapter, there are numerous counterexamples showing how the cells do not easily adhere to certain multilayer compositions. Quite surprisingly, the findings discussed here reveal that, via the nanoscale control over thin film properties that is afforded by the polyelectrolyte multilayer process, it is possible to actually fine-tune a surface—even if made from the same polyion combination—to be either highly cell adhesive or cell resistant. This is the first report stating that it is possible to direct the constituent polymers assembled into a thin film to exhibit a range of cell responses. According to the biomaterials literature, many of the polymers used here—PAA, PMA, and PAH—are often viewed as being cell adhesive. However, this chapter clearly identifies the fact that in the case of multilayers, it is not simply an issue of whether or not the individual constituent polymers are inherently resistant or adhesive; rather, it is important to consider how those polymers are blended together, especially in terms of the interrelated issues of the film conformation, the ionic crosslink density and fraction of unbound ionizable groups, and the swellability and hydration.

All the bioinert polymer systems consisted of at least one polyion possessing a high degree of non-ionized, unpaired groups in the as-prepared multilayer. These resistant films were consequently more loop-rich and rougher in general compared to their cell adhesive counterparts. For comparison purposes, two specific multilayer conditions—the 3.5/7.5 and 2.0/2.0 PAA/PAH systems—were studied more in depth, especially with regard to their protein adhesion, as seen in Chapter 4, their wettability after being processed in a variety of solutions to mimic physiological cell culture conditions, and their in situ film swelling under PBS. While wettability and protein adhesion characteristics were not such obvious indicators of preventing or promoting cell attachment, the swelling studies did show a drastic difference in the behavior of multilayers under physiological fluid environments. The bioinert 2.0/2.0 case swelled by 4 times its initial height in the physiological buffer, whereas the 3.5/7.5 system barely swelled at all. These results seem to also suggest that the more open 2.0/2.0

films, having a much weaker ionic stitching character, can more easily hydrate and swell in other fluids such as the cell media. In contrast, the 3.5/7.5 PAA/PAH multilayer, possessing a tightly ionically paired architecture, could presumably not hydrate and swell as much as a less strongly stitched film. By analogy, it is believed and fairly obvious, based on thickness measurements and bonding data, that other cell adhesive and cell resistant multilayers similarly possess structures with more or less tightly ionically stitched conformations.

Certainly, however, much more work is needed to confirm the findings presented here. The *in situ* swelling studies and protein analysis studies using the SPR method were performed only on the 3.5/7.5 and the 2.0/2.0 PAA/PAH systems, as already well-characterized representatives of cell adhesive and bioinert multilayers, respectively. The extension of these important studies to other systems is necessary in order to confirm the general presumption that loop-rich, partially ionized films swell more than their highly ionized and smoother counterparts.


In addition, further *in vitro* cell studies, including cell adhesion strength assays, cell migration studies, and cell function assays (e.g., measuring the amount of protein synthesis on various multilayers) are needed to fully elucidate the biocompatibility of polyelectrolyte multilayers. Long-term *in vitro*, as well as *in vivo* animal, studies are similarly necessary to determine the extent of the bioinertness, since for medical applications, continuous resistance to nonspecific fouling from cells and the reduction or prevention of fibrous encapsulation is obviously desirable. In fact, one of the major problems with PEO materials is their poor long-term performance *in vivo*.<sup>36</sup> Already, preliminary results have demonstrated the ability of PAA/PAAm films to remain cell resistant for several weeks; such experiments should be performed for other bioinert multilayer combinations.

Ideally, as discussed in Chapter 1, the bioinert multilayers presented here can serve as the cell resistant background, which simultaneously prevents nonspecific cell attachment yet promotes specific cell or protein adhesion via engineered ligand presentation. While some multilayers presented in this chapter (e.g., PAA/PAH or SPS/PAH deposited at pH 6.5/6.5 conditions) are adhesive, the observed cell attachment is nonspecific and therefore uncontrolled. Consequently, although these adhesive multilayers allow cell attachment, these films would not be such desirable candidates for biomaterials possessing controlled interactions with cells, which is an important demand. Instead, specific cell adhesive protein



sequences, such as the common RGD (arginine-glycine-aspartic acid) tripeptide, could be incorporated onto an inert multilayer background. The resulting composite bioinert and cell adhesive materials could be patterned or organized with micron-scale precision for various tissue engineering, cell array, or biosensing applications. A simple, large-scale example of patterning cells using multilayers, Figure 5.10 presents a cell adhesive TCPS dish that was half-coated with cell resistant PAA/PAAM multilayers. As the figure shows, the cells readily adhere to the untreated TCPS side but remain unattached and floating on the inert multilayer side.

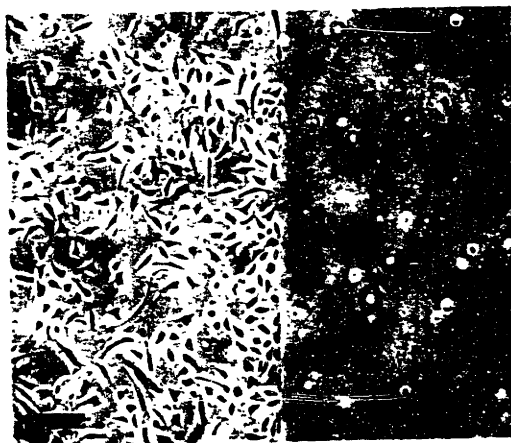


**Figure 5.10:** Phase contrast photograph of NR6WT fibroblasts seeded onto a TCPS dish half-coated with bioinert PAA/PAAM multilayers; the cells only attach onto the adhesive TCPS side (left side), but not on the cell resistant multilayer half (right side). (  = 250  $\mu\text{m}$ )

Considering the chemistry of the bioinert multilayers, it is clear that the films contain many free, unbound functional groups. For example, SPS/PAH films at 10.0/10.0 and PAA/PAH films at 2.0/2.0 abound in free amines and free acids, respectively. These groups provide numerous chemical sites whereby synthetic reactions could occur to even further modify the multilayers. Therefore, through rather straightforward chemistry, it is possible to tether RGD or other peptide sequences in order to selectively attract cells. Thus, for instance, not only is the 2.0/2.0 PAA/PAH system beneficially cell resistant but it inherently possesses a rich density of reactivity sites for further biochemical ligand modification. The ability to pattern multilayers<sup>37</sup> in much smaller dimensions than those presented in Figure 5.10 via photolithography, microcontact printing/stamping, inkjet printing, or other standard techniques, is currently underway. Already, there are promising results showing how RGD

can be selectively patterned into features (e.g., lines, circles, or other intricate shapes) with a resolution of  $\sim 50 \mu\text{m}$ . Such patterning is accomplished by only “activating” a precisely determined area of free chemical groups, which are subsequently reacted to tether RGD or another desired biomolecule.

In summary, this chapter has identified how polyelectrolyte multilayers may be tuned through the manipulation of pH and/or ionic strength conditions to be either highly cell adhesive or cell resistant. The inherent swellability and hydration characteristics of weakly ionized multilayers under physiological buffer conditions explain the bioinertness exhibited by those multilayer systems. Wettability and protein adsorption experiments were useful yet not extremely enlightening issues, relative to the swelling data, for determining the mechanism of cell resistance. Moreover, presumably serum proteins do adsorb onto even the hydrated cell resistant multilayers but remain in non-denatured conformations, which are unable to support cell attachment. The additional ability to then pattern those cell resistant films with biomolecular ligands further supports the rationale of using such thin film multilayer coatings as bio-interface materials.

## 5.6 References

- (1) Onda, M.; Lvov, Y.; Ariga, K.; Kunitake, T. Sequential Actions of Glucose Oxidase and Peroxidase in Molecular Films Assembled by Layer-by-Layer Alternate Adsorption. *Biotech. Bioeng.* **1996**, *51*, 163.
- (2) Onda, M.; Lvov, Y.; Ariga, K.; Kunitake, T. Sequential Reaction and Product Separation on Molecular Films of Glucoamylose and Glucose Oxidase Assembled on an Ultrafilter. *J. Ferment. Bioeng.* **1996**, *82*, 502.
- (3) Decher, G.; Lehr, B.; Lowack, K.; Lvov, Y.; Schmitt, J. New Nanocomposite Films for Biosensors: Layer-by-Layer Adsorbed Films of Polyelectrolytes, Proteins or DNA. *Biosens. Bioelect.* **1994**, *9*, 677.
- (4) Chung, A. J.; Rubner, M. F. Methods of Loading and Releasing Low Molecular Weight Cationic Molecules in Weak Polyelectrolyte Multilayer Films. *Langmuir* **2002**, *18*, 1176.
- (5) Qui, X.; Leporatti, S.; Donath, E.; Möhwald, H. Studies on the Drug Release Properties of Polysaccharide Multilayers Encapsulated Ibuprofen Microparticles. *Langmuir* **2001**, *17*, 5375.
- (6) Shi, X.; Caruso, F. Release Behavior of Thin-Walled Microcapsules Composed of Polyelectrolyte Multilayers. *Langmuir* **2001**, *17*, 2036.

- (7) Antipov, A. A.; Sukhorukov, G. B.; Donath, E.; Möhwald, H. Sustained Release Properties of Polyelectrolyte Multilayer Capsules. *J. Phys. Chem. B* **2001**, *105*, 2281.
- (8) Sukhorukov, G. B.; Antipov, A. A.; Voigt, A.; Donath, E.; Möhwald, H. pH-Controlled Macromolecule Encapsulation in and Release from Polyelectrolyte Multilayer Nanocapsules. *Macromol. Rapid Comm.* **2001**, *22*, 44.
- (9) Elbert, D. L.; Herbert, C. B.; Hubbell, J. A. Thin Polymer Layers Formed by Polyelectrolyte Multilayer Techniques on Biological Surfaces. *Langmuir* **1999**, *15*, 5355.
- (10) Serizawa, T.; Yamaguchi, M.; Matsuyama, T.; Akashi, M. Alternating Bioactivity of Polymeric Layer-by-Layer Assemblies: Anti- vs Procoagulation of Human Blood on Chitosan and Dextran Sulfate Layers. *Biomacromolecules* **2000**, *1*, 306.
- (11) Chluba, J.; Voegel, J. C.; Decher, G.; Erbacher, P.; Schaaf, P.; Ogier, J. Peptide Hormone Covalently Bound to Polyelectrolytes and Embedded into Multilayer Architectures Conserving Full Biological Activity. *Biomacromolecules* **2001**, *2*, 800.
- (12) Grant, G. G. S.; Koktysh, D. S.; Yun, B.; Matts, R. L.; Kotov, N. A. Layer-By-Layer Assembly of Collagen Thin Films: Controlled Thickness and Biocompatibility. *Biomed. Microdevices* **2001**, *3*, 301.
- (13) Gin, H.; Dupuy, B.; Bonnemaïson-Bourignon, D.; Bordenave, L.; Bareille, R.; Latapie, M. J.; Baquey, C.; Bezian, J. H.; Ducassou, D. Biocompatibility of Polyacrylamide Microcapsules Implanted in Peritoneal Cavity or Spleen of the Rat. Effect on Various Inflammatory Reactions In Vitro. *Biomat. Artif. Cells Artif. Organs* **1990**, *18*, 25.
- (14) Oka, J. A.; Weigel, P. H. Binding and Spreading of Hepatocytes on Synthetic Galactose [sic] Culture Surfaces Occur as Distinct and Separable Threshold Responses. *J. Cell Biol.* **1986**, *103*, 1055.
- (15) Malmsten, M.; Emoto, K.; Van Alstine, J. M. Effect of Chain Density on Inhibition of Protein Adsorption by Poly(ethylene glycol) Based Coatings. *J. Colloid Interface Sci.* **1998**, *202*, 507.
- (16) Wang, R. L. C.; Kreuzer, H. J.; Grunze, M. Molecular Conformation and Solvation of Oligo(ethylene glycol)-Terminated Self-Assembled Monolayers and Their Resistance to Protein Adsorption. *J. Phys. Chem. B* **1997**, *101*, 9767.
- (17) Chapman, R. G.; Ostuni, E.; Liang, M. N.; Meluleni, G.; Kim, E.; Yan, L.; Pier, G.; Warren, H. S.; Whitesides, G. M. Polymeric Thin Films That Resist the Adsorption of Proteins and the Adhesion of Bacteria. *Langmuir* **2001**, *17*, 1225.
- (18) McAuslan, B. R.; Johnson, G. Cell Responses to Biomaterials I: Adhesion and Growth of Vascular Endothelial Cells on Poly(hydroxyethyl methacrylate) Following Surface Modification by Hydrolytic Etching. *J. Biomed. Mater. Res.* **1987**, *21*, 921.
- (19) Shivakumar, K.; Nair, R. R.; Jayakrishnan, A.; Thanoo, B. C.; Kartha, C. C. Synthetic Hydrogel Microspheres as Substrata for Cell Adhesion and Growth. *In Vitro Cell. Dev. Biol.* **1989**, *25*, 353.
- (20) Ramsey, W. S.; Hertl, W.; Nowlan, E. D.; Binkowski, N. J. Surface Treatments and Cell Attachment. *In Vitro* **1984**, *20*, 802.
- (21) Ghosh, P.; Amirpour, M. L.; Lackowski, W. M.; Pishko, M. V.; Crooks, R. M. A Simple Lithographic Approach for Preparing Patterned, Micron-Scale Corrals for Controlling Cell Growth. *Angew. Chem. Int. Ed.* **1999**, *38*, 1592.

- (22) Tidwell, C. D.; Ertel, S. I.; Ratner, B. D.; Tarasevich, B. J.; Arte, S.; Allara, D. L. Endothelial Cell Growth and Protein Adsorption on Terminally Functionalized, Self-Assembled Monolayers of Alkanethiols on Gold. *Langmuir* **1997**, *13*, 3404.
- (23) López, G. P.; Albers, M. W.; Schreiber, S. L.; Carroll, R.; Peralta, E.; Whitesides, G. M. Convenient Methods for Patterning the Adhesion of Mammalian Cells to Surfaces Using Self-Assembled Monolayers of Alkanethiolates on Gold. *J. Am. Chem. Soc.* **1993**, *115*, 5877.
- (24) Hoffman, A. S. Thermally-Induced Hydrogels. *Polymer Preprints*, **2000**, *41*, 707.
- (25) Peppas, N. A.; Sahlin, J. J. Hydrogels as Mucoadhesive and Bioadhesive Materials: A Review. *Biomaterials* **1996**, *17*, 1553.
- (26) Nakayama, Y.; Anderson, J. M.; Matsuda, T. Laboratory-Scale Mass Production of a Multi-Micropatterned Grafted Surface with Different Polymer Regions. *J. Biomed. Mater. Res. (Appl. Biomater.)* **2000**, *53*, 584.
- (27) Altankov, G.; Grinnell, F.; Groth, T. Studies on the Biocompatibility of Materials: Fibroblast Reorganization of Substratum-Bound Fibronectin on Surfaces Varying in Wettability. *J. Biomed. Mater. Res.* **1996**, *30*, 385.
- (28) Horbett, T. A.; Waldburger, J. J.; Ratner, B. D.; Hoffman, A. S. Cell Adhesion to a Series of Hydrophilic-Hydrophobic Copolymers Studied with a Spinning Disc Apparatus. *J. Biomed. Mater. Res.* **1988**, *22*, 383.
- (29) Van Wachem, P. B.; Beugeling, T.; Feijen, J.; Bantjes, A.; Detmers, J. P.; Vanaken, W. G. Interaction of Cultured Human-Endothelial Cells with Polymeric Surfaces of Different Wettabilities. *Biomaterials* **1985**, *6*, 403.
- (30) Deligianni, D. D.; Katsala, N.; Ladas, S.; Sotiropoulou, D.; Amedee, J.; Missirlis, Y. F. Effects of Surface Roughness of the Titanium Alloy Ti-6Al-4V on Human Bone Marrow Cell Response and on Protein Adsorption. *Biomaterials* **2001**, *22*, 1241.
- (31) Flemming, R. G.; Murphy, C. J.; Abrams, G. A.; Goodman, S. L.; Nealey, P. F. Effects of Synthetic Micro- and Nano-Structured Surfaces on Cell Behavior. *Biomaterials* **1999**, *20*, 573.
- (32) den Braber, E. T.; de Ruijter, J. E.; Ginsel, L. A.; von Recum, A. F.; Jansen, J. A. Quantitative Analysis of Fibroblast Morphology on Microgrooved Surfaces with Various Groove and Ridge Dimensions. *Biomaterials* **1996**, *17*, 2037.
- (33) Singhvi, R.; Stephanopolous, G.; Wang, D. I. C. Review: Effects of Substratum Morphology on Cell Physiology. *Biotech. Bioeng.* **1994**, *43*, 764.
- (34) Rosengren, A.; Bjursten, L. M.; Danielsen, N.; Persson, H.; Kober, M. Tissue Reactions to Polyethylene Implants with Different Surface Topography. *J. Mater. Sci. Mater. Med.* **1999**, *10*, 75.
- (35) Elbert, D. L.; Hubbell, J. A. Surface Treatments of Polymers for Biocompatibility. *Annu. Rev. Mater. Sci.* **1996**, *26*, 365.
- (36) Ostuni, E.; Chapman, R. G.; Liang, M. N.; Meluleni, G.; Pier, G.; Ingber, D. E.; Whitesides, G. M. Self-Assembled Monolayers That Resist the Adsorption of Proteins and the Adhesion of Bacterial and Mammalian Cells. *Langmuir* **2001**, *17*, 6336.
- (37) Yang, S. Y.; Rubner, M. F. Micropatterning of Polymer Thin Films with pH-Sensitive and Cross-linkable Hydrogen-Bonded Polyelectrolyte Multilayers. *J. Am. Chem. Soc.* **2002**, *124*, 2100.

## **Chapter 6: Conclusions and Outlook**

### **6.1 Thesis Summary and Outlook**

This thesis has attempted to explore the rationale of using polyelectrolyte multilayer thin films as biomaterials. As examples of nanostructured polyelectrolyte complexes, multilayers follow a history of such complexes being used as coacervations and films for cell and protein encapsulation, membranes, and other biomedical coatings. While the field of polyelectrolyte multilayers is growing at a significant rate, only a few studies have examined their potential as implantable biomaterials. Many investigations have already shown the possibility of using such thin films as biosensors, since a variety of enzymes or other proteins may easily be formed into layers with synthetic polyions. Controlled release therapies also seem promising, especially from the fact that substrates of any size, shape, or type—colloids, nanoparticles, cells, and drug crystals—may be coated with multilayers.

Two major areas were presented in this thesis—1) the discovery and investigation of a unique pH-induced phase separation which yields micro- and nanoporous thin films<sup>1</sup> and 2) the interactions of polyelectrolyte multilayers with proteins and with mammalian cells. The first topic dealt with a pH-driven spinodal decomposition, which occurs on potentially many

different multilayer systems at a transition pH dependent on the  $pK_a$  values and assembly conditions of the constituent polyions. As a model system, the 3.5/7.5 (or 3.5/7.75) PAA/PAH combination was discussed in terms of the processing variables used to induce the porosity and how the resulting film thickness, refractive index roughness, and morphology could be modified. The study identified two distinct porous structures achieved by controlling the time, temperature, and rinsing conditions—1) a percolating, interconnected nano- or microporous morphology developed at shorter processing times, cooler temperatures, and without neutral water rinsing, and 2) a discrete, circular throughpore morphology obtainable rapidly in acid at elevated treatment temperatures or instead developed when any initially acid-exposed porous film was immersed in neutral water for several hours.

A bond breaking and reformation mechanism was proposed that serves to reorganize the multilayer, which is presumably ionically stitched in highly intermingled conformations without significant coordinated charge pairing. By exposure to the acidic water, the film could rearrange into a more cooperatively stitched, and thus more favorable, architecture. The observation that all films, if immersed in neutral water for at least one hour, developed smoother surfaces with many discrete throughpores generally having smaller pore sizes relative to the initial porous morphologies suggests that such a discrete-pore containing structure is highly favorable. The reduction of the high surface energy due to the large amount of additional surface area created from the pores helps to explain this ultimate secondary reorganization.

Further investigations were deemed necessary to confirm the mechanism of the spinodal decomposition and to develop a free energy model to help explain the porosity transformation. Other issues, including the use of ionic strength and surfactants to induce the porosity at pH conditions other than at  $pH \sim 2.4$ , should be examined. Studying the permeability and transport properties of such porous thin films is also a necessity. Finally, these nano- and microporous multilayer thin films should be investigated for their potential in biomedical applications. Such tailorable porous coatings may greatly enhance the current membrane<sup>2-5</sup> as well as the drug delivery and controlled release<sup>6-10</sup> performance of multilayer thin films. Furthermore, the findings described in this thesis uniquely identified, for the first time, the ability to systematically introduce nano- and/or micropores into multilayer coatings,

surely a useful contribution to the field of polyelectrolyte multilayers as a whole and specifically for potential biomaterial, optical, microelectronic, and membrane applications.

The second major topic of this thesis examined how polyelectrolyte multilayers interact with both proteins and cells, an essential issue for determining the biocompatibility of multilayer thin films. Remarkably, even subtle changes in the chemistry and structure of the thin films resulted in dramatic differences in the attachment and proliferation of a model highly adhesive mammalian fibroblast cell line. In addition, this thesis importantly revealed that simple changes in the molecular-level processing alone of otherwise reportedly always cell adhesive polyions (e.g., PAA and PAH) may result in powerful differences in the cell response to the multilayers assembled from them. Interestingly, for every multilayer combination, there was no observable difference in the overall cell response with respect to the identity of the outermost film layer, suggesting the fact that the chemical and physical nature of the entire film structure, not just the surface, governs the interaction of cells with a multilayer.

While there had been several previous cell studies with multilayer assemblies, this thesis uniquely and importantly conveyed how the cell response depends upon the underlying multilayer molecular architecture, an issue not previously investigated. By understanding and manipulating the structure of the thin films, it was possible to not only advantageously create bioinert surfaces, which are essential aspects of current biomaterials research, but also to engineer a single multilayer combination to be either cell adhesive or cell resistant. Previously, several studies have shown how the wettability, film thickness, and layer conformation of weak polyelectrolyte multilayers, in particular, may be readily and systematically controlled by adjusting simple processing parameters, such as the pH of the polyion solutions.<sup>11,12</sup> By analogy, this thesis has revealed that controlling the assembly pH and ionic strength conditions enables the design of tunable cell-interactive multilayers. Furthermore, with such an approach as demonstrated here, it should be possible to identify numerous other cell adhesive and cell resistant multilayer combinations simply by manipulating the underlying molecular architecture.

In Chapter 5, an argument was made that all of the bioinert polymeric systems were able to swell substantially more than the adhesive films; this hypothesis was verified by examining, with fluid cell AFM measurements, the in situ swelling behavior of the 2.0/2.0

and 3.5/7.5 PAA/PAH multilayers, which represented the case of a bioinert and a cell adhesive system, respectively. As predicted, a 2.0/2.0 PAA/PAH film immediately swelled substantially more than a 3.5/7.5 PAA/PAH film in physiological buffer, confirming the concept that weakly ionically crosslinked multilayers are able to swell significantly in buffer and cell media, while more tightly ionically stitched films are not. This high degree of swelling and its associated hydration render bioinert films to be highly water-rich surfaces. Although proteins may bind and interact with the hydrated bioinert multilayers, the mammalian cells do not perceive those proteins as being able to support cell adhesion. In essence, from the cells' perspective, the proteins appear to be dissolved in the buffer rather than be anchored and denatured on a surface in order to allow subsequent cell attachment.

Although there has been significant progress in identifying both cell adhesive and cell resistant multilayer systems, certainly more work is needed to verify these findings, especially to confirm the prediction that other weakly ionically crosslinked multilayers, besides the 2.0/2.0 PAA/PAH combination, exhibit a high degree of swelling and hydration. Studying the molecular conformations of proteins on various multilayer surfaces would also be valuable in elucidating the mechanisms by which proteins can interact with and attach to cell resistant multilayers yet to which cells cannot.

In vitro cell culture studies have already demonstrated some of the fundamental biocompatibility issues of multilayers with a highly adhesive fibroblast cell line. Additional in vitro studies, such as cell migration, cell adhesion strength assays, and cell function assays (e.g., protein or extracellular matrix (ECM) synthesis) would be quite useful. Eventually, in vivo animal studies would be necessary to test the performance of such films under living conditions and reveal the capability of cell resistant multilayers to exhibit long-term bioinertness. Incorporating biodegradable polymers, which controllably resorb over time under physiological conditions, into bio-interfacing multilayers is yet another consideration, especially for tissue engineering applications and devices.

Multilayers should also be investigated for their ability to resist bacteria, not just mammalian cell attachment. The ability to resist bacterial adhesion as a means by which to reduce infection both in medical implants and in human habitats and surroundings is a major demand in public health<sup>13-15</sup>; if certain antibacterial agents, such as silver ions,<sup>14</sup> nitric oxide,<sup>15</sup> and even certain polycations and polyanions<sup>13</sup> were assembled into multilayers, then the



resulting films could easily conformally coat and beneficially render, via simple aqueous-based deposition processes, virtually any surface to possess antibacterial qualities.

Given its simplicity, versatility, nanoscale control, and the ability to create conformal coatings on materials of any size or shape as well as the potential to tune the adhesion of cells, the multilayer deposition of polyelectrolytes may inspire a new process to make bio-interactive surfaces. Tailorable, pre-designed features, ranging from the film roughness to the wettability to the number of available free charges all may easily be manipulated in fabricating polyelectrolyte multilayers. These attributes enable polyelectrolyte multilayers to be highly promising candidates for biomaterials. In addition, many fundamental issues regarding how the body's cells and proteins perceive and interact with synthetic biomaterials are still elusive; perhaps the advantages in assembling coatings with controlled chemical and physical attributes will enable multilayers to be an ideal system for investigating and helping to understand general cell-biomaterial interactions.

The capability to present onto bio-inert multilayers a variety of cell-adhesive biomolecules, such as fibronectin or the RGD amino acid sequence, via several different approaches should also expand the versatility of polyelectrolyte multilayers for bio-interface materials. Such micropatterning of cell-adhesive and -resistant features on a surface should provide opportunities for making controlled implant surfaces, cellular networks and arrays, as well as biosensors. Furthermore, because the polyelectrolytes used to assemble multilayers are in solution, the polymers are able to flow into tiny, intricate geometries, such as, for example, the common medical devices of cardiovascular stents and synthetic blood vessel prostheses; multilayers could then easily be created to fabricate conformal bioactive coatings with highly tailorable structural features as well as predictable, favorable interactions with living cells. Ultimately, fibrous encapsulation and inflammatory tissue responses would hopefully be abated as undesirable cells would not be able to adhere to the multilayer-coated implants. In these cardiovascular implant examples, rather than fibroblasts or inflammatory cells, endothelial blood vessel cells could instead be directed via appropriate signaling ligands and growth factors to interact favorably and controllably with the implant. It should be reiterated that certain wettable multilayers are now being used to coat some types of contact lenses. These contact lenses are among the first commercial products developed using polyelectrolyte

multilayer technology and further suggest the overall biocompatibility of such nanostructured coatings.

Overall, polyelectrolyte multilayers should greatly expand the possibilities for controlling cell-biomaterial interactions and producing micro- and nanoporous materials. By manipulating the molecular architecture of multilayers, particular those films assembled from weak, pH-dependent polyelectrolytes, this thesis has revealed how it is possible to develop multilayers with controlled porosity and tunable cell interactions. Furthermore, with the versatility of this technique, it is possible to assemble complex heterostructured multilayer thin films composed of: synthetic polyions that may be conductive or electroactive<sup>16,17</sup>; nanoparticles (e.g., silver)<sup>18</sup> or polyelectrolytes that may be inherently antibacterial; biopolymers, such as enzymes that have bio-sensing capabilities<sup>19,20</sup>; as well as cell-resistant (e.g., PAA/PAAm or 2.0/2.0 PAA/PAH) components, all of which may be micropatterned. The release of drug or other therapeutic agents is also viable. Thus, their unique ability to be tuned to be either cell adhesive or resistant, together with the pH-induced porosity, enables polyelectrolyte multilayers to be envisioned as a new nanoscale-processed alternative for effectively engineering bio-interfaces.

## 6.2 References

- (1) Mendelsohn, J. D.; Barrett, C. J.; Chan, V. V.; Pal, A. J.; Mayes, A. M.; Rubner, M. F. Fabrication of Microporous Thin Films from Polyelectrolyte Multilayers. *Langmuir* **2000**, *16*, 5017.
- (2) Tieke, B.; van Ackern, F.; Krasemann, L.; Toutianoush, A. Ultrathin Self-Assembled Polyelectrolyte Multilayer Membranes. *Eur. Phys. J. E* **2001**, *5*, 29.
- (3) Dubas, S. T.; Farhat, T. R.; Schlenoff, J. B. Multiple Membranes from "True" Polyelectrolyte Multilayers. *J. Am. Chem. Soc.* **2001**, *123*, 5368.
- (4) Dai, J. H.; Jensen, A. W.; Mohanty, D. K.; Erndt, J.; Bruening, M. L. Controlling the Permeability of Multilayered Polyelectrolyte Films through Derivatization, Cross-linking, and Hydrolysis. *Langmuir* **2001**, *17*, 931.
- (5) Krasemann, L.; Tieke, B. Composite Membranes with Ultrathin Separation Layer Prepared by Self-Assembly of Polyelectrolytes. *Mat. Sci. Eng. C* **1999**, *8/9*, 513.
- (6) Antipov, A. A.; Sukhorukov, G. B.; Donath, E.; Möhwald, H. Sustained Release Properties of Polyelectrolyte Multilayer Capsules. *J. Phys. Chem. B* **2001**, *105*, 2281.
- (7) Chung, A. J.; Rubner, M. F. Methods of Loading and Releasing Low Molecular Weight Cationic Molecules in Weak Polyelectrolyte Multilayer Films. *Langmuir* **2002**, *18*, 1176.

- (8) Shi, X.; Caruso, F. Release Behavior of Thin-Walled Microcapsules Composed of Polyelectrolyte Multilayers. *Langmuir* **2001**, *17*, 2036.
- (9) Sukhorukov, G. B.; Antipov, A. A.; Voigt, A.; Donath, E.; Möhwald, H. pH-Controlled Macromolecule Encapsulation in and Release from Polyelectrolyte Multilayer Nanocapsules. *Macromol. Rapid Comm.* **2001**, *22*, 44.
- (10) Qui, X.; Leporatti, S.; Donath, E.; Möhwald, H. Studies on the Drug Release Properties of Polysaccharide Multilayers Encapsulated Ibuprofen Microparticles. *Langmuir* **2001**, *17*, 5375.
- (11) Yoo, D.; Shiratori, S. S.; Rubner, M. F. Controlling Bilayer Composition and Surface Wettability of Sequentially Adsorbed Multilayers of Weak Polyelectrolytes. *Macromolecules* **1998**, *31*, 4309.
- (12) Shiratori, S. S.; Rubner, M. F. pH-Dependent Thickness Behavior of Sequentially Adsorbed Layers of Weak Polyelectrolytes. *Macromolecules* **2000**, *33*, 4213.
- (13) Tiller, J. C.; Liao, C.-J.; Lewis, K.; Klibanov, A. M. Designing Surfaces That Kill Bacteria on Contact. *Proc. Natl. Acad. Sci.* **2001**, *98*, 5981.
- (14) Klueh, U.; Wagner, V.; Kelly, S.; Johnson, A.; Bryers, J. D. Efficacy of Silver-Coated Fabric to Prevent Bacterial Colonization and Subsequent Device-Based Biofilm Formation. *J. Biomed. Mater. Res. (Appl. Biomater.)* **2000**, *53*, 621.
- (15) Nablo, B. J.; Chen, T.-Y.; Schoenfisch, M. H. Sol-Gel Derived Nitric-Oxide Releasing Materials that Reduce Bacterial Adhesion. *J. Am. Chem. Soc.* **2001**, *123*, 9712.
- (16) Cheung, J. H.; Stockton, W. B.; Rubner, M. F. Molecular-Level Processing of Conjugated Polymers. 3. Layer-by-Layer Manipulation of Polyaniline via Electrostatic Interactions. *Macromolecules* **1997**, *30*, 2712.
- (17) Stockton, W. B.; Rubner, M. F. Molecular-Level Processing of Conjugated Polymers. 4. Layer-by-Layer Manipulation of Polyaniline via Hydrogen-Bonding Interactions. *Macromolecules* **1997**, *30*, 2717.
- (18) Joly, S.; Kane, R.; Radzilowski, L.; Wang, T.; Wu, A.; Cohen, R. E.; Thomas, E. L.; Rubner, M. F. Multilayer Nanoreactors for Metallic and Semiconducting Particles. *Langmuir* **2000**, *16*, 1354.
- (19) Lvov, Y.; Ariga, K.; Ichinose, I.; Kunitake, T. Assembly of Multicomponent Protein Films by Means of Electrostatic Layer-by-Layer Adsorption. *J. Am. Chem. Soc.* **1995**, *117*, 6117.
- (20) Caruso, F.; Möhwald, H. Protein Multilayer Formation on Colloids Through a Stepwise Self-Assembly Technique. *J. Am. Chem. Soc.* **1999**, *121*, 6039.

# THESIS PROCESSING SLIP

FIXED FIELD: ill. \_\_\_\_\_ name \_\_\_\_\_

index \_\_\_\_\_ biblio \_\_\_\_\_

► COPIES: Archives Aero Dewey Barker Hum  
Lindgren Music Rotch Science Sche-Plough

TITLE VARIES: ►  \_\_\_\_\_

NAME VARIES: ►  \_\_\_\_\_

IMPRINT: (COPYRIGHT) \_\_\_\_\_

► COLLATION: \_\_\_\_\_

► ADD: DEGREE: \_\_\_\_\_ ► DEPT.: \_\_\_\_\_

► ADD: DEGREE: \_\_\_\_\_ ► DEPT.: \_\_\_\_\_

SUPERVISORS: \_\_\_\_\_

NOTES:

cat'r:	date:
DEPT: Nat Science	page: 796
YEAR: 2002	DEGREE: Ph.D.
NAME: HENDERSON, James Daniel	